Coastal dune behavior and the role of sediment supply in the aeolian system

MSc Thesis Yichuan Gong

Delft University of Technology

November 2017

Coastal dune behavior and the role of sediment supply in the aeolian system

M.Sc. Thesis

Yichuan Gong

November 2017

Delft University of Technology
Faculty of Civil Engineering and Geosciences
Department of Hydraulic Engineering

Graduation Committee:

Prof. dr. ir. S.G.J. Aarninkhof	Delft University of Technology, Chair
dr. ir. S. de Vries	Delft University of Technology
dr. ir. B.C. van Prooijen	Delft University of Technology
dr. ir. B.M. Hoonhout	Delft University of Technology
dr. ir. P.G.M. Rauwoens	The Catholic University of Leuven

Preface

This thesis describes the findings of my graduation work to obtain the degree of Master of Science at the Faculty of Civil Engineering and Geosciences at Delft University of Technology.

First, I am grateful to my daily supervisor: Sierd de Vries. Thank you for always being available when I needed you. Your time and effort are indispensable for me to complete the thesis. Thank you for all your input given in the process of my graduation and on this document.

I would like to thank Stefan Aarninkhof for chairing my graduation committee. Your feedbacks during committee meetings gave me a lot of inspirations. And thank you for your kind encouragement.

Next I would like to thank Bas Hoonhout for your valuable advice and helping me with the model. I also would like to thank the rest of my graduation committee, Bram van Prooijen and Pieter Rauwoens, for your valuable discussions and insights.

Finally a great thank to my parents and girlfriend for your unconditional support throughout my entire study time. And I would like to thank my friends in the thesis room who provided me a pleasant environment during my graduation.

Abstract

This thesis explores the nature of coastal dune behavior and the role of sediment supply in the aeolian system. The relationship between aeolian sediment transport and dune behavior on decadal timescales is not yet well-known. The influences of relevant processes on the aeolian system deserve more research.

The first part of the thesis conducts a data analysis based on the Dutch JARKUS dataset, which provides yearly measured profiles along the Dutch coast. A series of parameters derived from the profile measurements have been used to represent the dune behavior quantitatively. Two locations with different coastal orientations, the Rijnland and Ameland coasts, have been studied.

The theoretical wind transport capacity calculated for the two coasts showed very different results, where the transport capacity in cross shore direction for Ameland was found offshore dominant with very small onshore component while the one for Rijnland was found onshore dominant with much larger onshore component. The calculated actual dune growth rates along the two coasts had much less values than the transport capacity but demonstrated similar trend: Rijnland experienced more dune accretion than Ameland. The spatial variations in coastal morphology derived from the measurements have been correlated to the alongshore varying dune behavior, showing that a larger dune accretion is usually linked to a wider active dune but no obvious relationship can be identified between beach width and dune growth rate.

The second part of the thesis discusses a modeling study using the AeoLiS model. The inconsistency between the actual dune accretion and the theoretical onshore wind transport capacity was probably because the sediment availability dominated the aeolian sediment transport, which inspired an attempt to analyze the role of sediment supply in the aeolian system through a modeling study. Therefore AeoLiS has been used to simulate aeolian sediment transport, dune volume changes and the combined effect of erosion and accretion processes in the coastal systems.

In the modeling study, 11 scenarios have been simulated. By comparing the simulation results of the different scenarios, the influences of several different processes on the aeolian sediment transport have been analyzed. Dune vegetation was found to be necessary to acquire dune accretion. Sediment sorting and beach armoring were found to be able to significantly reduce the aeolian sediment transport, indicating the important role of sediment supply in the aeolian system. And the more the nonerodible roughness elements existed on the bed, the more the aeolian transport could be reduced. In the onshore wind dominant system, the existence of the offshore wind reduced the onshore aeolian transport in the model. In the offshore wind dominant system, the offshore wind needed to be filtered out to enable the model to reproduce the pattern of onshore aeolian transport and dune accretion. For Rijnland which experienced mainly onshore winds, the modeled dune accretion volume was relatively larger than the measured dune accretion based on the data analysis. For Ameland where the present winds were mainly offshore, the simulated and measured dune accretion volumes were quite close. Similar to the trends in the wind transport capacity and the dune growth rate, the modeled dune accretion volume for Rijnland was also larger than the one for Ameland.

Content

1. Introduction

This document is a Master thesis report, which intends to explore how erosive and accretive processes govern dune behavior and the influences of sediment supply on the aeolian system. This introduction chapter will introduce the background knowledge and the main concerns of the thesis.

To begin with, this introduction will present some basic facts about the coastal dunes and their relevance to engineering practice. Then the theoretical background about dune behavior and aeolian system will be presented. Later some background knowledge about data analysis and numerical modeling will be discussed. Finally the research questions and the thesis outline will be given. This introduction can be regarded as the combination of a general introduction of the thesis content and a literature review of the theoretical background of the thesis.

1.1. Coastal dunes and their roles in engineering practice

Coastal dunes are sandy ridges located behind beaches, built up by beach sand through the process of aeolian transport. As the wind moves the sediment into the rear of beaches, the sediment accumulates and the dunes grow higher and wider (Willian Nickling, 1990). The mechanism that controls the growth and the morphology of coastal dunes is governed by the interaction between wind, sediment supply, and coastal morphologic features. Many factors could have influences on dune building process, including wind speed and direction, grain size composition, beach width, beach slope, moisture content, beach armoring, vegetation present, etc. (Bauer et al., 2009). Figure 1 shows a picture of coastal dunes located on the Rijnland coast near IJmuiden. In the picture, the dune area is characterized by the sandy ridges partly covered by vegetation.

Figure 1. Coastal dunes on the Rijnland coast near IJmuiden.

From an engineering point of view, the roles of coastal dunes in protecting the coastal area are indispensable. Coastal dunes usually act as natural buffer when storms come, protecting the coastal area from wave impact, inundation and salt water intrusion. They also have essential

ecological and recreational values, providing unique habitats for specialized flora and fauna. Coastal maintenance is quite important for coastal countries like The Netherlands and measures like artificial beach nourishment are executed regularly there. Understanding the coastal dune behavior and aeolian system could help optimizing the strategies of coastal zone management and decision making about, for example, the frequency and amount of beach nourishment.

1.2. Coastal dune behavior and aeolian sediment transport

Dunes are often treated as natural barrier protecting hinterland from flooding. Marine processes along with storm surges erode coastal dunes, while aeolian sediment transport over beach results in dune growth. Depending on the balance between marine and aeolian processes, dune volume and coastal morphology change over time. Understanding the dune building processes will help improving the maintaining strategies. Unlike traditional approaches which enhance dunes when a certain function is not satisfied, Aarninkhof et al. (2010) proposed to apply Building with Nature type approaches. Their ecodynamic innovation explored the environmental benefits of dune building processes and help maintain dunes' protective function.

Although coastal dunes can protect hinterland during storm events, the safety levels these dunes can provide are vulnerable and variable, because of the dynamic topographic features of these dunes. A lot of efforts have been spent on understanding the dune building processes and their effects on dune behavior. While many traditional studies regard wind force as a main factor which governs aeolian transport and dune growth, several coastal studies have shown some other factors like beach profiles, sediment properties could also have important impacts.

To understand the dune behavior, aeolian forcing like wind which builds dunes and marine forcing like waves and surge which erodes dunes should be considered simultaneously. Whether the dunes will experience erosion or accretion depends on the net result of all the relevant processes. Changes in frequency and magnitude of storms and high tides have powerful impact on dune erosion and accretion behavior (Pye and Blott, 2008). In their study, dune toe erosion and accretion records are compared with storm surges in order to find correlation between them. Ruessink and Jeuken (2002) investigated the dynamics of the dunefoot along the Dutch coast and use landward retreat and seaward advance in meters as descriptive parameter. Some recent publications use morphologic variability (Bochev-van der Burgh et al., 2011) or dune volume changes per year (de Vries et al., 2012) as terms to describe dune behavior and show erosion or accretion rates.

Marine processes during storm events usually contribute to erosion of the dunes. Kriebel and Dean (1985) calculated the changes in waterline position by solving sediment transport equations numerically and found a relation between the depth and the waterfront position. Their model has been verified in several cases. Larson et al. (2004) developed an analytical modelling approach to assess dune erosion quantitatively. Their research combined wave impact theory and sediment supply to explain dune behavior under high waves and storm surges attack. Many other publications were also devoted to analyzing coastal dune erosion qualitatively and quantitatively and assessing the safety levels of the dunes (e.g. van de Graaff (1977); Callaghan et al. (2008); den Heijer et al. (2012)).

While dune erosion during storms can be severe, storm events only occur rarely. The process that happens more regularly is the aeolian transport when sufficient wind force occurs. Sufficient wind will transport erodible sediment from the beach in onshore direction and then build dunes. A lot of research on aeolian transport has been invested in both desert and coastal regions. As a leading authority on the study of aeolian transport in deserts, Bagnold (1937) investigated the mechanism of aeolian transport and identified the interaction between wind and sand as well as the main influencing factors. Kawamura (1951) studied the relation between sand flow speed and wind frictional velocity and obtained the expression of the limiting frictional velocity for incipient motion of sand grains $V_{\tau t}$. The threshold velocity is affected by the grain diameter, the gravitational acceleration, the sand grains' density and the density of the air (Bagnold, 1954).

In coastal regions, the processes are not completely the same as in desert. Precipitation can wet the beach sand in coastal regions, which rarely happens in desert. Marine forcing like waves and tides is absent in desert as well. Davidson-Arnott et al. (2008) conducted experiments to explore the effects of surface moisture and fetch on aeolian transport. They found sediment transport rates are reduced when surface moisture content increases. Wind tunnel experiments were conducted and showed some effects of beach slope on threshold friction speed (Iversen and Rasmussen, 1994). Arens (1996) compared actual rates of transport with potential rates and analyzed the deviation. His study showed aeolian transport depends much more on moderate conditions rather than extreme conditions and the threshold wind velocity for aeolian transport is around 5-10 m/s. Extreme events which are usually accompanied by precipitation have little impact on blowouts, the main features of aeolian transport, compared to mild conditions (Jungerius et al., 1991).

1.3. Measured dune development along the Dutch coast

The Dutch JARKUS dataset including yearly profile measurements provides a practical resource for studying coastal sediment supply and its relation with dune behavior. From the JARKUS dataset, dune volume changes can be acquired and used to study the spatial and temporal variations of dune growth rates. And more understanding of the relation between different governing factors and dune behavior could be gained from the analysis of the dataset. The insight gained will help future modeling of sediment processes and dune behavior.

The Dutch JARKUS dataset provides yearly measured profiles along the entire Dutch coast since 1965, which includes the regions of foreshore, beach and dune with a spatial interval of 250m alongshore. Analyzing the JARKUS data can help exploring the relation between coastal dune behavior and sediment processes. With the development of measuring and sensing techniques, the data gathering methods for coastal morphology have changed. Many data collection and selection methods and their accuracies are introduced in the study of Bochev-van der Burgh et al. (2011), such as leveling, aerial photography and laser altimetry. Southgate (2011) explored the possibilities of improving forecasts of beach volume of the Dutch coast with the help of data analysis of the JARKUS dataset. In his study, a more detailed description of the JARKUS dataset can be found. When analyzing the JARKUS data, the dune volume (changes) is first deliberated. Van Straaten (1961) defined the dune foot as the position with distinct change in profile slope between

beach and dune. The dune volume can be defined as the sand volume between the dunefoot level and a certain level landward (de Vries et al., 2012).

Meteorological data like wind data can be obtained from the Royal Dutch Meteorological Institute (KNMI). Guillen et al. (1999) analyzed the decadal evolution of the Holland coast and dune position and found correlations between dune behavior and storm conditions. Fryberger (1979) compared the morphologies of dunes with local wind conditions and discerned some characteristic wind parameters like drift potentials.

Besides aeolian transport, marine processes also have essential effects on dune behavior. So marine data is also important and can be obtained from monitoring stations. The impact of storms can be analyzed with the data from WL/Delft Hydraulics. Only three big storm events are recorded over last 60 years along the Holland coast. The most severe storm along the Dutch coast was in 1953 with an erosion of approximately 80-100 m^3/m (WL/Delft Hydraulics, 1978). A 1 in 20 year return probability storm occurred on 03-01-1976 with a mean erosion of 36 m^3/m (WL/Delft Hydraulics, 1978). Another big storm with a mean erosion of 23 m^3/m occurred on 01-02-1983 (WL/Delft Hydraulics, 1984). Scale model reproduction of storm conditions and beach profile was conducted, showing a large proportion of eroded sediment from dunes are deposited over a limited distance rather than transported further offshore (Vellinga, 1986). And field data showed the post-storm recovery of the profiles was fast (Pye and Blott, 2008). Dunes and sand slopes could form within several days.

A good application of the dataset JARKUS was done by Keijsers et al. (2014). Based on the measurements from the JARKUS dataset, they investigated the influence of erosive and accretive forces on dune volume changes and how it was governed by regional climate and local topography. The region being studied was chosen along the northwest Dutch coast, from Noord-Holland in the west to Schiermonnikoog Island in the east. Storminess being derived from water level measurements represented erosive force and transport potential being calculated from local wind data represented accretive force. Dune volumes have been calculated from the annual elevation measurements, obtained from the JARKUS dataset. The results show considerable temporal variations in dune volume changes, storminess and transport potential. While the dune volume changes have been linked to the storminess in several locations, the correlation between dune volume changes and transport potential is generally weak.

1.4. Bed surface properties and sediment supply

The building processes of coastal dunes need continuous sediment supply, which transports sediment to the beach-dune system by aeolian transport (Hoonhout and de Vries, 2017). Although only a small amount of sediment in the nearshore will finally reach the dunes, the importance of the sediment supply to the safety levels of dunes is irreplaceable (Aagaard et al., 2004). The aeolian sediment supply to coastal system can be affected by the sediment availability and bed surface properties (van der Wal, 1998). Limited sediment availability may usually be one of the reasons for the inconsistency between measured dune growth and theoretical wind transport capability (Lynch et al., 2016). The understanding of the influence of sediment supply on the aeolian system and the

relationship between sediment supply and bed surface properties still lacks depth.

Bed surface properties have a great influence on aeolian sediment transport. The co-occurrence of erodible and nonerodible grains on the bed makes the spatiotemporal variations in bed surface properties very important for sediment supply. To investigate the influence of nonerodible grains, Tan et al. (2013) did systematic experiments and examined aeolian sediment transport over various gravel beds under different wind conditions. They found that aeolian sediment transport can be significantly reduced by gravel beds and the extent of reduction was strengthened by increasing gravel size. Numerical modeling was also conducted to study the influence of roughness elements on the shear stress distribution over a bed with both erodible and nonerodible grains (Turpin et al., 2010). Typically, the roughness density λ is used to describe the coverage of nonerodible grains and the shear stress distribution over roughness arrays (Raupach et al., 1993).

Although the roughness density λ can cope with the instantaneous influence of roughness elements on shear stress distribution and aeolian sediment transport, it cannot deal with the temporal variations in bed surface properties. The extent of exposure of roughness elements is subject to change because large grains tend to emerge over time due to winnowing of fine sediments. The winnowing of fines and the resultant emergence of nonerodible roughness elements result in time-dependent bed surface properties and aeolian sediment transport (Nickling and McKenna Neuman, 1995). Even for beds with low volumetric concentrations of nonerodible roughness elements, the surface will be armored over time and eventually the erosion of fine grains can be negligible (McKenna Neuman et al., 2012). Therefore, process-based simulation is required to cope with all these temporal variations of bed surface properties occurring in the real world.

In the coastal beach area, spatial variations in bed surface properties exist widely and have been studied by many researchers. Dong et al. (2004) conducted wind tunnel experiments. In their experiments, an area of gravels was positioned downwind of an area of sand. Results of the experiments showed the erosion pattern over gravel area was different from over sandy area and the sand cloud over gravel area was significantly reduced compared to that over sandy area. These spatial variations in bed surface properties require an aeolian sediment transport model which can distinguish between sediment transport capacity and sediment availability in relation to bed surface properties.

1.5. Aeolian sediment transport modelling

Aeolian sediment transport is the main process that build the coastal dunes. By changing the sediment transport capacity and/or the sediment availability, the bed surface properties such as bed slopes, nonerodible elements, and moisture can exert influence on the aeolian sediment transport rate (Kocurek and Lancaster, 1999). The typical approach to assess this influence is by using velocity threshold. But this approach is insufficient to cope with the spatial and temporal variations in bed surface properties in the real world. A new model called AeoLiS was recently presented which simulates the sediment availability rather than parameterizes through the velocity threshold, to cope with the spatiotemporal variations of sediment availability (Hoonhout

& de Vries, 2016).

The spatiotemporal variability of sediment availability depends on the bed surface properties. The existing modeling approaches use a single parameter, velocity threshold, to deal with the influence of the bed surface properties on the sediment transport capacity and sediment availability. Bagnold (1937) studied the relation between the sediment transport and the wind speed distribution and proposed an aeolian sediment transport model. In his model, the velocity threshold was used to demonstrate the effects of surface properties on sediment transport capacity, showing the threshold wind speed to move sediment decreases when grain size decreases. Many later studies followed the approach of Bagnold (1937) and proposed many different methods for parameterizing the bed surface properties. For example, Sørensen (2004) derived an explicit formula for aeolian sediment transport, relating the dimensionless transport rate to the dimensionless friction velocity. However, the models using the velocity threshold are not able to simulate the spatiotemporal variations of bed surface properties well.

Sherman and Li (2012) evaluated eight aeolian sand transport models, including the model of Bagnold (1937) and some later proposed models, and estimated the shear velocities using wind profile data. They compared the models with field data and found the Bagnold (1937) model outperformed the other later models and made the best fit. Bed surface properties were considered by many researchers as the reasons of poor performance of the aeolian sediment transport models. For example, moisture content can make modeling and prediction of sediment transport difficult through complex interaction with wind conditions (Bauer et al., 2009). Vegetation has important impact on reduction of sand erosion by wind and it is not easy to characterize the distribution of vegetation in models (Okin, 2008). Other factors which may explain partially the poor performance of the models are salt crusts (e.g., Nickling and Ecclestone, 1981), bed slopes (e.g., Iversen and Rasmussen, 2006), shell pavements (e.g., van der Wal, 1998; McKenna Neuman et al., 2012), and sorted and armored surfaces (e.g., Gillies et al., 2006; Cheng et al., 2015). Many authors recommended using modified velocity threshold to account for the influence of these bed surface properties on the aeolian sediment transport (Hotta et al., 1984; Nickling and Ecclestone, 1981; King et al., 2005).

Two fundamentally different concepts, sediment transport capacity and sediment availability, need to be coped with in an aeolian sediment transport model. The difference becomes more evident over a bed with spatiotemporal variations in bed surface properties (Hoonhout and de Vries, 2016). Using the velocity threshold alone to manage the variations of bed surface properties is insufficient and defective because it changes inherently in time and space (Stout, 2004). All of these limitations ask for simulation of bed surface properties and sediment availability. Hoonhout and de Vries (2016) presented a new model approach which explicitly defined sediment availability according to de Vries et al. (2014) and introduced multifraction aeolian sediment transport approach. This model approach is called AeoLiS (Aeolian sediment transport with Limited Supply; https://github.com/openearth/aeolis-pythont). By simulating rather than parameterizing, the model could cope with spatiotemporal variations in bed surface properties and distinguish between sediment transport capacity and sediment availability. As a relatively new model approach, AeoLiS has not been applied broadly. The model has been used to predict the recovery

of Fire Island in the United States, which gave satisfying results compared to the corresponding data analysis (Janssen, 2016). And some efforts have been spent to combine AeoLiS with other models in order to integrate aeolian sediment transport with other coastal processes (Velhorst, 2017).

1.6. Problem definition

The Dutch JARKUS dataset provides yearly measured profiles along the Dutch coast. What kind of parameters derived from the profile measurements can describe the dune behavior quantitatively is not yet well-known. Along the Dutch coast, dune behavior varies significantly. The influences of the different coastal orientations and the morphologic variability along the coast on the alongshore varying dune behavior are not known as well. Therefore the first part of this thesis focuses on exploring the spatial varying dune behavior and its relationship with other coastal features, based on the method of data analysis.

To further understand the coastal beach-dune system, the AeoLiS model is used to simulate the aeolian sediment transport and the combined effect of erosion and accretion processes. The influences of the relevant factors like sediment supply on the aeolian system require more research. Though having been validated for the Sand Motor, the predictive skill of AeoLiS at other locations needs to be understood better as well. Therefore the second part of the thesis applies the AeoLiS model on two different locations along the Dutch coast to explore the roles of different relevant processes in the aeolian system.

1.7. Research questions

The main research question in this research is as follows:

- What is the relationship between aeolian sediment transport and dune behavior on decadal timescales along the Dutch coast, and what are the roles of erosive and accretive processes in the relationship?

The main question is divided into following sub-questions:

1. What parameters represent/quantify dune behavior?
2. What are the theoretical aeolian transport capacity and the dune growth rates along the Dutch coast under different coastal orientations and how do they compare with each other?
3. How do the spatial variations existing in coastal morphology correlate to the alongshore varying dune behavior?
4. How to simulate aeolian sediment transport, dune volume changes and the combined effect of erosive and accretive processes?
5. How do relevant processes affect the aeolian sediment transport and what is the role of sediment supply in the aeolian system?

1.8. Thesis outline

This thesis constitutes four parts:

Part I concerns the implementation of data analysis based on the yearly measurements from the JARKUS dataset. In Chapter 2, research questions one will be answered. First the two studied locations are presented: the Ameland and Rijnland coasts. Then the methods for calculating wind transport capacity and quantifying dune volume and changes are provided. Chapter 3 presents of results of data analysis. In this chapter, research questions two and three will be answered. The dune behavior is described quantitatively by several parameters derived from the measurements, based on the methods presented in Chapter 2. By analyzing the spatiotemporally varying dune behavior along the two coasts, the relation between wind transport capacity and dune growth rates is discussed. Coastal orientation, as one of the possible influencing factors, is explored by comparing the differences in dune behavior between Ameland and Rijnland. Then the alongshore variability in coastal morphology is presented and correlated to the alongshore varying dune growth rates, where the relationship between the dune growth rates and the coastal morphologic features like beach width and active dune width are discussed.

Part II concerns the modeling study for aeolian sediment transport and sediment supply that inspired by the previous data analysis. The AeoLiS model is studied and applied to further investigate the relation between aeolian sediment transport and dune behavior. In Chapter 4, research question four will be answered. This chapter discusses the methods for setting up the model, including the model topography, wind data, tide data, etc. In total 11 scenarios with different parameter settings are designed. Some important strategies used in the model setup are also included. Chapter 5 presents the results of the modeling study, based on which research question five will be answered. By comparing the results of different scenarios, the influences of the concerned processes on the aeolian sediment transport are discussed. Especially the role of sediment supply in the aeolian system is targeted for particular focus.

Part III involves discussions about model performance on the two concerned coasts, model validation and model calibration. Then general conclusions are provided by addressing the research questions, followed by the recommendations.

Part IV includes appendices which provide additional results for both the data analysis and the modeling study.

i. DATA ANALYSIS

Part I

DATA ANALYSIS

2. Methodology data analysis

This chapter aims to explain the methods of data analysis which are used to assess coastal dune behavior and aeolian sediment transport quantitatively in two locations: the Ameland coast and the Rijnland coast. To begin with, these two concerned locations will be introduced. Then the methodology used for data analysis is discussed. The methodology consists of 3 steps. In step 1, the cumulative theoretical sediment transport volumes are calculated to assess the aeolian transport capacity. In step 2, the volume changes of the active dunes in a specific period are derived from the profile measurements obtained from the JARKUS dataset. In step 3, the alongshore distributions of the dune growth rates are calculated for the two concerned locations respectively.

In this chapter the first research question is answered:

What parameters represent/quantify dune behavior?

2.1. The Ameland Island and the Rijnland Coast

The dune behavior of the two locations, Ameland and Rijnland, will be studied based on data analysis. The reason why studying the dune behavior for two locations is due to one of the interests of the thesis: the influence of coastal orientations on dune behavior.

The Ameland Island is one of the Dutch Wadden Islands, located between the Terschelling Island and the Schiermonnikoog Island. Ameland acts as a barrier island separating the Wadden Sea from the North Sea. The thesis concerns the north part of the Ameland coast which faces the North Sea, an approximately 25km long coast consists of beaches and sand dunes. The Ameland coast concerned is indicated in Figure 2 with the red color.

The Rijnland coast is located between the south breakwater around the IJmuiden which protects the North Sea Canal in the north and the breakwater of the Scheveningen harbor in the south. As a 41km long subsection of the Holland coast, the Rijnland coast is also characterized by sandy beaches and dunes. The Rijnland coast is shown in Figure 2 by the orange color.

Figure 2. The locations of the Ameland coast and the Rijnland coast (Source: www.Freeworldmap.net).

2.2. Theoretical wind transport capacity

In this section, the method of calculating the theoretical wind transport capacities for Ameland and Rijnland will be presented. Here the wind transport capacity represents the potential of the present wind, which does not take the sediment supply into account. First the imposed wind data is introduced. Next the spatial dimensions and coastal orientations of the two concerned coasts are discussed. Then the method for calculating the wind transport capacity is presented in detail.

2.2.1. Wind data

The meteorological data is acquired from the Royal Dutch Meteorological Institute (KNMI). Here the data from the wind station of De Kooy has been used, a coastal station located near Den Helder (see Figure 3 for reference). Figure 4 shows the wind rose of the wind data in the period 2006-2016 measured at the station of De Kooy. Most of the large wind components are in the third quarter which represents the directions between western and southern directions, especially from the southwest direction. According to the hourly averaged wind speed time series (see Figure 5), most time the wind speeds are roughly in the range of 0-15m/s, but sometimes the wind speeds can reach the order of 20m/s or 25m/s.

Figure 3. The location of the station of De Kooy (source: the Royal Dutch Meteorological Institute (KNMI))

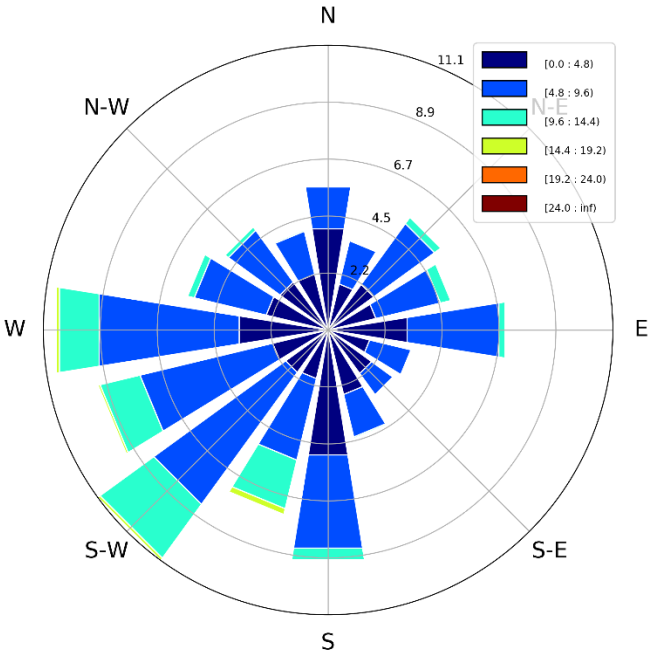

Figure 4. Wind rose of the wind data for the wind transport capacity.

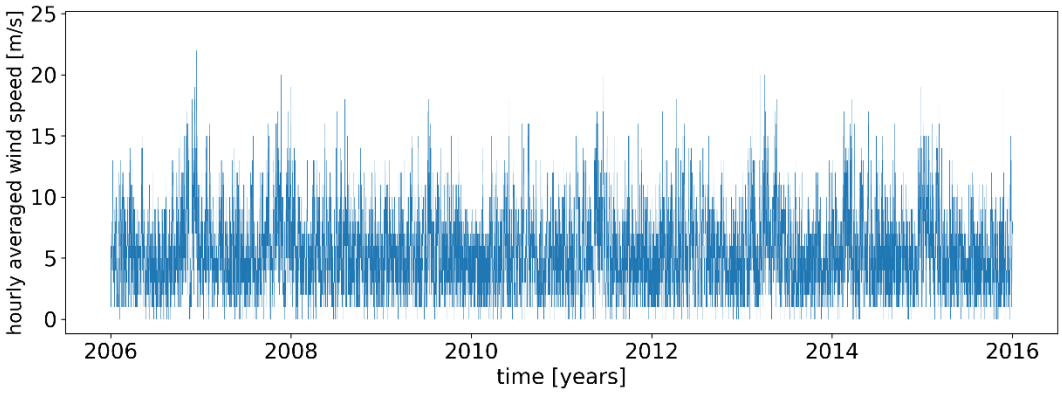

Figure 5. Hourly averaged wind speed time series of the wind data for the wind transport capacity

2.2.2. Spatial dimensions and coastal orientations of Ameland and Rijnland

The theoretical wind transport capacities are calculated for the two concerned locations: Ameland and Rijnland. Figure 6 shows the spatial dimensions and the coastal orientations for Ameland (top panel) and Rijnland (bottom panel) respectively. Note the figures are not to scale and only for illustrative purpose. The alongshore span of the concerned domain for the Ameland coast is $24160\mathrm{m}$. Similarly, the alongshore length for Rijnland is $41000\mathrm{m}$. Note that these two values are the approximate lengths of the concerned domain of the coasts, which do not necessarily represent the exact lengths of the Ameland and Rijnland coasts.

As one of the concerned influencing factors, the coastal orientations of the two coasts are very different. Here the coastal orientations are taken as the normal directions of the coastlines. From Figure 6 (top panel), it is found that the north coast of Ameland extends more or less from the west to the east. Therefore the normal direction of the coastline is approximately towards the north with the angle taken as $\theta_c = 360°$. As for Rijnland, the coastline extends approximately from the

southwest to the northeast, where the coastal orientation is approximately to the northwest with the angle of $\theta_c = 312°$, see Figure 6 (bottom panel). In the figure, the directions of the cross shore sediment transport and alongshore sediment transport are indicated as well.

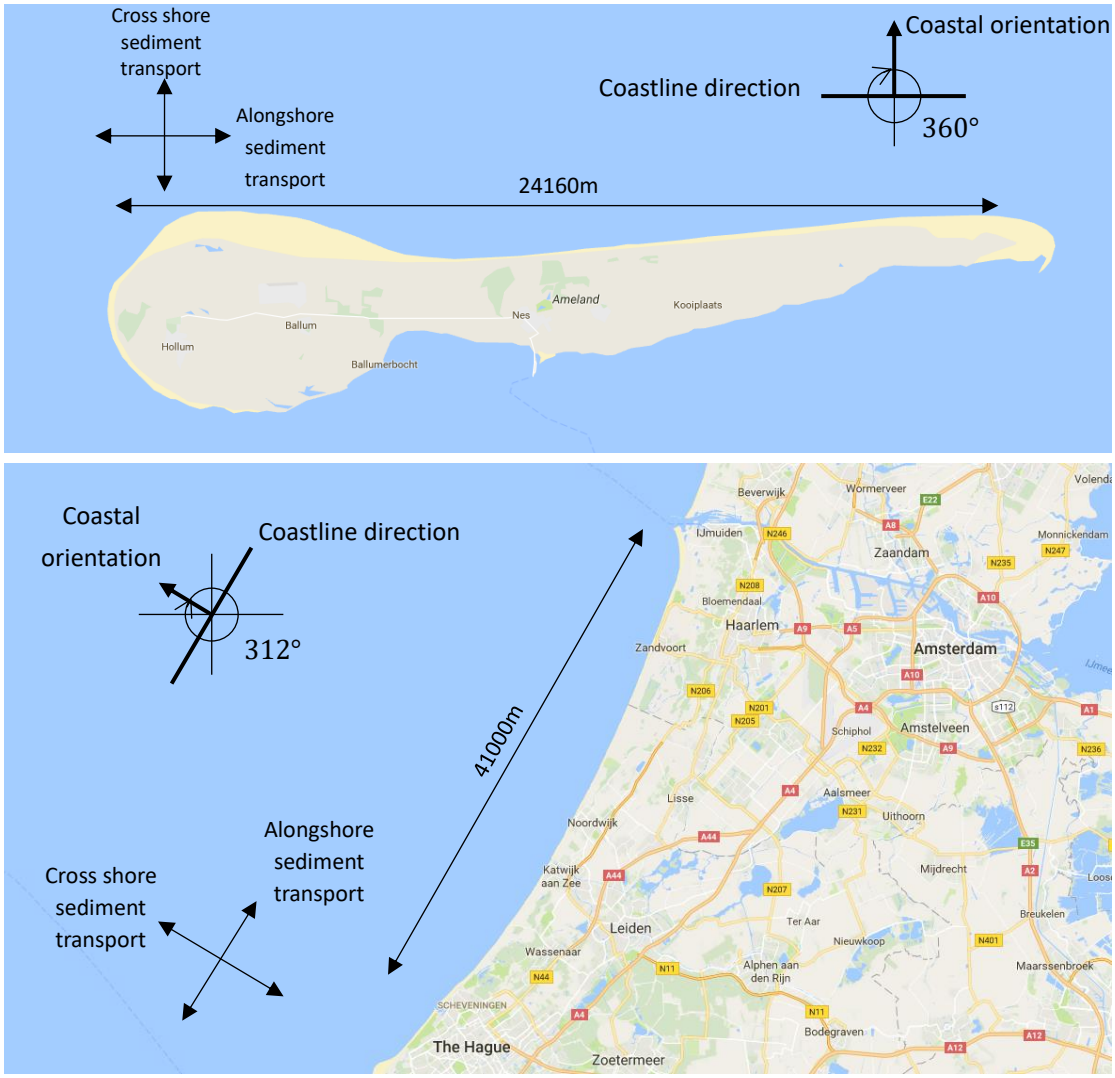

Figure 6. The spatial dimensions and the coastal orientations of Ameland (top panel) and Rijnland (bottom panel).

2.2.3. Calculating wind transport capacity

The cumulative theoretical sediment transport volume $Q\ [\mathrm{m}^3]$ represents the total wind transport capacity in the specific period. Here the period is between January 1, 2006 and December 31, 2016. The hourly averaged measured wind speed $u_{10}\ [\mathrm{m/s}]$ and the wind direction $\theta_u\ [°]$ measured at 10m height are from the KNMI station of De Kooy. The instantaneous theoretical sediment transport rate $q\ [\mathrm{kg/m/s}]$ has been obtained with the Bagnold (1937) type formulation:

$$q = C\frac{\rho_a}{g}\sqrt{\frac{d_n}{D_n}}(u_* - u_{*th})^3 \quad (1)$$

where the C factor is around 2.5 for wide range grain size, the air density $\rho_a = 1.25\ [\mathrm{kg/m}^3]$, the particle density $\rho_p = 2650.0\ [\mathrm{kg/m}^3]$, the shear velocity $u_* = \alpha * u_{10}\ [\mathrm{m/s}]$, the shear velocity threshold $u_{*th} = \alpha * 3.87\ [\mathrm{m/s}]$, the conversion factor from free-flow wind velocity to shear

velocity $\alpha = 0.058$, the gravitational constant $g = 9.81\ [\mathrm{m/s^2}]$, the nominal grain size $d_n = 335\ [\mu\mathrm{m}]$ and a reference grain size $D_n = 250\ [\mu\mathrm{m}]$.

The cumulative theoretical sediment transport volumes in cross shore direction $Q_{cs}\ [\mathrm{m^3}]$ and alongshore direction $Q_{as}\ [\mathrm{m^3}]$ have been obtained with time integration:

$$Q_{cs} = \sum q * \frac{\Delta t * \Delta y}{(1-p)*\rho_p} * f_{\theta_u,cs} \tag{2}$$

$$Q_{as} = \sum q * \frac{\Delta t * \Delta x}{(1-p)*\rho_p} * f_{\theta_u,as} \tag{3}$$

where the temporal resolution $\Delta t = 3600\ [\mathrm{s}]$, the approximate beach width $\Delta x = 100\ [\mathrm{m}]$, the alongshore span of the domain for the Ameland coast $\Delta y = 24160\ [\mathrm{m}]$, the alongshore span of the domain for the Rijnland coast $\Delta y = 41000\ [\mathrm{m}]$, the porosity $p = 0.4$ and $f_{\theta_u,cs}$ and $f_{\theta_u,as}$ are the factors to account for the cross shore and alongshore directions respectively. Note that θ_c represents the coastal orientation of the coast (normal direction of the coastline). For the Ameland coast $\theta_c = 360°$, while for the Rijnland coast $\theta_c = 312°$. The factor for the alongshore direction is defined as:

$$f_{\theta_u,as} = \sin(\theta_c - \theta_u) \tag{4}$$

The factor for the cross shore direction $f_{\theta_u,cs}$ has a twofold definitions. The first definition only takes the onshore winds into consideration and all the offshore winds are neglected. In other words, the results can be seen as the onshore component of the cross shore transport capacity. That means when the factor $f_{\theta_u,cs}$ is negative, it is replaced by zero:

$$f_{\theta_u,cs} = \max(0; \cos(\theta_c - \theta_u)) \tag{5}$$

In fact, the cross shore transport capacity based on this definition represents the potential onshore transport towards the dune, which can be linked to the potential dune accretion.

The second definition takes both the onshore and offshore winds into account. The results can be seen as the net transport capacity in the cross shore direction. So the negative values for the factor $f_{\theta_u,cs}$ will be kept:

$$f_{\theta_u,cs} = \cos(\theta_c - \theta_u) \tag{6}$$

The cross shore transport capacity based on the second definition can indicate whether the dominant direction of the net wind transport capacity is onshore and towards the dune or offshore towards the sea. Later in Chapter 3, the results of the theoretical wind transport capacity for the two locations will be discussed, including the alongshore transport capacity as well as the cross shore transport capacity based on the two different definitions.

2.3. Dune volume (changes)

In order to assess dune behavior quantitatively, dune volume has to be defined and calculated. In this thesis, the dune volume and the dune growth rate are calculated dependent on time and space. The following two subsections discuss how dune volumes and changes are defined and calculated in detail. Figure 7 below shows the brief procedure to acquire the dune growth rates from the JARKUS dataset.

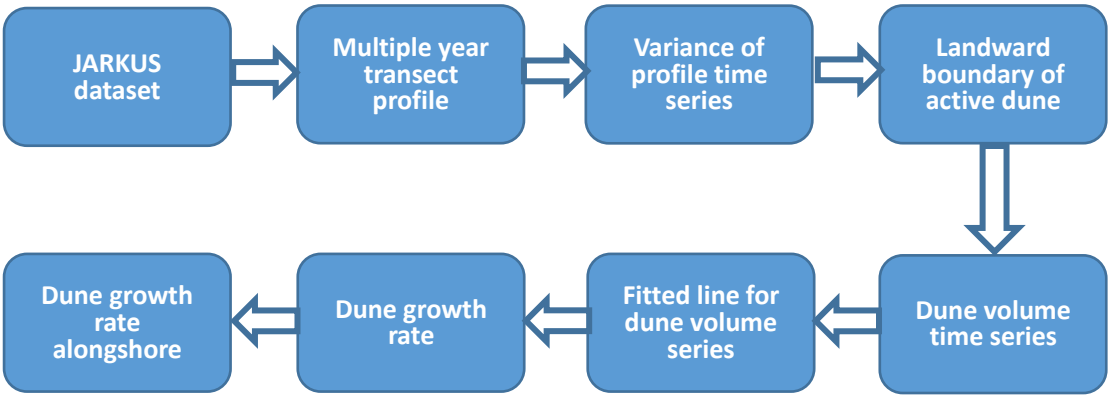

Figure 7. The brief procedure to acquire the dune growth rates from the JARKUS dataset.

2.3.1. Defining active dune and dune volume

This section discusses the definitions of two key factors: active dune and dune volume. With the definitions, the procedure of quantifying the dune behavior will be presented in the next section. No general definition for dune volume really exists, different researchers may use different definitions based on their specific concerns. Here the dune volume has been extracted from the active dune. Because of the aeolian transport and possible storm events, the coastal dune profile is changing over the years. But in the cross shore direction, some sections of the profiles have very large temporal variations though other sections just remain more or less the same over years. Figure 8 (top panel) shows an example of dune evolution for an arbitrary transect (transect id = 8008400). The horizontal axis represents the cross shore coordinate relative to the rsp (rijks strand paal, national beach pole of The Netherlands). The vertical axis in the top panel represents the surface altitude relative to NAP, which is the Dutch vertical datum being widely used in Western Europe. From the figure it could be seen that the section with the cross shore distance around x = 50m has distinctly large temporal variability in the vertical direction. In fact, this section is the active dune being concerned.

The dune volume here has been defined as the volume of sand within the range of active dune: under the dune surface, above the dunefoot level and extended until the landward limit of the active dune. In order to extract the dune volume from the profile time series, the exact boundary of the active dune should be determined. The dunefoot level along the Dutch coast is usually taken as +3 NAP (Ruessink and Jeuken, 2002). So the intersection point of the profiles and the dunefoot level has been set as the seaward boundary of the active dune.

The landward boundary of the active dune is determined based on a multiple year profile time series. The location where the profile time series showing negligible temporal variability in vertical direction has been taken as the landward boundary of the active dune. Therefore the variance of the multiple year profile time series along the cross shore direction has been calculated for each transect. Figure 8 (bottom panel) shows the resultant variance of the corresponding profile time series (transect id = 8008400). This variance value represents the vertical variability of the time series. The location of the negligible variance (the point with the orange asterisk marker) has been taken as the landward boundary. Therefore the dune volume has been taken as the volume enclosed by the dune surface, the dunefoot level and the seaward and landward boundary of the

active dune (indicated by the gray area in the top panel of Figure 8).

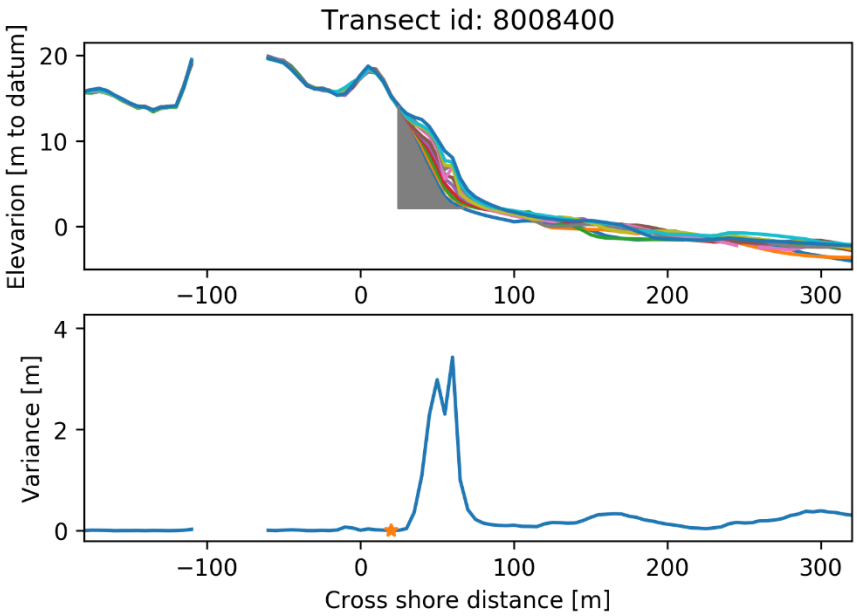

Figure 8. Example dune evolution in the top panel and the corresponding variance in the bottom panel (transect id = 8008400). The active dune volume is calculated from the gray area in the top panel. The orange asterisk marker indicates the landward boundary of the active dune. The horizontal axis represents the cross shore coordinate relative to the rsp (rijks strand paal). The vertical axis in the top panel represents the surface altitude relative to NAP.

2.3.2. Quantifying dune behavior

Dune volume and dune growth rates will be used to analyze quantitatively the dune behavior and the spatio-temporal variations in dune behavior. After defining the active dune and dune volume in section 2.3.1, absolute dune volumes and dune growth rates can be calculated. Here in this section, the procedure of quantifying the dune behavior based on a series of parameters derived from the JARKUS dataset is presented.

Firstly, the data such as cross shore coordinates, alongshore identifiers of transects (transect id) and surface altitude were extracted from the JARKUS dataset. Here for this thesis, the period is from the year of 2006 to 2016 and the locations are the entire Rijnland coast and Ameland coast (the north coast). The raw data needs some pre-process: after filtering out the data points with the unrealistic 'Fill Value', the remaining data points have been interpolated. Because only the coastal dune area is considered by the study, all the data points with surface altitude above +20m NAP and below -15m NAP have not been taken into account and been removed.

With the pre-processed data points, one transect profile can be obtained for each year and each alongshore location. So a multiple year profile time series has been plotted for each location (see Figure 8 top panel for an example). Then the variance of the profile time series which represents the vertical variability has been calculated for each location (see Figure 8 lower panel for an example). For every profile, the point with negligible variance in the landward direction has been

used to define the dune volume, which has already been discussed above in section 2.3.1.

Then based on the definitions in section 2.3.1, the dune volume values for each year and each location have been obtained. So dune volume time series for each location can be obtained (see Figure 9 for an example). The blue dots in the figure represents the calculated dune volumes for each year. A positive linear trend for the dune volumes can be recognized in the figure. Because of the absolute dune volumes being sensitive to the position of the landward limit, the dune volume changes between different years ($DVC = DV_t - DV_{t-1}$) have been considered.

After removing the points with infinite dune volume value, a regression analysis has been done for each transect. In the dune volume time series figure for a particular location, for example Figure 9, dune volumes are plotted against time. So the dune volume change between two adjacent points divided by time interval ($(DV_t - DV_{t-1})/\Delta t$) has been taken as the dune volume change gradient, i.e. the dune growth rate. The regression analysis is to find a straight fitted line for the dune volume series with least root mean square error (RMSE), see the red line in Figure 9. So the slope of this fitted line is the dune growth rate for the specific location. Finally the dune volume time series has been calculated for the entire Ameland coast and Rijnland coast, generating dune growth rates for all the locations. And the results of the dune growth rate have been plotted alongshore, which will be shown and discussed in detail in chapter 3 which presenting the results of data analysis.

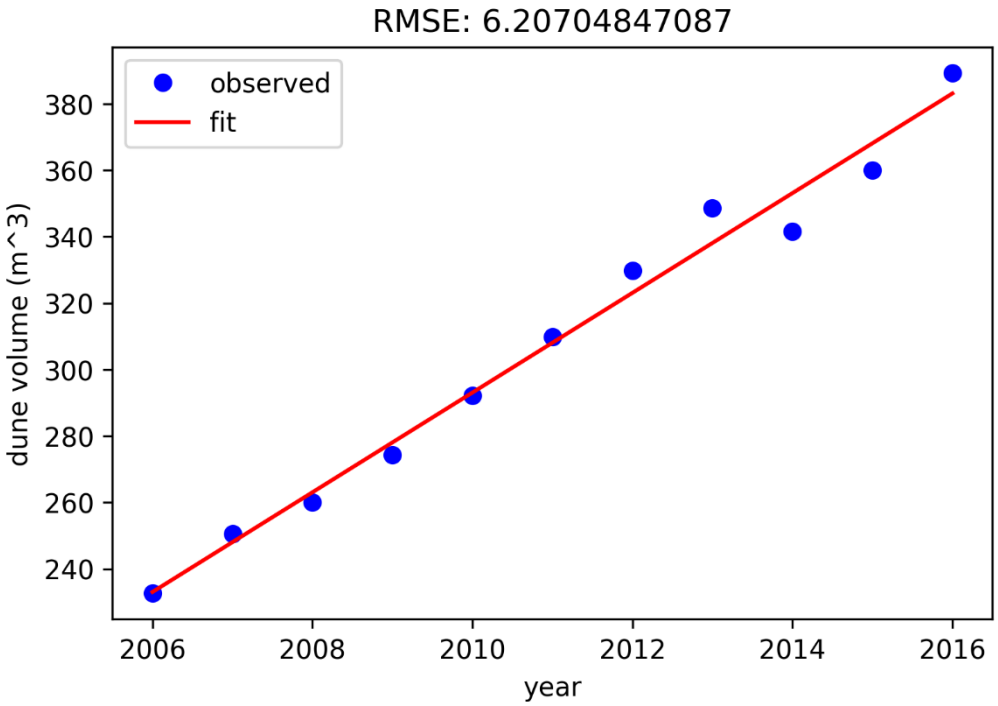

Figure 9. Example of dune volume time series (transect id = 8008400). The blue dots in the figure represents the calculated dune volumes for each year. The red line is the fitted line for the dune volume time series based on the regression analysis, where the slope of the line is the dune growth rate.

3. Results data analysis

In this chapter, the results of data analysis after applying the methods described in chapter 2 will be discussed. The resultant spatial variability in dune behavior is analyzed and correlated to the coastal features like coastal orientations and coastal morphology. Firstly the results of the calculation of wind transport capacity for the two concerned locations are shown and the influence of coastal orientation on the results are discussed. Then the calculated alongshore dune growth rates for the two concerned locations are presented and again the different coastal orientations are used to explain the difference in the dune growth rates between the two locations. The calculated wind transport capacity is then compared to the actual dune growth rate, which indicates the importance of sediment supply to the aeolian system. Then the alongshore morphologic variability existing in the coastal system is discussed. Finally the relationship between beach width, active dune width and dune growth rate is analyzed.

The questions which will be answered in this chapter are research questions two and three:

What are the theoretical aeolian transport capacity and the dune growth rates along the Dutch coast under different coastal orientations and how do they compare with each other?

How do the spatial variations existing in coastal morphology correlate to the alongshore varying dune behavior?

3.1. Theoretical wind transport capacity

According to the method discussed in chapter 2, the total wind transport capacity (or cumulative theoretical sediment transport volume) has been calculated for the Ameland coast and the Rijnland coast respectively. The period concerned is between January 1, 2006 and December 31, 2016. Here the calculated results for the transport capacity are discussed. The possible explanation for the results based on the influence of coastal orientations is discussed as well.

3.1.1. Results of wind transport capacity

In the alongshore direction, the calculated cumulative theoretical sediment transport volume for the Ameland coast is $Q_{as,Ameland} = 57000m^3$, while the one for Rijnland is $Q_{as,Rijnland} = 73000m^3$. As for in the cross shore direction, there are two results for both Ameland and Rijnland which based on two different definition stated in section 2.2.3. Based on the first definition which neglects all the offshore winds, the cumulative wind transport capacity calculated for Ameland is $Q_{cs,Ameland} = 2050000m^3$ while the one for Rijnland is $Q_{cs,Rijnland} = 11077000m^3$. Based on the second definition which considers both the onshore and offshore winds, the calculated cumulative wind transport capacity for Ameland is $Q_{cs,Ameland} = -11138000m^3$ while the one for Rijnland is $Q_{cs,Rijnland} = 4858000m^3$.

The values above are total transport capacity for the entire period and the entire domain. To make

it convenient to compare, the values have been converted into transport capacity per year per running meter. The periods for the two locations are the same: 11 years. The cross shore span, the average beach width, used for Rijnland is about 88m. The average beach width of Ameland is about 115m. Then the total wind transport capacity in the alongshore direction per year per running meter for Ameland is $q_{as,Ameland} = 45.1 m^3/yr\ /m$, while the one for Rijnland is $q_{as,Rijnland} = 75.4\, m^3/yr\ /m$. Therefore the values of the alongshore wind transport capacity for the locations are in the same order of magnitude, though the value for Rijnland is relatively larger. Maybe the prevailing wind from the southwest is more beneficial to the alongshore transport for Rijnland than Ameland, because of the different coastal orientations of the two locations.

For the wind transport capacity in the cross shore direction, two definitions are applied. First the results based on the first definition which neglects all the offshore winds are discussed. In other words, the results are the onshore component of the cross shore wind transport capacity. Similarly to the alongshore transport capacity, the values for the cross shore transport capacity are also converted into "per year per running meter". As stated in section 2.2.2, the alongshore span of the domain for the Ameland coast is $24160\mathrm{m}$; while for the Rijnland coast is $41000\mathrm{m}$. And the period of calculation is 11 years. If taking the period and the alongshore span of the domain into consideration, the wind transport capacity in the cross shore direction per year per running meter without considering the offshore winds can be calculated. So this value for Ameland is $q_{cs,Ameland} = 7.7 m^3/yr\ /m$; while for Rijnland is $q_{cs,Rijnland} = 24.6 m^3/yr\ /m$. It is found that as for the wind transport capacity in the onshore direction per year per running meter, the value for Rijnland is more than three times as large as the value for Ameland. Note that the cross shore transport capacity without considering the offshore winds represents the potential onshore transport capacity on the beach which blows sediment towards the dune. The results of calculated wind transport capacity per year per meter in both alongshore and cross shore directions are summarized in Table 1.

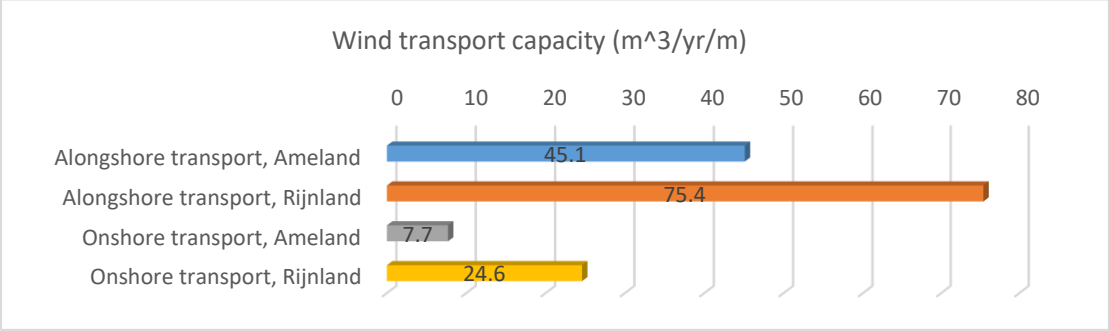

Table 1. Summary of the calculated wind transport capacity per year per running meter. Note that here the onshore transport represent the cross shore transport capacity without considering the offshore winds, i.e. the onshore component of the cross shore transport capacity.

According to the second definition which considers both the onshore and offshore winds, the net transport capacity in the cross shore direction has been calculated for the two locations. Based on the results, whether the cumulative transport capacity in cross shore direction is onshore or offshore can be discerned. The negative value for Ameland, $Q_{cs,Ameland} = -11138000 m^3$, indicates that the cumulative wind transport capacity is offshore which tends to transport sediment towards the sea. The positive value for Rijnland, $Q_{cs,Rijnland} = 4858000 m^3$, indicates

that the cumulative wind transport capacity is onshore which tends to transport sediment towards the dune. Because the values of cross shore transport capacity based on the second definition are only used to indicate whether the cumulative transport is onshore or offshore, they are not converted into “per year per running meter” and not listed in Table 1.

3.1.2. Influence of coastal orientation on wind transport capacity

The coastal orientations are considered as the normal directions of the concerned coastlines, which could be one of the possible explanations for the difference in wind transport capacity between the two concerned locations. As discussed in section 2.2.2., the coastal orientations for the Ameland coast and the Rijnland coast are quite different: $\theta_c = 360°$ for Ameland while $\theta_c = 312°$ for Rijnland (see Figure 6 for reference). Most of the large wind components are from the quarter between western and southern directions, especially from the southwest direction, see Figure 4. Therefore the dominant winds are considered onshore for Rijnland but offshore for Ameland.

In the section 3.3.1 the results of the cross shore wind transport capacity which considers both the onshore and offshore winds have been shown: $Q_{cs,Ameland} = -11138000m^3$ for Ameland and $Q_{cs,Rijnland} = 4858000m^3$ for Rijnland. These two values indicate that the net wind transport capacity in the cross shore direction is offshore for Ameland but onshore for Rijnland. That can be explained by the different costal orientations between the two places. For Rijnland with the coastal orientation $\theta_c = 312°$, the dominant winds from the west to the southwest are considered as onshore winds, which is beneficial to the onshore sediment transport and dune growth. But for Ameland with $\theta_c = 360°$, the dominant winds are considered offshore, leading to the cumulative cross shore wind transport capacity being offshore.

As for the resultant cross shore transport capacity when only considering the onshore winds, the value of the onshore wind transport capacity per year per running meter for Rijnland is more than three times as large as the value for Ameland: for Ameland $q_{cs,Ameland} = 7.7m^3/yr\ /m$ while for Rijnland $q_{cs,Rijnland} = 24.6m^3/yr\ /m$. This could also be explained by the different coastal orientations between the two places. The dominant winds are considered onshore for Rijnland but offshore for Ameland. More onshore wind is more favorable to onshore aeolian transport than offshore wind. Theoretically, more sediment could be transported towards the dune. Therefore the different coastal orientations can be a possible reason why the unit onshore wind transport capacity for Rijnland is more than three times as large as the one for Ameland. In a word, the coastal orientations can have significant influences on the theoretical wind transport capacity.

3.2. Dune volume and dune growth rate

The results of wind transport capacity shown before are the theoretical transport capacity for the two coasts, rather than the actual aeolian transport that the two coasts really experienced. In most cases, the actual transport cannot reach the value of theoretical transport capacity, because of limiting factors like limited sediment availability. The influences of sediment availability on aeolian transport which has been explored by modelling study will be discussed in latter chapter. Here in

this section, the results of dune volume and dune growth rate based on the methods of data analysis presented in chapter 2 are discussed and the influences of coastal orientations on the dune growth rates are explored.

3.2.1. Results of dune volume and dune growth rate on the Ameland coast

The dune volume values have been calculated for all transect locations of the entire Ameland coast for the period between 2006 and 2016, using the methods mentioned in chapter 2. From the slope of the fitted line of the dune volume time series, the dune growth rates for all transect locations have been obtained and plotted alongshore, shown in Figure 10. The vertical axis represents the dune growth rate value with the unit of "cubic meter per year per running meter $(\mathrm{m}^3/\mathrm{yr}/\mathrm{m})$", while the horizontal axis represents the alongshore identifier of transect (transect id) which corresponds to the alongshore coordinate. The second horizontal axis on the top represents the alongshore distance of the coast. The locations with the small id (left side of the figure) are in the west part of the Ameland coast, while the large values of id (right side of the figure) represent the east part of the coast. And the positive values on the vertical axis represent dune accretion while negative values for dune erosion.

From the result figure a relatively large spatial variation alongshore for the dune growth rate can be recognized from the west to the east for the Ameland coast. The result shows several peaks in the domain for the dune growth rate, while for most locations the dune growth rate values remain very small. As for the peaks, for example at around id = 3000200 and id = 3001150, the dune growth rates can reach the order of 20 $\mathrm{m}^3/\mathrm{yr}/\mathrm{m}$. For the location with the id from 3000750 to 3001100, the dune growth rate values are less than 10 $\mathrm{m}^3/\mathrm{yr}/\mathrm{m}$. The section between id = 3000400 and id = 3000700 even has more or less dune volume balance. The dunes located near id = 3000300 experiences serious erosion with more than 20 $\mathrm{m}^3/\mathrm{yr}/\mathrm{m}$. Generally speaking, the Ameland coast experienced a trend of dune accretion for the period from 2006 to 2016. However, this trend of dune growth was relatively weak.

3.2.2. Results of dune volume and dune growth rate on the Rijnland coast

Similar to the Ameland coast, the dune volume values and dune growth rates have also been calculated for all transect locations for the entire Rijnland coast. The results of the dune growth rates along the Rijnland coast during the period from 2006 to 2016 are shown in Figure 11. The vertical axis is the dune growth rate in $[\mathrm{m}^3/\mathrm{yr}/\mathrm{m}]$. Positive values represent dune accretion while negative values stand for dune erosion. The horizontal axis is the alongshore identifier of transect (transect id). The second horizontal axis on the top represents the alongshore distance of the coast. The locations with small id (left side of the figure) are in the north side of the Rijnland coast, while large id (right side of the figure) represent the south part of the coast.

From the figure it is found that the dune growth rate of Rijnland also has large spatial variation. Most locations in the domain experience dune accretion or volume balance and dune erosion seldom happens. The values of dune growth rate have three peaks in the domain which have very large dune accretion, around id = 8005850, id = 8008150 and id = 8008700. At these peaks, the dune growth rates can reach the values of 40 or even 60 $\mathrm{m}^3/\mathrm{yr}/\mathrm{m}$. The section between id =

8006300 and id = 8006700 has dune growth rate values more or less close to zero. Other part which experiencing dune accretion generally has the dune growth rates in the order of about 10 $\mathrm{m}^3/\mathrm{yr}/\mathrm{m}$. Generally speaking, during the period from 2006 to 2016, the condition for Rijnland was favorable to dune growth and most part of the region indeed experienced dune accretion.

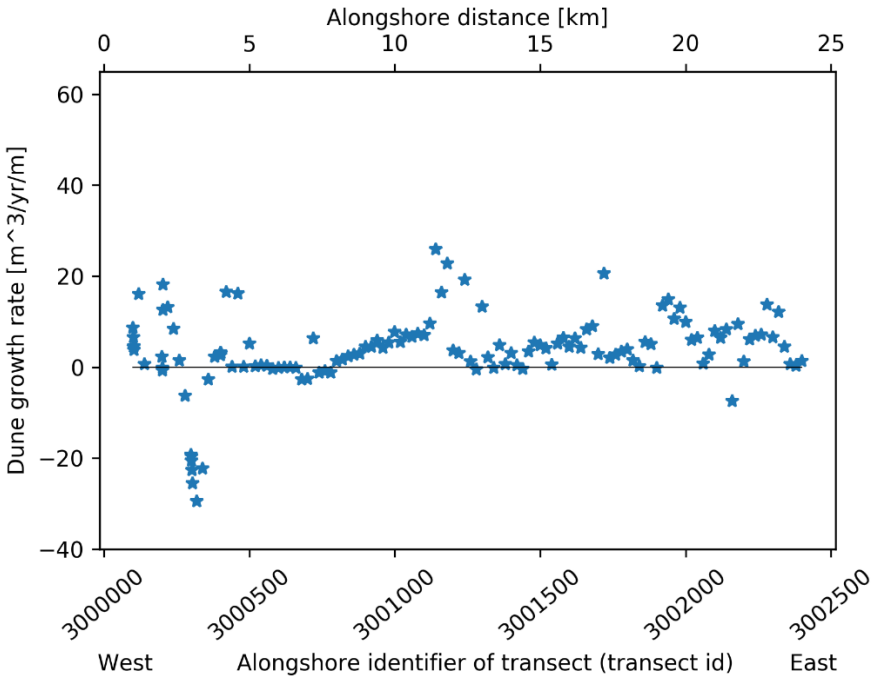

Figure 10. Dune growth rates along the Ameland coast. Positive values of dune growth rate represent dune accretion while negative values represent dune erosion. The transect id on the bottom horizontal axis represents the alongshore location, which corresponds to the alongshore distance on the top axis.

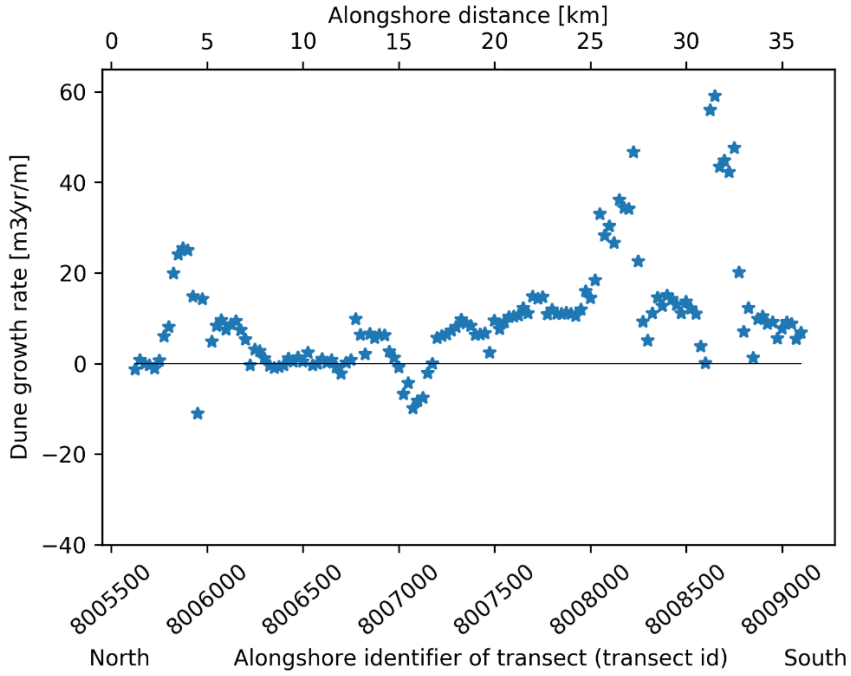

Figure 11. Dune growth rates along the Rijnland coast. Positive values of dune growth rate represent dune accretion while negative values represent dun erosion. The transect id on the bottom horizontal axis represents the alongshore location, which corresponds to the alongshore distance on the top axis.

3.2.3. Influence of coastal orientation on dune growth rates

From the results shown above, it is found that the alongshore distributions of the actual dune growth rates derived from the measurements for Ameland and Rijnland are quite different. By comparing the results shown in Figure 10 and Figure 11, it is found that for the peak values of dune accretion, Rijnland have much larger values than Ameland. As for the other locations not belonging to the peaks, the Ameland coast usually has the dune accretion values around 5 m^3/yr/m, while Rijnland has values around 10 m^3/yr/m. The derived dune growth rates are the net results combining both dune accretion and intermittent dune erosion. After checking the dune volume time series for both Rijnland and Ameland, it is found that for most of the transects which experienced dune accretion, no significant erosion in the time series was discerned in the concerned period. Considering the low probability of very large erosion events in the concerned period, it is inferred that generally the condition for Rijnland is more favorable to onshore aeolian transport than for Ameland, resulting in more dune accretion for the Rijnland coast.

The coastal orientations could play a role in explaining the different dune growth rate patterns between Ameland and Rijnland. With the coastal orientation approximately towards the northwest with the angle $\theta_c = 312°$, the dominant wind from the third quarter is considered onshore for the Rijnland coast. But for Ameland with the coastal orientation towards the north with $\theta_c = 360°$, most winds are considered offshore. Onshore wind can entrain sediment in the intertidal zone and transport it towards the land, resulting in dune accretion, while offshore is considered having no obvious contribution to dune growth. With onshore winds blowing frequently, sediment is transported onshore to build the dunes persistently on the Rijnland coast. Therefore Rijnland has larger values of dune growth and annual dune erosion seldom happens there. For Ameland which is offshore wind dominated, the onshore wind component which builds the dunes is smaller, resulting in smaller values of dune growth rate.

3.3. Relationship between wind transport capacity and measured dune growth rate

In section 3.1, the result of the onshore wind transport capacity per year per running meter has been shown, which is the theoretical sediment transport volume that wind could transport. The results of dune growth rate for the two locations discussed in section 3.2 are the actual dune accretion (or erosion) volumes derived from the measurements. These dune growth rate values can also be considered as “volumes per year per running meter” because they are yearly average volumes based on regression analysis and for transects with unit width. Therefore, to some extent the wind transport capacity section 3.1 and the dune growth rate in section 3.2 can be compared with each other.

The onshore wind transport capacity per year per running meter is $7.71\mathrm{m}^3/\mathrm{yr}/\mathrm{m}$ for the Ameland coast while $24.56\mathrm{m}^3/\mathrm{yr}/\mathrm{m}$ for Rijnland. However, for both Ameland and Rijnland, most locations in the domain have the dune accretion volumes much less than the theoretical capacity, see Figure 10 and Figure 11. In other words, generally the actual dune accretion cannot

reach the sediment volume that wind can transport onshore theoretically.

One of the possible reasons for such kind of inconsistency between capability and reality can be the appearance of intermittent erosion. During the concerned period from 2006 to 2016, some erosion events could have happened. The high water levels during the erosion events may reach the dunefoot levels and get the dunes eroded, leading to the dune accretion volumes being less than the theoretical transport capacity. Another important factor accounting for the inconsistency is the limited sediment availability. In the aeolian system with limited sediment availability, the sediment available for transport is less than the transport capacity of the present wind. Even the wind appears to be very strong, the actual sediment transport and resultant dune growth are restrained by the limited available sand.

For both the onshore wind transport capacity and the actual dune growth rate, Rijnland got higher values than Ameland. This can be explained by the different coastal orientations between the two coasts, as stated in sections 3.1.2 and 3.2.3. However, the transport capacity and the dune growth rate are affected by the coastal orientations to different extents. The unit onshore transport capacity for Rijnland is more than three times as large as the value for Ameland. But the actual dune growth rates for most locations along the Rijnland coast are no more than two times as large as the values for the Ameland coast. Such difference in the extents of the influence of coastal orientation may also due to the limited sediment supply.

Therefore the inconsistency between the theoretical wind transport capacity and the actual dune growth rate shows the importance of the sediment availability for assessing and understanding the dune behavior. It inspired an attempt to explore the roles of sediment supply and sediment availability in the aeolian system by conducting a modeling study, which will be the second part of the thesis.

3.4. Alongshore morphologic variability in the coastal beach-dune system

To understand the coastal beach-dune system better, here the spatial variability of coastal morphology along the Rijnland coast in the period between the year of 2006 and 2016 will be discussed. Figure 12 show the measured locations of waterline, dunefoot and landward boundary of the active dune. The results are the averaged location over the concerned period. From the figure it can be recognized that in the section between id=8005500 and id=8006000, the waterline and the entire beach-dune system significantly protrude into the sea. The difference of the positions in cross shore direction between this protruding region and the adjacent region (from id=8006000 to the right hand side in Figure 12) can be hundreds or even more than one thousand meters. The reason for the significant protrusion of the entire coastal system may be the existence of the groyne of the North Sea Canal located in the north of the Rijnland coast. The alongshore sediment transport is blocked by the groyne. A large amount of sediment has been deposited next to the groyne and created a very wide beach area, forcing the beaches and dunes moving seaward.

Since it is not handy to analyze the region from id = 8006000 to the right from Figure 12 (left panel), a zoom-in figure has been plotted for the cross shore distance between -200m and 300m, see

Figure 12 (right panel). From the figure it's found that the alongshore variabilities of the measured locations in this region are actually not small. The waterline protrudes into the sea in several locations. For other locations the waterline are concave and setting back landward. Note that usually the dunefoot and landward dune boundary have the same trend with the waterline, which means they follow the waterline to protrude seaward or concave backward at same locations. In the following two sections, the results of the width of beach and the width of active dune will be shown separately and analyzed in more detail.

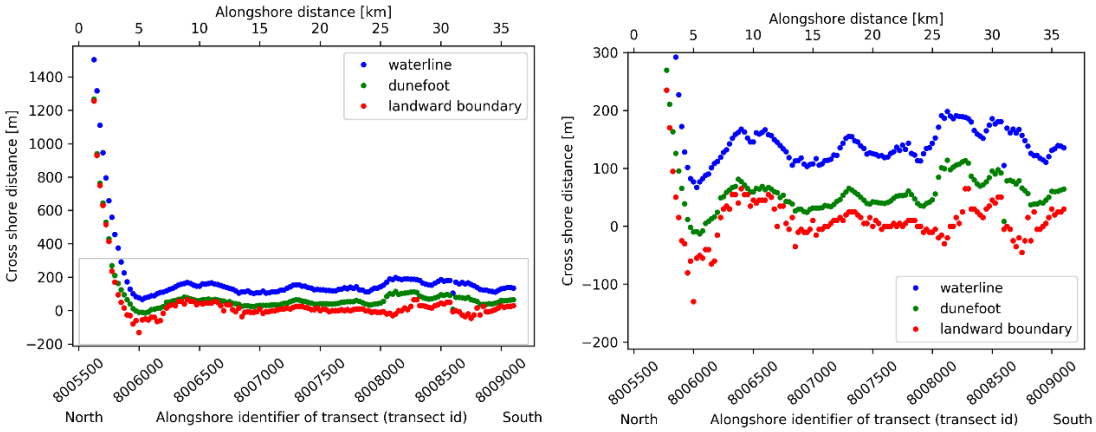

Figure 12. Measured locations of waterline, dunefoot and landward boundary of the active dune along Rijnland. Right panel is the enlarged view of the left panel for the area specified by the square. The results are the average over the concerned period from 2006 to 2016. The vertical axis represents the cross shore coordinate relative to the rsp (rijks strand paal).

3.4.1. Alongshore morphologic variability of the beach width

Beach width is defined as the cross shore distance between waterline and dunefoot. The locations where the waterline protrudes much into the sea does not necessarily also have very wide beach, because the dunefoot may follow the waterline to protrude seaward at the same locations. Here the beach width alongshore is extracted from Figure 12 and analyzed separately. Figure 13 shows the values of derived beach width along the Rijnland coast. The results are the average over the concerned period. Compare to the measured locations of the waterline and dunefoot in cross shore direction shown in Figure 12, the beach width values have much smaller order of magnitude. In the region between id=8005500 and id=8006000, the waterline protruded into the sea for more than 1000m, but the beach width was only hundreds of meters. That's because not only the waterline is located more seaward, but also the dunefoot is located more seaward. In other words, the entire beach-dune system is located more seaward.

Since it is not handy to analyze the part from the id = 8006000 to the right from Figure 13 (left panel), a zoom-in view of the beach width alongshore in the range from 50m to 120m is shown in Figure 13 (right panel). It is recognized that for the region from id=8006000 towards the south (to the right in Figure 13), the beach width shows some alongshore variations. The average beach width in this region is between 80m to 90m. The difference between two beach width values can be more than 20m, which accounts for more than 20% of the average width. Although having large spatial variability, the beach width values in this region just oscillate around the average width value and no prominent trend can be derived merely based on this plot.

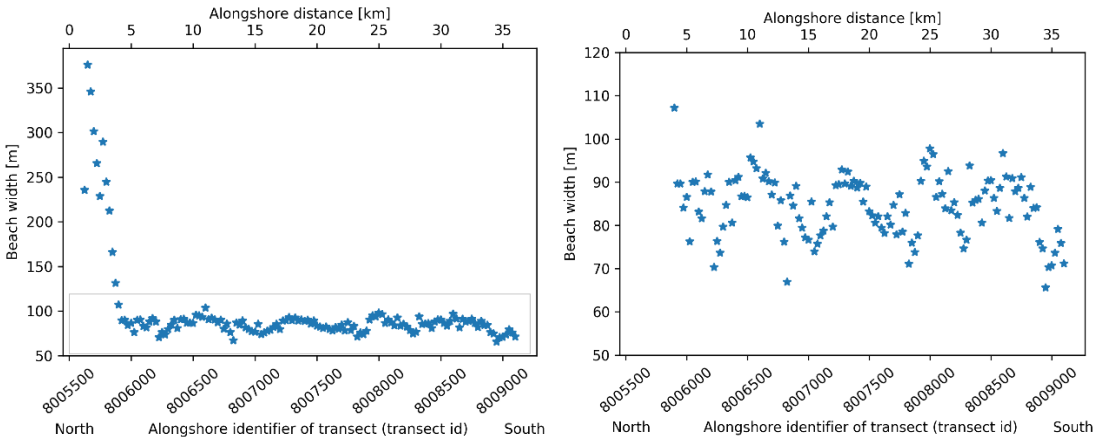

Figure 13. Beach width along Rijnland. Right panel is the enlarged view for the area specified by the square in the left panel. The results are averaged over the concerned period from 2006 to 2016.

3.4.2. Alongshore morphologic variability of the width of active dune

As stated previously in chapter 2, the active dune is a part of the dune where the corresponding multiple year profile series showing large temporal variability. Therefore the width of active dune is the distance in cross shore direction between the dunefoot and the landward active dune boundary (see Figure 12 for reference). The calculated values for the width of active dune have been plotted along the Rijnland coast, see Figure 14. The results are averaged over the concerned period. Here, the results are quite different compared to the measured locations and the beach width shown in Figure 12 and Figure 13. At the north end of the domain (left end of Figure 14), active dunes are not wide at all though the beaches there are very wide. Along the Rijnland coast, the width of active dune shows a large spatial variability. There are three peaks which have very wide active dunes, around id = 8005900, id = 8008150 and id = 8008700. And the width values there could reach the order of 100m or more. If disregarding the three peaks, the width values of active dune for the rest locations vary dynamically from 10m to 50m. And generally the south half of the Rijnland coast (disregarding the peaks) has wider active dunes, with the width values around 40m, than the north part which is about 20m wide.

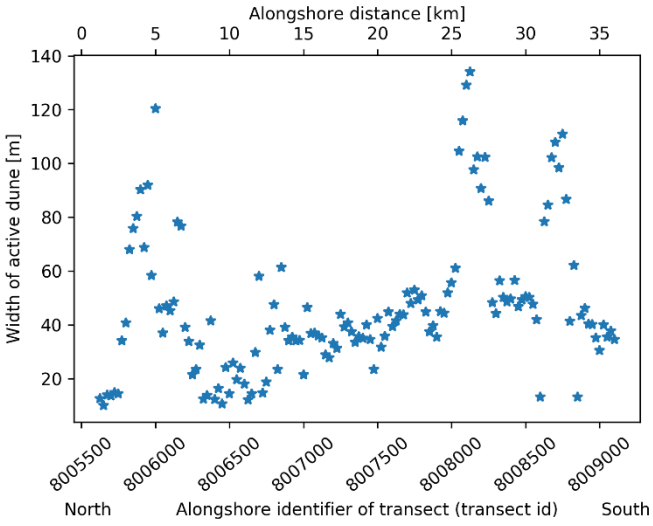

Figure 14. Width of active dune along the Rijnland coast. The results are the average over the concerned period from 2006 to 2016.

3.5. Relationship between beach width, active dune width and dune growth rate

Based on the obtained alongshore distribution of dune growth rate, beach width and active dune width along Rijnland (shown in Figure11, Figure 13 and Figure 14), the relation between them has been analyzed. Two more figures are provided with linear regression analysis, showing the possible correlations between the concerned three parameters. As stated before, the dune growth rate, beach width and active dune width are averaged over the concerned period (from 2006 to 2016).

3.5.1. Relationship between width of active dune and dune growth rate

First the dune growth rate alongshore in Figure 11 and the width of active dune alongshore in Figure 14 are compared. From these two figures, it can be recognized that the dune growth rate and the active dune width seems have some sort of correlation. In both plots, three peaks can be discerned at the same locations: around id = 8005900, id = 8008150 and id = 8008700. Within these peak region, the dunes have very large active dune width as well as very high dune accretion values. Other locations which are not within the peaks also show similar trends in both figures: generally the south part of the coast (right side in figures) has wider active dunes and bears more dune accretion than the north part.

To further explore the relation between the active dune width and the dune growth rate, the dune growth rate is plotted against the width of active dune in Figure 15. The red line is the fitted line of the scatters based on the least squares linear regression. A positive correlation can be identified between the dune growth rate and the active dune width. The coefficient of determination (R^2) of 0.354 for the line fit also indicates the correlation is discernible. Therefore it can be concluded that the dune growth rate is correlated to the width of active dune: a larger dune accretion is usually linked to a wider active dune. One of the possible reasons for this correlation is that much of the sediment transported onshore is deposited on the front dune slope, from the dunefoot to the top of dune. The entire front dune slope moves seaward as the onshore wind transport continues. Therefore the active dunes become wider as more grains are transported and deposit on them.

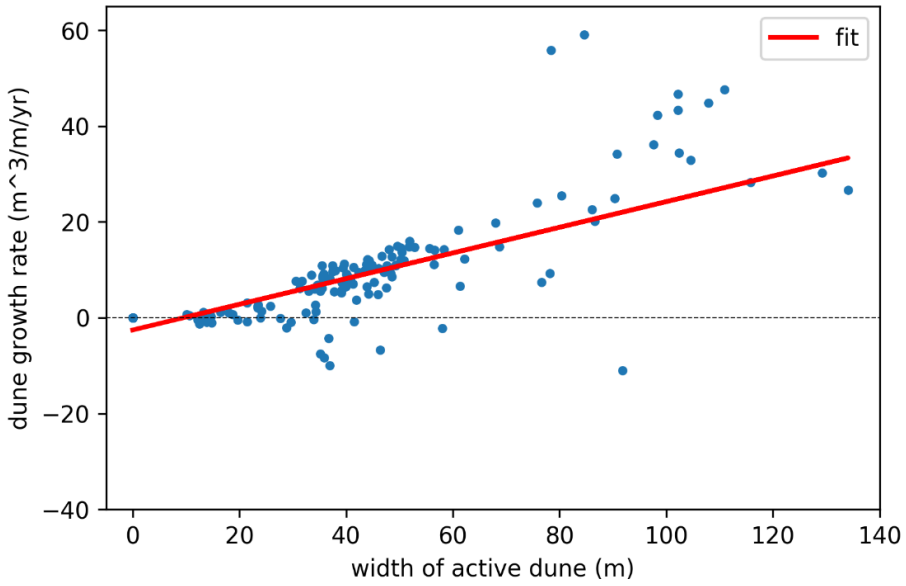

Figure 15. Correlation between width of active dune and dune growth rate along Rijnland. The red line is the fitted line which represents the least squares linear regression. The coefficient of determination (R^2) equals 0.354.

3.5.2. Relationship between beach width and dune growth rate

Here the alongshore distribution of the dune growth rates for Rijnland is compared with the alongshore distribution of the beach width to explore the influence of the beach width. In Figure 13, which shows the alongshore distribution of the beach width, the north region between id = 8005500 and id = 8006000 has considerably wide beach with the width of hundreds of meters. Intuitively it is expected that wider beaches may provide more sediment and longer fetch for aeolian transport, resulting in more dune accretion and wider active dunes. However, this has not been reflected in the results of dune growth rate and active dune width at all (see Figure 11 and Figure 14). Oppositely, the active dunes at the north part are relatively narrow (less than 20m), and the dune growth rates there even reach zero. From the location with id = 8006000 to the south (to the right in Figure 13), the beach width values vary around 85m but have no evident peak, while the dune growth rates and the active dune width values both have two obvious peaks with very large values around id = 8008150 and id = 8008700.

To further demonstrate the relation between the beach width and the dune growth rate, the calculated dune growth rate is plotted against the beach width in Figure 16. Note that in this figure the width values larger than 110m are filtered out to make the result more generic. Again the red line represents the least squares linear regression. The slope of the fitted line almost approaches 0. The corresponding coefficient of determination (R^2) of 0.008, which is much smaller than the R^2 for Figure 15, also indicates here the correlation is trivial. A wider beach does not necessarily have a large dune accretion (or dune erosion). Therefore it is concluded that no necessary association can be distinguished between the beach width and the dune growth rate along the Rijnland coast. This may be explained by sediment sorting and beach armoring. As the onshore aeolian transport continues, the dry beach experiences sediment sorting where fine grains are picked up and transported onshore while nonerodible roughness elements emerge from the bed. Gradually the

dry beach gets armored and does not act as sediment source any more. Only the intertidal area where hydraulic mixing happens can provide available sediment. Therefore no matter how wide the beach is, the sediment availability which mostly depends on the intertidal area remains more or less the same.

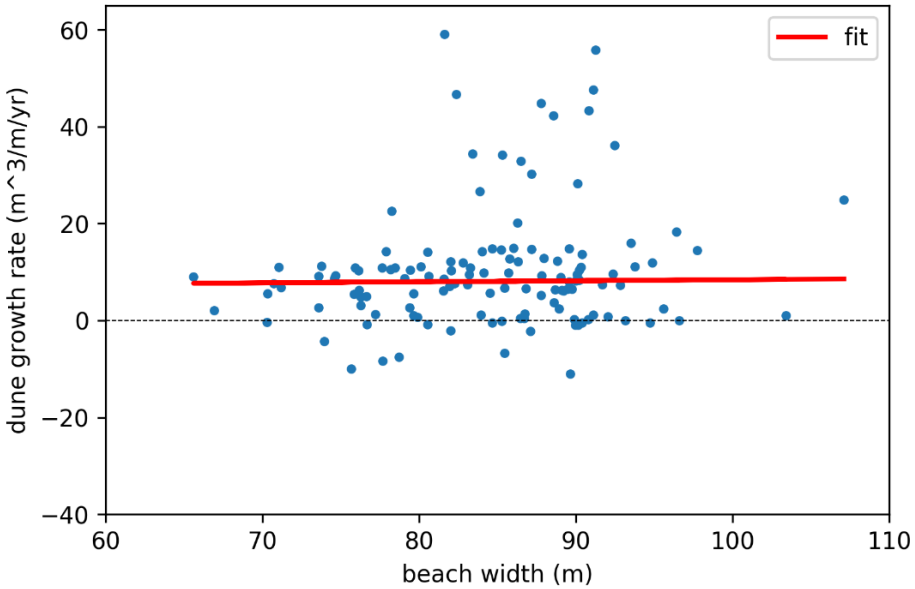

Figure 16. Correlation between beach width and dune growth rate along Rijnland. The red line is the fitted line which represents the least squares linear regression. The coefficient of determination (R^2) equals 0.008.

3.6. Conclusions data analysis

A data analysis has been done for the Rijnland and Ameland coasts under different coastal orientations. Based on the yearly profile measurements from the Dutch JARKUS dataset, a series of parameters has been derived to represent the dune behavior quantitatively.

The theoretical onshore aeolian transport capacity for Rijnland is more than three times larger than the value for Ameland. The measured dune growth rates along the Rijnland coast are generally larger than the ones for Ameland as well. One of the possible reasons for these differences is the different coastal orientations between the two concerned coasts, which introduce more onshore wind and dune accretion to Rijnland than Ameland. For both coast, the measured dune growth rates are smaller than the theoretical onshore wind transport capacity, indicating the potentially important role of sediment supply in the aeolian system.

The derived coastal morphology shows large alongshore variability. When correlating the alongshore morphologic variability to the dune growth rates, the results show that a larger dune accretion is usually linked to a wider active dune, while no necessary association can be distinguished between beach width and dune growth rates.

ii. MODELING STUDY

Part II

MODELING STUDY

4. Methodology modeling study

The inconsistency between the wind transport capacity and the measured dune growth rates revealed in the data analysis inspired an attempt to explore the importance of sediment supply by a modeling study. In this chapter, the method of the modeling study will be discussed, mainly including the model setup and the scenario settings. Some skills used for constructing the model such as the vegetation strategies are also discussed here. The purposes of the modelling study are to evaluate the relationship between aeolian sediment transport and dune behavior, and the role of sediment supply to the aeolian system. Some of the results of previous data analysis are also considered in the constructed model.

The question which will be answered in this chapter is research question four:

How to simulate aeolian sediment transport, dune volume changes and the combined effect of erosive and accretive processes?

4.1. Model description and setup

The AeoLiS model is a process based model which is able to simulate aeolian sediment transport and compute the spatiotemporal varying sediment availability. The model simulates the supply-limitations and bed surface properties rather than parameterizes through the velocity threshold (Hoonhout & de Vries, 2016). The model approach generalizes the existing model concepts such as the shear velocity threshold and critical fetch.

In the aeolian transport processes, the combined effect of erosion and deposition represents the net entrainment of sediment. The net entrainment depends on the balance between the saturated sediment concentration c_{sat} $[\mathrm{kg/m^2}]$ and the instantaneous sediment transport concentration c $[\mathrm{kg/m^2}]$. All the sediment transport is assumed to happen near the bed surface and no vertical dimension is considered in the control volume.

The AeoLiS model computes the equilibrium or saturated sediment transport rate q_{sat} $[\mathrm{kg/m/s}]$ using an empirical sediment transport formulation (e.g. Bagnold 1937):

$$q_{sat} = \alpha C \frac{\rho_a}{g} \sqrt{\frac{d_n}{D_n}} (u_z - u_{th})^3$$

in which u_z $[m/s]$ is the wind velocity at height z $[m]$ and u_{th} $[m/s]$ is the velocity threshold. The properties of the sediment in aeolian transport are represented by a series of parameters: C $[-]$ is an empirical parameter to account for the grain size distribution width, ρ_a $[\mathrm{kg/m^3}]$ is the density of the air, g $[\mathrm{m/s^2}]$ is the gravitational constant, d_n $[m]$ is the nominal grain size, D_n $[m]$ is a reference grain size. α $[-]$ is a constant to account for the conversion of the measured wind velocity to the near-bed shear velocity. The model setup will be described in detail in the following sub-sections.

4.1.1. Model domain and topography

The modelling study chooses transects from the two concerned coasts: the Rijnland coast and the Ameland coast (North coast of the island). For Rijnland, the transect with transect id = 8007350 is chosen. For Ameland, the transect with transect id = 3000900 is chosen. The location of the chosen transects are shown in Google map, see Figure 17. The chosen transects have the shapes that can more or less represent most of the other transects. And the altitude measurements of the chosen transects have no missing points.

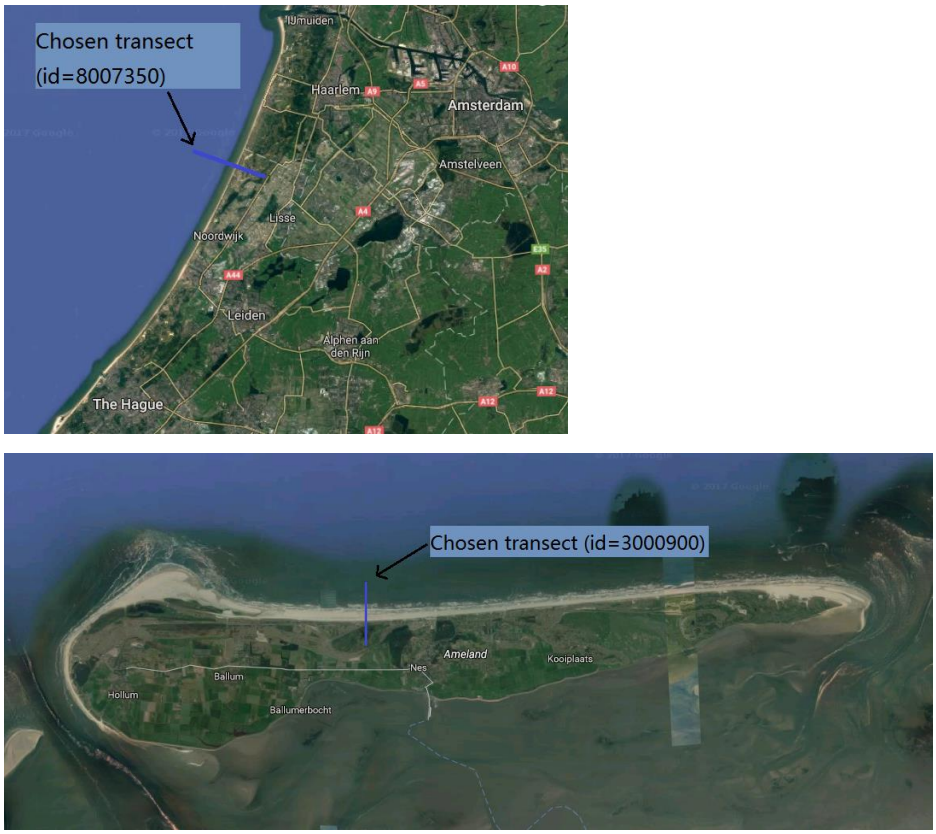

Figure 17. Locations of the chosen transects in Google maps. Top panel shows the location of chosen transect for Rijnland while the bottom panel shows the one for Ameland.

The model is set as two-dimensional (2DV), with the x-axis representing the cross shore direction and the z-axis representing the altitude. All the y coordinates in the alongshore direction are set to zero. The topography of the chosen transects are obtained from the JARKUS dataset using the method stated in chapter 2. The measurements of the year of 2016 are chosen. Here the obtained transect profiles are discrete measurement points in the range from the back of the dune to the beach section below the sea level.

The discrete altitude data is then interpolated to gain a continuous profile. To cope with the x-axis setting of the AeoLiS model, the x-axis of the profiles are adapted to start from seaside with x = 0 on the left towards the land on the right. In the AeoLiS model, sediment cannot be transported over the water surface. So the profile section being permanently underwater is not computed in the model and of less interest. The very back of the dune is of less interest as well because it's no

longer considered as active dune. Therefore only the middle part of the profiles are taken and will be applied in the model as the topography. The model topography is presented in Figure 18 for Rijnland (left panel) and Ameland (right panel).

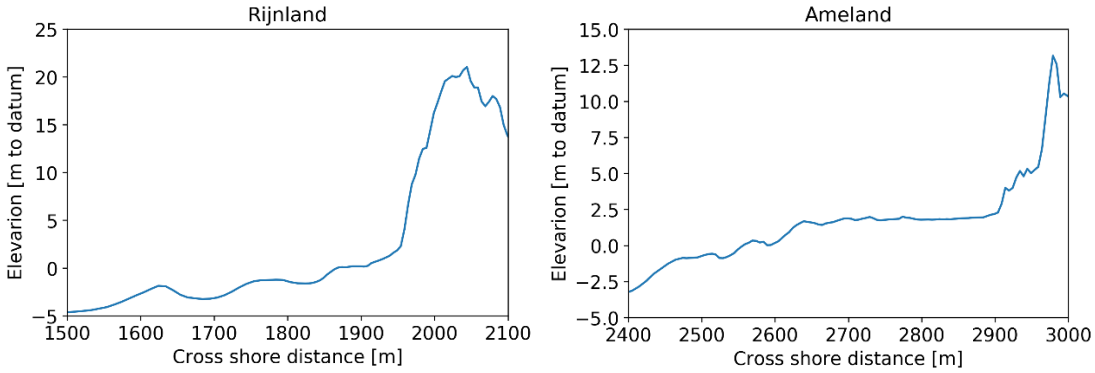

Figure 18. The applied model topography for Rijnland (Left panel) and Ameland (right panel).

4.1.2. Computational grid

The concerned model domain is discretized into a finite number of computational grid cells. Here the object to be discretized is the sand bed which interacts with wind near the bed surface. A finer grid resolution can reproduce the real world more accurately but needs more computational time. So the decision was based on the balance between the computational time and the desired model accuracy.

The AeoLiS model simulates the processes of beach armoring and sediment sorting because the spatiotemporal variations in grain size distributions may vary in both the horizontal and the vertical. Therefore the bed is discretized in both horizontal and vertical directions (2DV). In the horizontal direction, the bed is discretized into grid cell with the length of 1m. In the vertical direction, the bed is divided into 3 bed layers. As one of the possible varying input parameters, the layer thickness in the model has been chosen as 0.05m and 0.10m.

4.1.3. Boundary conditions

The offshore boundary condition for the aeolian transport is defined as a zero-flux boundary, which means that sediment cannot be transported over the water surface. The location of this boundary condition is not fixed. It follows the movement of the water line, which is induced by the tidal forcing. Note that, as stated before, the actual computational domain is not starting from the water line but from somewhere further seaward. The onshore boundary for aeolian transport has a constant transport gradient and the location of this boundary condition is the onshore boundary of the computational domain.

4.1.4. Hydrodynamic and meteorological input

The main hydrodynamic input being considered is the tides. Because of the tides, the intertidal area is flooded periodically. Hydraulic mixing could happen in this region, breaking the beach

armoring and affecting the sediment supply. The tide data is acquired from the local tide stations measured by Rijkswaterstaat, part of the Dutch Ministry of Infrastructure and the Environment. For the Rijnland coast, the station of IJmuiden is chosen, which is the nearest tide station for the concerned transect. For the Ameland Island, the station of Wierumergronden is chosen for the same reason. The data gives tidal level every ten minutes. In order to run one-year simulations, the time span of the tide data is chosen from 1 July, 2016 to 30 June, 2017 for both concerned locations. Figure 19 shows the imposed tide data for Rijnland (top panel) and Ameland (bottom panel).

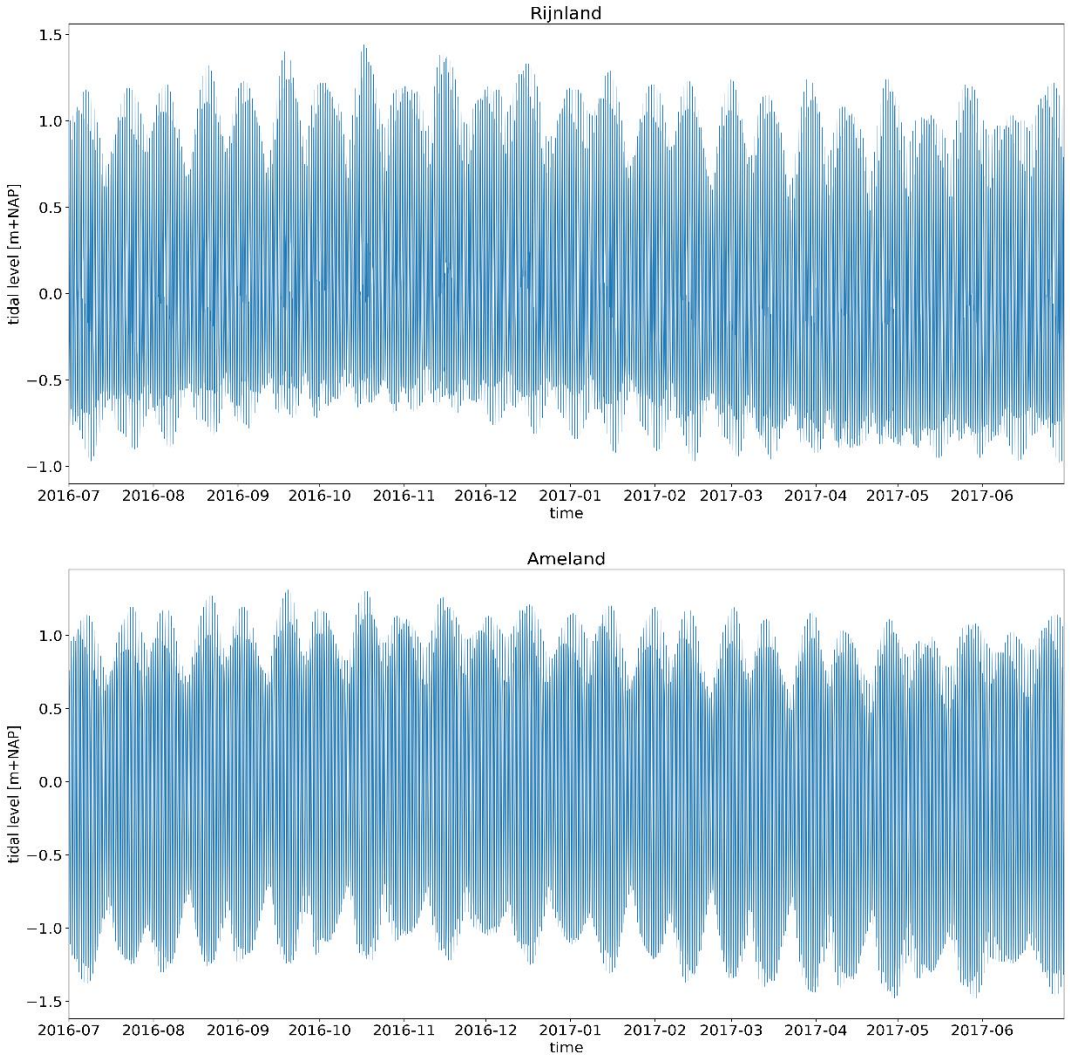

Figure 19. Imposed tide data for Rijnland (top panel) and Ameland (bottom panel)

The meteorological input for the model run is the wind data, including the hourly average wind speed and the corresponding wind direction. For both Rijnland and Ameland, the realistic wind data measured at the nearest stations is used. The Royal Dutch Meteorological Institute (KNMI) records time series of meteorological data in many stations. For Rijnland, the wind station of IJmuiden is used. For the Ameland coast, the wind station of Hoorn (Terschelling) is chosen. The concerned periods of the wind data for both locations are chosen as the same as the tide data, i.e. from 1 July, 2016 to 30 June, 2017.

Figure 20 shows the wind rose and the wind speed time series for Rijnland (top panels) and for Ameland (bottom panels). In the wind roses, colors represent the magnitude of wind speed while the lengths in radial direction represent the frequency of occurrence. Note the two wind roses cannot be compared directly because of the different scales of color legend. From the wind roses it is found that for both Rijnland and Ameland, most of the strong winds come from the west to the southwest. And the wind speed values for Rijnland are larger than the ones for Ameland, see the figures of wind speed time series.

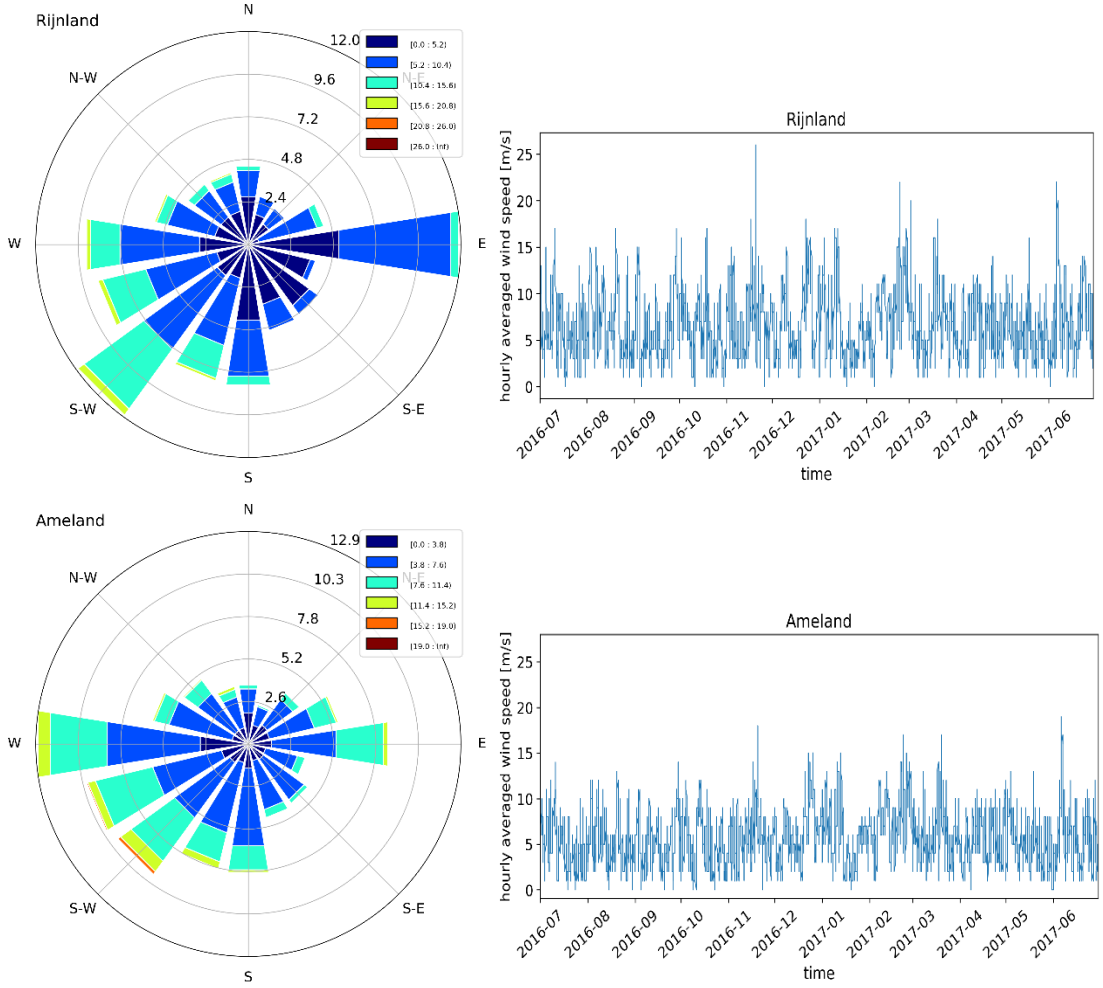

Figure 20. Wind roses and wind speed time series for Rijnland and Ameland. Top panels are for Rijnland; bottom panels are for Ameland.

4.1.5. Sediment fraction settings

As for the sediment fractions, four patterns of settings have been used. Pattern 1 has two grain size fractions (nfractions = 2), 0.0003m and 0.0320m, with the distribution of 95% and 5% respectively. Pattern 2 has only one grain size (nfractions = 1), 0.0003m. Pattern 3 has two grain size fractions (nfractions = 2), 0.0003m and 0.0320m, but the percentage of the finer grains reduces to 85% while the coarser grains account for 15%. These three patterns are chosen for illustrative purpose which allows to explore the influence of beach armoring and nonerodible roughness elements. Pattern 4 has 11 grain size fractions (nfractions = 11), with the grain size and distribution shown in Figure 21. The grain size and distribution of Pattern 4 adopt the sediment fraction settings for the Sand Motor

located on the Delfland coast in The Netherlands (https://github.com/openearth/aeolis-course/tree/master/sandmotor/models/original), considering no available data for the sediment fractions for the Rijnland and Ameland coasts and the relatively close distances between these two coasts and the Sand Motor.

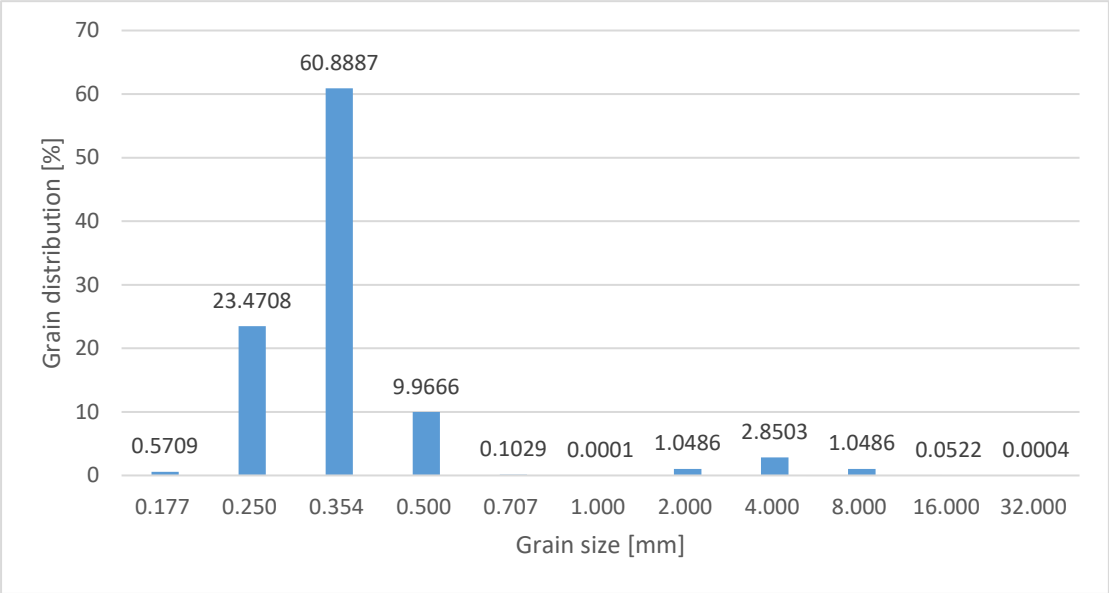

Figure 21. Grain size and grain size distribution of the sediment fraction pattern 4.

4.1.6. Other parameter settings

The total simulation time is set to 1 year (tstop = 31449600.0 seconds), in order to see the long term effect. The choice of time step is a compromise between computational time and desired accuracy. And a time step of 120 seconds is chosen to gain a relatively high temporal resolution. The rest of the parameter settings for the constructed model adopts the default settings (http://aeolis.readthedocs.io/en/latest/defaults.html).

4.2. Model runs

This section discusses 11 scenarios that have been simulated in order to better understand how relevant processes affect the aeolian sediment transport and dune behavior, and what is the role of sediment supply in the aeolian system. The influence of a certain process can be assessed by comparing the model results of several certain scenarios with only the concerned parameter settings being different. Both Rijnland and Ameland have been modelled and all the scenarios have a simulation time span of 1 year. Table 2 gives the description of each scenario. The terms in the table will be explained below. Scenario #1 can be seen as the base scenario. The purpose of each scenario setting and the way of comparing model results (choosing which scenarios to assess which processes) will be illustrated in the next chapter concerning the model results.

In Table 2, six options of model settings have been listed. Every scenario has unique scenario settings. ‘Transect location’ determines which place the chosen transect belongs to. ‘Rijnland’

means that the transect belonging to the Rijnland coast with transect id = 8007350 is chosen and will be used for the model domain and topography. Similarly, 'Ameland' means the transect from the Ameland coast with transect id = 3000900 is chosen. 'Vegetation' indicates whether the vegetation strategies are applied or not. The vegetation strategies will be explained in detail in the following subsection. 'Sediment fraction settings' indicates which sediment fraction pattern is used. The settings of the four sediment fraction patterns have already been described in section 4.1.5. The bed is divided into three bed layers with equal layer thickness. Two values for the layer thickness have been used, 0.05m and 0.10m. As one of the possible influencing factors, the influence of wind speed is explored by applying two kinds of wind speed: 'Normal' wind speed indicates the wind speed values measured by wind stations are used; 'Increased' wind speed means the wind speed values for every measurement point in the time series has been increased with 20% while the directions remains the same. 'Existence of offshore winds' indicates whether the offshore winds exist in the imposed wind input or get filtered out. The adopted method for filtering out the offshore winds will be explained in the later subsection.

	Description of scenarios					
Scenario number	Transect location	Vegetation	Sediment fraction settings	Layer thickness	Wind speed	Existence of offshore winds
#1	Rijnland	Yes	Pattern 1	0.05m	Normal	Yes
#2	Rijnland	No	Pattern 1	0.05m	Normal	Yes
#3	Rijnland	Yes	Pattern 1	0.10m	Normal	Yes
#4	Rijnland	Yes	Pattern 2	0.05m	Normal	Yes
#5	Rijnland	Yes	Pattern 3	0.05m	Normal	Yes
#6	Rijnland	Yes	Pattern 1	0.05m	Normal	No
#7	Rijnland	Yes	Pattern 1	0.05m	Increased	Yes
#8	Rijnland	Yes	Pattern 4	0.05m	Normal	No
#9	Ameland	Yes	Pattern 1	0.05m	Normal	Yes
#10	Ameland	Yes	Pattern 1	0.05m	Normal	No
#11	Ameland	Yes	Pattern 4	0.05m	Normal	No

Table 2. Settings of the model scenarios.

4.2.1. Vegetation strategies

In the dune area in the real world, many kinds of specialized vegetation inhabit and form a natural defense. Vegetation can reduce the local wind shear, therefore lowering the wind transport capacity in the region. Figure 22 shows some photos of dune vegetation on the Rijnland coast. To enable the sediment leave the soil surface and be transported by the wind, the wind shear velocity should exceed a certain threshold. This velocity threshold largely depends on the bed surface properties like vegetation, moisture, roughness elements, etc.


Figure 22. Dune vegetation on the Rijnland coast.

In the model, the shear velocity threshold is initially calculated based on the grain size, then updated based on the other bed surface properties. In order to simulate the influence of the existing vegetation on the dunes on the aeolian sediment transport, the vegetation strategies have been applied in the constructed model. The method is to impose a threshold mask to locally increase the wind shear velocity threshold in the dune area. For both Rijnland and Ameland, the dune area with the bed level above +3m NAP which is the level of the dunefoot has been imposed to an increased velocity threshold. In the dune area, the calculated instantaneous wind shear velocity threshold is increased with a factor. This factor is 1.1 times the altitude difference between the concerned point and +3m NAP. The value of 1.1 is chosen to force the sediment deposition gently distributes over the dune area. If applying a too large value, the velocity threshold at the dunefoot will already be very large that most of the sediment will deposit at the dunefoot rather than being transported further onshore. Therefore the enlargement of the threshold is related to the altitude of the point: the point with higher altitude gets higher velocity threshold. After imposing the created threshold mask in the model, the dune area can be seen as being covered by vegetation. The region will have increased velocity threshold and reduced wind transport capacity, making the transported sediment settle and deposit on the dune.

Here the resultant velocity threshold of scenario #1 is taken as an example to illustrate the effectiveness and feasibility of the applied vegetation strategies. Figure 23 shows the resultant shear velocity threshold of scenario #1 including the vegetation effects. There are two curves in the figure. The two curves in the figure show the cross shore distribution of the threshold of the last time step, so at the end of one year simulation. The red curve is the threshold of the smaller grain size fraction (0.0003m) while the black curve shows the one for the lager grain size fraction (0.0320m).

By comparing the two curves, it is found that they have the similar trend. On the left hand side of the figure, a large part has no threshold value at all. That’s because this region is always underwater

and the sediment cannot be transported over this region. Then from somewhere near x = 1930m, the threshold starts to have low values. Actually, the location of this point is the location of waterline and it will vary around the mean water line following the tidal forcing. Going to the right, from somewhere around x = 1960m the threshold value starts to increase and becomes very high. In fact this point is the dunefoot and it is the starting point of the imposed threshold mask. The interesting thing is that the velocity threshold within the dune area has the same shape as the topography of the dune. But that is not surprising. Because the imposed threshold mask is based on the topography to increase the velocity threshold. Although having the same trend and shape, the abstract values of the threshold of the larger sediment fraction represented by the black curve are much larger (almost ten times larger) than the ones for the smaller sediment fraction represented by the red curve. That is due to the initial wind shear velocity threshold is proportional to the square root of the grain size, where larger grains have larger velocity threshold (Bagnold, 1937). The cross shore distribution of the velocity threshold for another time, 6 hours earlier than the end of simulation, was also obtained though it is not shown in the figure. It is found that the point where threshold value start to increase does not change over time because is the location of the dunefoot. But the location where the threshold starts to have low value has changed from x = 1930m to around x = 1870m. That is because this point is the water line and it will change with tidal level.

The result of the computed threshold values clearly demonstrates the imposed vegetation strategies. After applying the vegetation strategies, it is expected that the sediment that picked up and transported towards the dune will deposit on the dune from the location of dunefoot, because of the imposed enlarged velocity threshold. The resultant topography for the scenarios with the vegetation strategies will be shown and discussed in the next chapter concerning the model results.

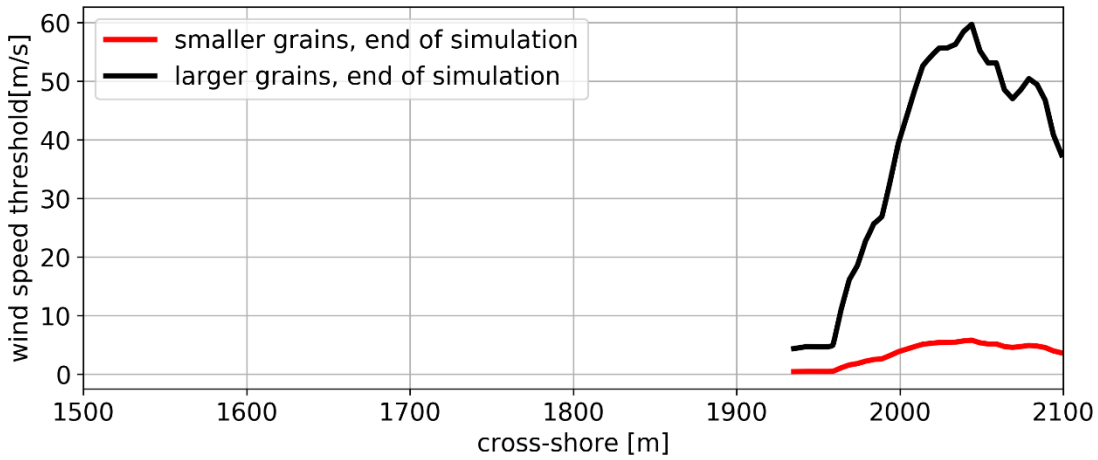

Figure 23. Cross shore distribution of the wind shear velocity threshold of scenario #1. The red curve is the threshold for the smaller grain size fraction. The black curve represents the threshold for the larger grain size fraction. The two curves are at the end of simulation.

4.2.2. Filtering out of the offshore wind

As shown in the Figure 20 (top panel), the dominant wind direction of Rijnland is around the Southwest, considered as onshore for the Rijnland coast. And Figure 20 (bottom panel) shows the

dominant wind for the Ameland coast blows from the West to the Southwest, considered as offshore. However, the wind that really contributes to the dune growth is the onshore wind. So an attempt has been made to filter out the offshore wind for both Rijnland and Ameland. For Rijnland with the coastal orientation of 312 degrees (normal direction of the coast), all the winds with the direction between 42 degrees and 222 degrees has been filtered out and replaced by zero wind speeds. For Ameland which has the coastal orientation approximately towards the North (normal direction of the coast), all the winds with the direction between 90 degrees and 270 degrees has been filtered out and replaced by zero wind speeds. Figure 24 shows the wind roses for Rijnland (left panel) and Ameland (right panel) after filtering. Note that the zero wind speeds are not shown in the wind roses. Then the remaining wind data has been imposed into the model for scenarios #6, #8, #10 and #11, forming four scenarios with only the contribution of onshore wind to the dune growth.

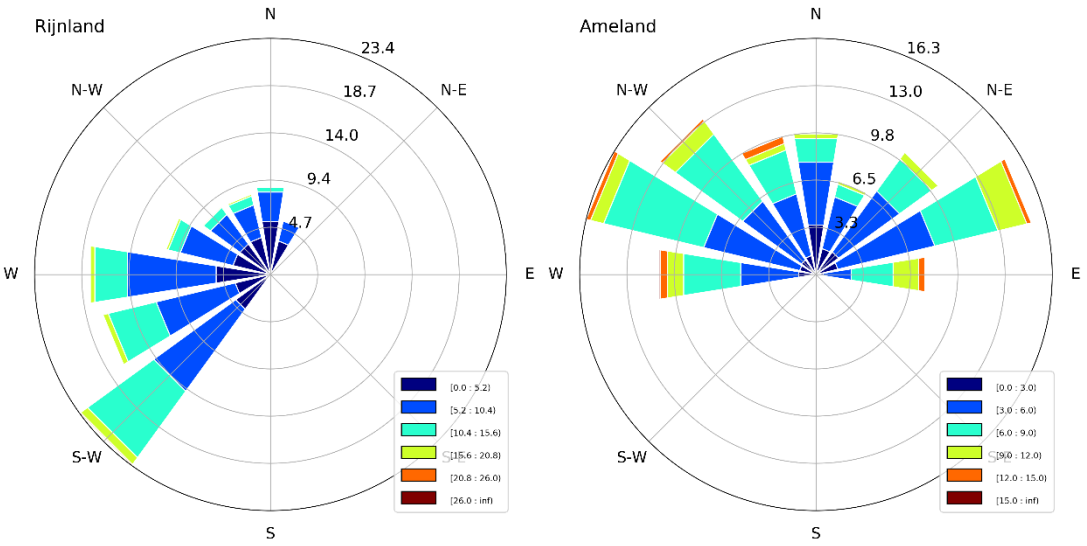

Figure 24. Wind roses after filtering out the offshore winds. Left panel is for Rijnland and right panel is for Ameland.

5. Results modelling study

In this chapter, the results of the modelling study will be discussed. The modelling study has run 11 scenarios with different parameter and input settings. The results of the model simulations have been analyzed in order to evaluate how the relevant processes affect the aeolian sediment transport and the role of sediment supply in the aeolian system. Firstly the results of scenario #1 are presented and analyzed, in order to show what kind of output a model run can give. Next the influences of vegetation and layer thickness are discussed. Then the influences of sediment sorting and nonerodible elements are analyzed to explore the importance of sediment supply to the aeolian sediment transport. After this, the influences of offshore wind are discussed. Finally the model results are compared to the results obtained from data analysis.

The question which will be answered in this chapter is research question five:

How do relevant processes affect the aeolian sediment transport and what is the role of sediment supply in the aeolian system?

5.1. Model output description and analysis

This section discusses in detail about the output of a model run. In other words, it answers the questions like “what kind of output does a model run give?” and “how can the output be analyzed?” Scenario #1 can be seen as a base scenario and this section is based on the output of scenario #1. In the later sections, the results of scenario #1 will be compared with the output of other scenarios.

5.1.1. Topography and bed level change

The topography and bed level change are important output for this thesis study. After running scenario #1 with a simulation time scale of 1 year, the initial and final topography of the chosen transect from the Rijnland coast is shown in Figure 25 (top panel). In order to show the beach erosion and dune growth clearly, an enlarged view of the topography in the range from y = -4m to y = 14m is also shown in Figure 25 (middle panel). The horizontal axis represents the x-coordinate in cross shore direction. It only shows the section with the cross shore coordinates between 1500m and 2100m because only this part was taken as the model domain. The vertical axis is the bed level with respect to the NAP datum. The blue line represents the initial topography while the black line is the final topography after 1 year simulation. The corresponding bed level change of the domain is shown in the bottom panel which has the same horizontal axis as the other panels. This bed level change is obtained by subtracting the initial bed level from the final bed level after 1 year simulation in the top panel. Therefore, positive values in that figure mean deposition while negative values mean erosion.

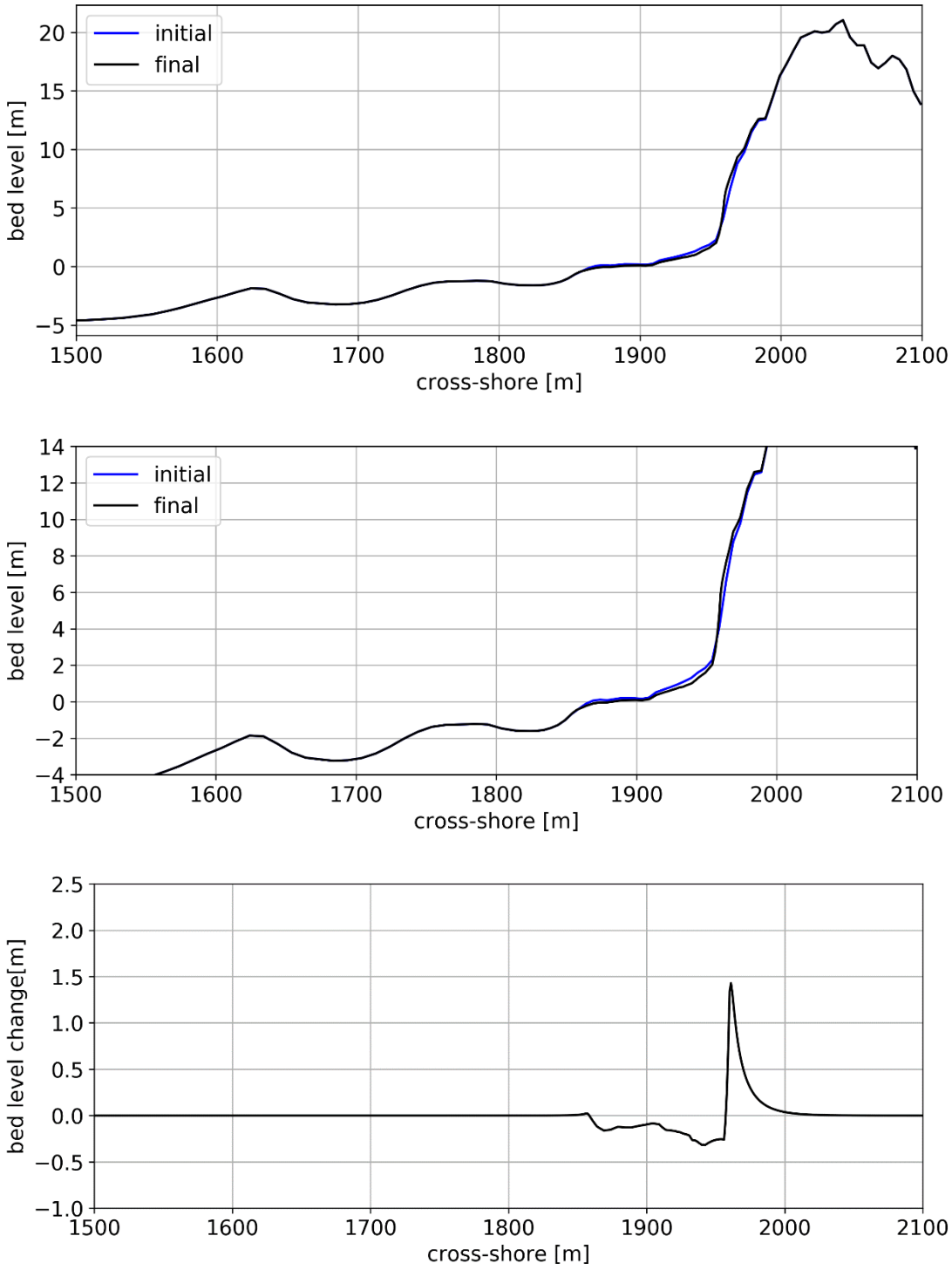

Figure 25. Resultant profiles and bed level change of the scenario #1. Top panel shows the initial and final profile of the concerned transect. Middle panel is the enlarged view of the top panel. Bottom panel shows the corresponding bed level change.

The mean water level is around +0m NAP to +0.5m NAP and the tidal level varies between -1.0m NAP and +1.5m NAP, see Figure 19 for the imposed tide data. That means the intertidal area is approximately between 1850m and 1950m in the cross shore direction. From the Figure 25 it is found that the region from x = 1500m to x = 1850m has neither erosion nor deposition. In fact, this

region is below the lowest tide and always remains underwater. As stated previously in the boundary conditions, the model has a zero-flux offshore boundary which does not allow sediment transport above water. Therefore, the zero bed level change in that region is resulted from the offshore boundary condition. In the section from x = 2000m to x = 2100m, which located on the top and the back of the dune, the bed level change also more or less equals to zero. This is mainly because of the high wind shear velocity threshold caused by the imposed vegetation strategies which has been discussed in the chapter concerning the modelling methodology.

In the region between 1850m and 2000m, obvious erosion and deposition can be recognized. The intertidal area (between 1850m and 1950m) experiences erosion where the maximum erosion can exceed 0.25m, see Figure 25 (bottom panel). The altitude of the dunefoot, the interface between beach and dune, is around +3m NAP where the corresponding cross shore coordinate being around 1950m. At the point of dunefoot, erosion turns into deposition and reach the maximum deposition height of 1.4m immediately. Then the value of deposition decays relatively quickly and reaches zero around x = 2000m. The reason why the transition from erosion to deposition at the interface being so sudden is because of the beach width being relatively narrow which results in the intertidal area being close to the dunefoot location. Actually, the dunefoot is the starting point of imposed high wind shear velocity threshold. That's why the dunefoot is the point where erosion turns into deposition. The surface area between the bed level change curve and the horizontal zero line within the accretion region has been calculated. In fact this value is the modeled dune accretion volume. From Figure 25, the dune accretion of scenario #1 is calculated to be $15.83\mathrm{m}^3/\mathrm{yr}/\mathrm{m}$. This value will be used to be compared with the value of other scenarios in the following sections. The figures visualize the erosion and deposition vividly, showing the beach around mean water line get eroded and the front slope of the dune obtains accretion. Generally speaking, scenario #1 demonstrates the beach erosion and dune accretion well and gives a dune accretion of $15.83\mathrm{m}^3/\mathrm{yr}/\mathrm{m}$, which is considered not very large.

5.1.2. Erosion and deposition processes

In brief, the processes that scenario #1 experiences are beach erosion and dune accretion. Therefore the output of scenario #1 regarding sediment entrainment (pickup) and instantaneous sediment concentration (Ct) is analyzed here, in order to demonstrate the processes of erosion and deposition. First the output for both the small grains and large grains at a location in the intertidal zone will be discussed. Then the output for the small grains at a location on the front dune slope will be presented.

First consider the output in the intertidal zone. Scenario #1 has two grain size fractions with 0.0003m and 0.0320m. Figure 26 shows the time series of the sediment entrainment (pickup), the instantaneous sediment concentration (Ct) and the corresponding wind speed of the two grain size fractions for the location of x = 1930m. Note that this point where x = 1930 is located in the intertidal area in front of the dunefoot where beach experiences erosion (see Figure 25 for reference).

The figure shows that when the larger grain size fraction is considered, the large sediment fraction represented by the green dots has zero pickup and zero concentration for the entire simulation

period. That is because the larger fraction has very high wind shear velocity threshold, making it quite difficult to entrain and transport theses large grains. Similarly for the location on the front dune slope where dune accretion happens, the large grain size fraction also has zero pickup and zero concentration (figures are not shown), because of the high velocity threshold.

Now the results of the smaller grain size fraction are considered, represented by the black dots in the pickup figure and by the red dots for Ct. The positive pickup values mean the sediment particles are picked up from the bed surface which results in erosion. The pickup (the black dots in the top panel of Figure 26) has several peaks while most of the time it stays zero, meaning the particles get picked up a few times while most of the time they just stay on the bed surface. The Ct represented by the red dots in Figure 26 (middle panel) is the instantaneous sediment concentration integrated over saltation height. The Ct figure has similar trends compared to the pickup figure. Usually when the pickup is high, the concentration is also high, which means that the local entrainment has big contribution to the local sediment concentration. But the Ct figure has more peaks than the pickup figure. That is because the local concentration does not entirely depend on the local erosion but is also influenced by the sediment transported by the wind from the upwind region. When comparing to the local wind time series, it is found that both the pickup and the concentration Ct, especially the Ct, correspond quite well with the wind series. When the wind has a peak, the pickup and the Ct are large as well. After all, wind is the main driving force of sediment entrainment and transport.

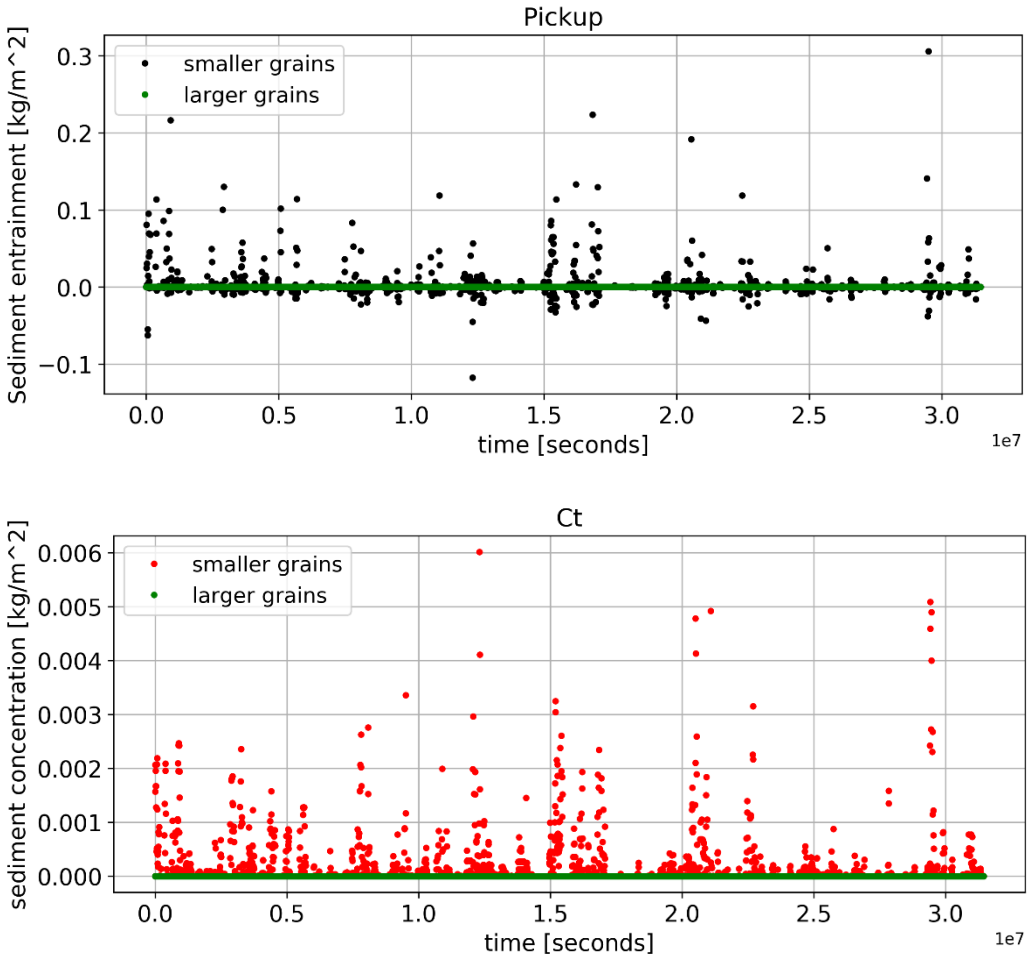

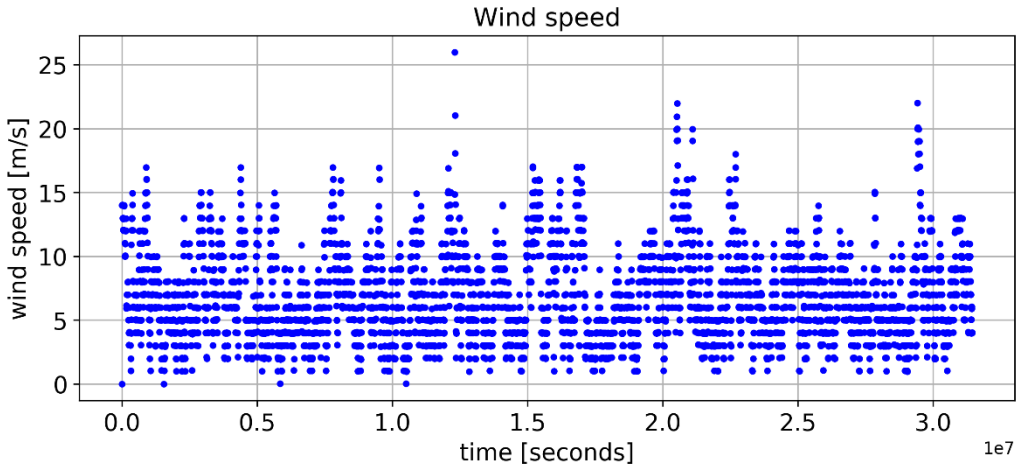

Figure 26. Time series of sediment entrainment (top panel), concentration (middle panel) and the corresponding wind time series (bottom) for the scenario #1. The green dots represents the results of the larger grain size fraction while the other dots are all for the smaller grains. The chosen location is x = 1930 in the intertidal zone. Total length of the horizontal axis in seconds equals 1 year.

Secondly, for the smaller grain size fraction on the front dune slope where sediment get deposited (x = 1970m, see Figure 25 for reference), the time series of the local pickup, Ct and the corresponding wind speed are shown in Figure 27. The negative pickup values mean the sediment particles get deposited on the bed surface. Similar to the output for the intertidal zone, the results of the pickup, concentration and wind speed on the front dune slope correspond quite well with each other and have peaks at the same times. That can be explained by the deposition process: when the wind is strong, more sediment get picked up and transported to the front dune, resulting high local sediment concentration. Because of the high velocity threshold caused by vegetation, a lot of particles deposit on the dune slope, giving rise to negative pickup peaks. Here the results of Ct (middle panel in Figure 27) have smaller order of magnitude than the results in the intertidal area (middle panel in Figure 26). That may be because the grains transported towards the dune has already started to deposit since the dunefoot. So here for the point of x = 1970m which is located more landward than the dunefoot, the sediment concentration has relatively small values.

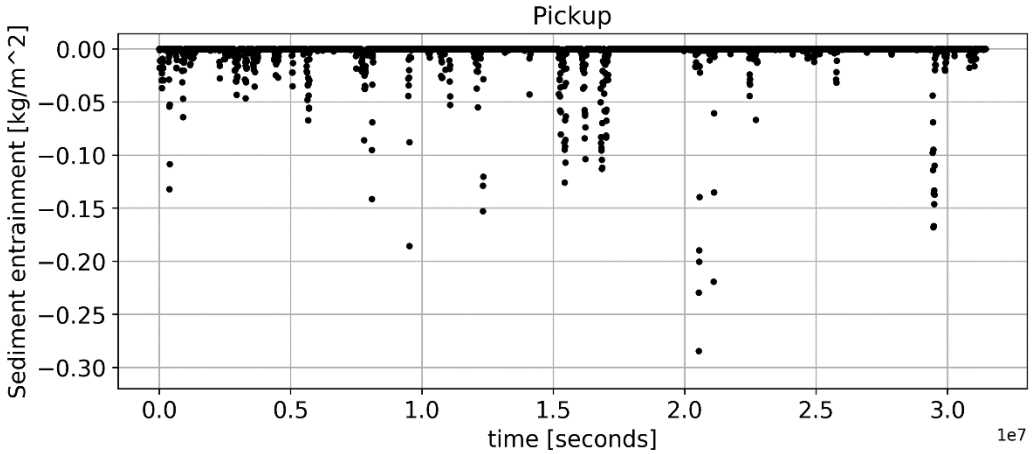

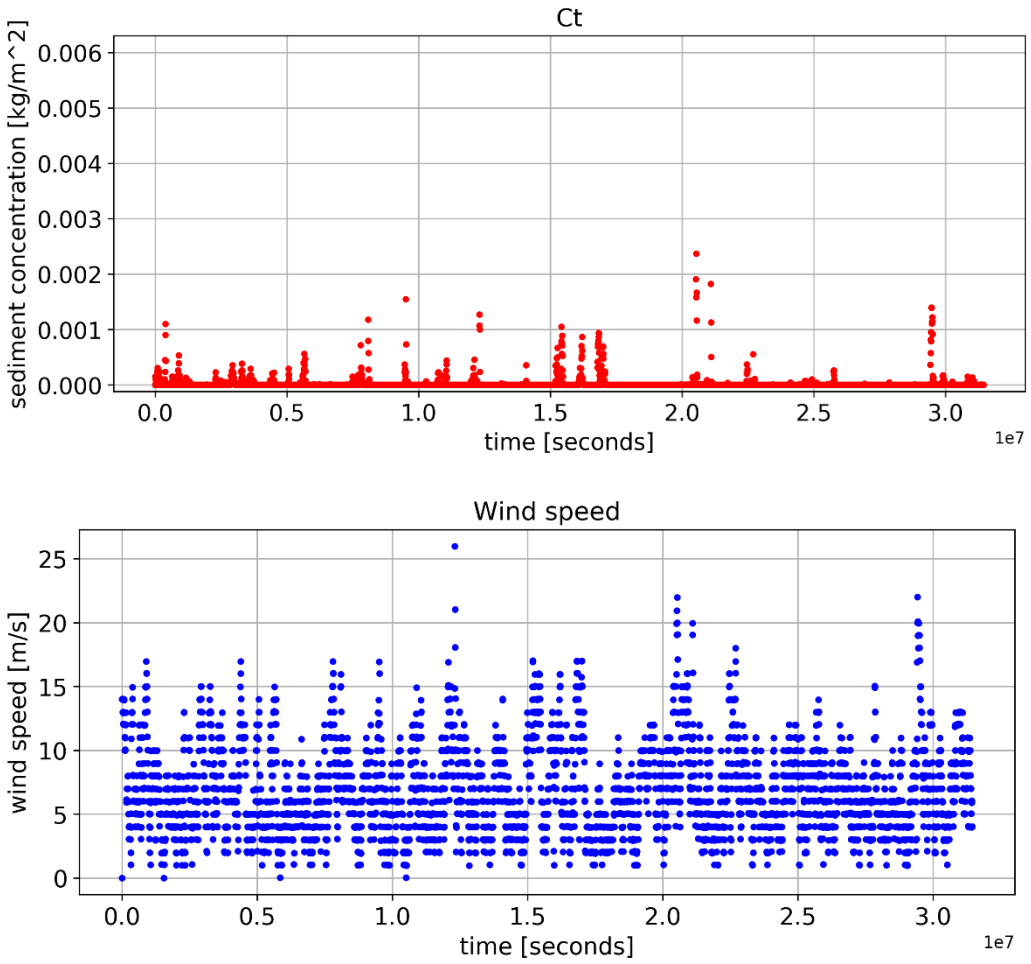

Figure 27. Time series of sediment entrainment (top panel), concentration (middle panel) result and corresponding wind time series (bottom) of the smaller grain size fraction for the scenario #1. The chosen location is x = 1970 on the front dune slope. Total length of the horizontal axis in seconds equals 1 year.

5.2. Scenario #2 – Vegetation

The purpose of scenario #2 is to illustrate the effect of the vegetation strategies imposed in the dune area. The only difference between scenario #2 and scenario #1 is that scenario #2 has no vegetation strategies applied. Figure 28 shows the initial and final topography along the cross shore direction of the chosen transect. Compared to the topography output of scenario #1 shown in Figure 25, the profile of scenario #2 only experiences erosion. The maximum erosion depths are the same for the two scenarios. No obvious deposition happens in the domain of scenario #2. Not only the beach in the intertidal area got eroded, but also the entire dune was eroded to some extent. In reality, various kinds of vegetation present on the front slope, the top and the back of dunes. Generally the vegetation on dunes significantly increases the surface roughness, resulting in increased wind shear velocity threshold. And the high velocity threshold enforces the sediment near the bed surface getting deposited, leading to dune growth rather than dune erosion in Figure 28. Therefore the comparison of the topography output between scenarios #2 and #1 proves the necessity and feasibility of the implementation of vegetation strategies.

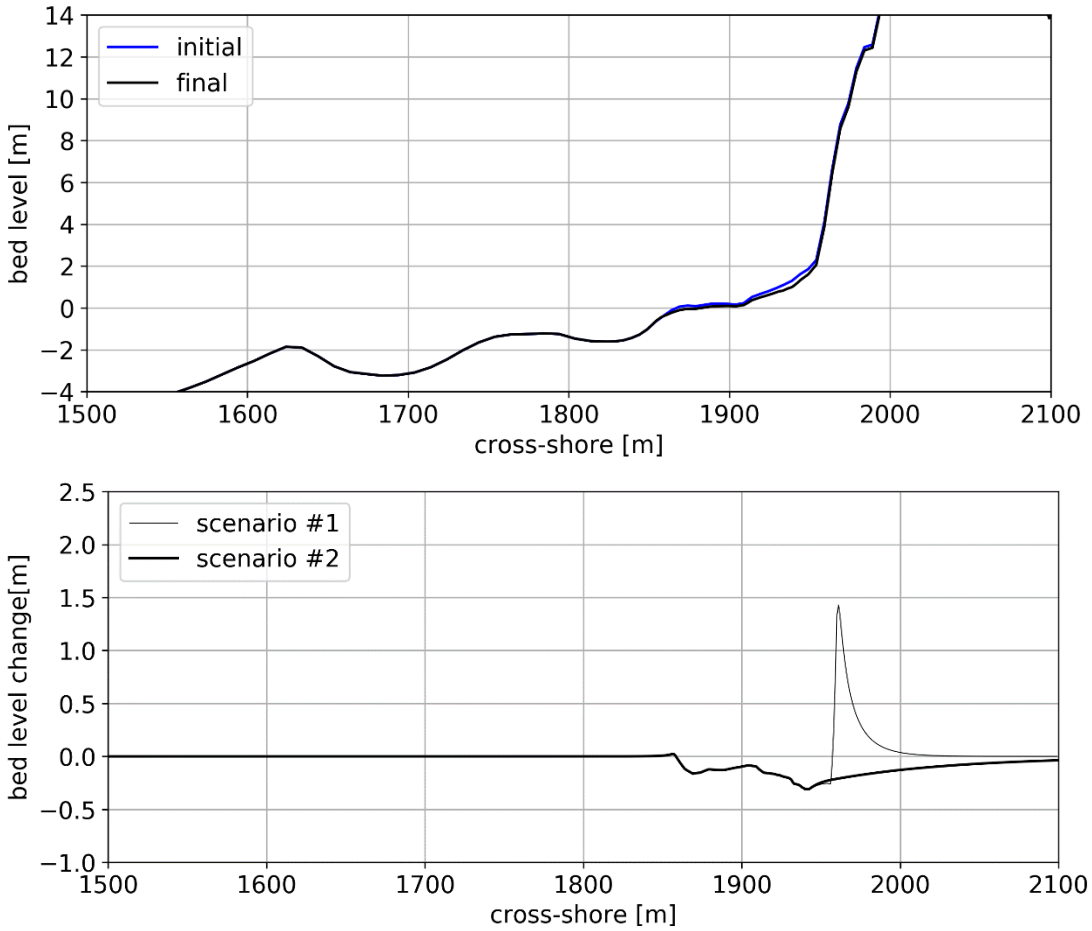

Figure 28. Resultant profiles and bed level change of the scenario #2. Top panel is the enlarged view of the initial and final profile of the concerned transect. Bottom panel shows the bed level change, where both scenarios #1 and #2 are shown for convenient comparison.

5.3. Scenario #3 – Layer thickness

As discussed before, the bed is discretized into computational grids in horizontal and vertical directions in order to simulate the process of sediment sorting. In the vertical direction, the bed is discretized into several bed layers (three layers for the thesis study) with a certain thickness. Scenario #3 is built and ran to test the influence of layer thickness on the aeolian sediment transport. Figure 29 shows the results of scenario #3 including the initial and final topography of the chosen transect and the corresponding bed level change. Compared to the results of scenario #1 with the layer thickness of 0.05m (see Figure 25), the erosion and deposition in scenario #3 which has 0.10m layer thickness are both larger. The largest erosion in scenario #1 is 0.319m in the intertidal zone while the one in scenario #3 reaches 0.424m, which is more than 32% larger. The largest deposition in scenario #1 is 1.429m while the one in scenario #3 can reach 1.713m, so about 20% larger. The dune accretion volume derived from the bed level change is $19.14\mathrm{m}^3/\mathrm{yr}/\mathrm{m}$, which is 21% larger than the volume of $15.83\mathrm{m}^3/\mathrm{yr}/\mathrm{m}$ for scenario #1. With doubled layer thickness, the profile in scenario #3 gets distinctly larger erosion and deposition, showing that the influence of layer thickness on aeolian sediment transport in the model is quite significant and important. A possible explanation for this is that a thicker bed layer in the model may provide more

available sediment to be picked up and transported, resulting in more beach erosion and aeolian transport. However, the calibration of this input parameter may need delicate in-situ sampling and precise soil layer analysis. And the AeoLiS model documentation does not provide an instruction to determine the layer thickness. So an instruction about how to determine the layer thickness based on soil data can be a future step to improve the AeoLiS model.

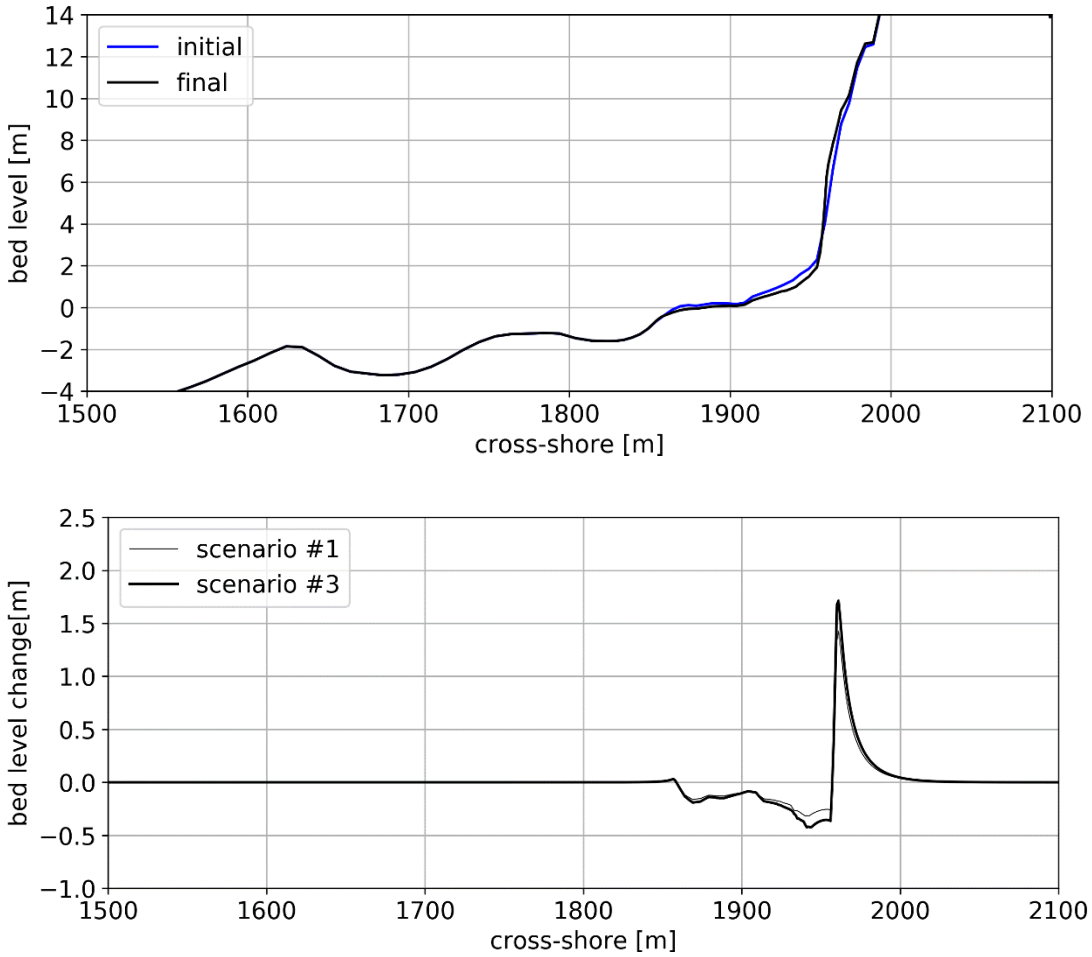

Figure 29. Resultant profiles and bed level change of the scenario #3. Top panel is the enlarged view of the initial and final profile of the concerned transect. Bottom panel shows the bed level change, where both scenarios #1 and #3 are shown for convenient comparison.

5.4. Sediment sorting and nonerodible roughness elements

For the availability-limited aeolian system that this thesis concerns, sediment availability is one of the vital factors that determine the aeolian sediment transport. When the available sediment is limited, the sediment availability determines the sediment entrainment and therefore the actual erosion of the bed. The bed surface properties vary with time and space because of the sediment sorting and the consequent emergence of nonerodible elements, resulting in the spatiotemporal variations in the sediment availability. In order to explore the role of sediment supply to the aeolian system, one of the main concerns of the thesis study, scenarios #4 and #5 are simulated and their results will be discussed below with more details.

5.4.1. Sediment sorting and beach armoring

Sediment sorting is a process that fines get eroded and deposited downwind, leading to a coarsening of the bed surface (Bagnold, 1937). Sediment sorting could happen for a bed consisting of both erodible and nonerodible fractions. Scenario #4 which has only 1 sediment fraction with the grain size of 0.0003m was simulated and compared with scenario #1.

Figure 30 shows the initial and final profile and the consequent bed level change of scenario #4. From the Figure 30 it is found that both the erosion and deposition have significant larger values compared to scenario #1 in Figure 25. Approaching the dunefoot location, the erosion depth for scenario #4 increases rapidly. Then it suddenly turns into a large deposition of almost 4m. The reason for the sudden change is the beach width being relatively narrow, making the intertidal area being close to the dunefoot location. The dune accretion volume derived from the bed level change for scenario #4 is $40.30\mathrm{m}^3/\mathrm{yr}/\mathrm{m}$, which is incredibly larger than the accretion of $15.83\mathrm{m}^3/\mathrm{yr}/\mathrm{m}$ for scenario #1. The deep erosion hole and the steep slope around the dunefoot in the final profile are considered unrealistic in the natural coastal system. Figure 31 shows the pickup and concentration time series for x = 1930m, a point in the intertidal zone. Compared to the results of scenario #1 in Figure 26, the pickup of scenario #4 is far more efficient. And the concentration for scenario #4 is also larger than the one in scenario #1, though they both have the similar trend.

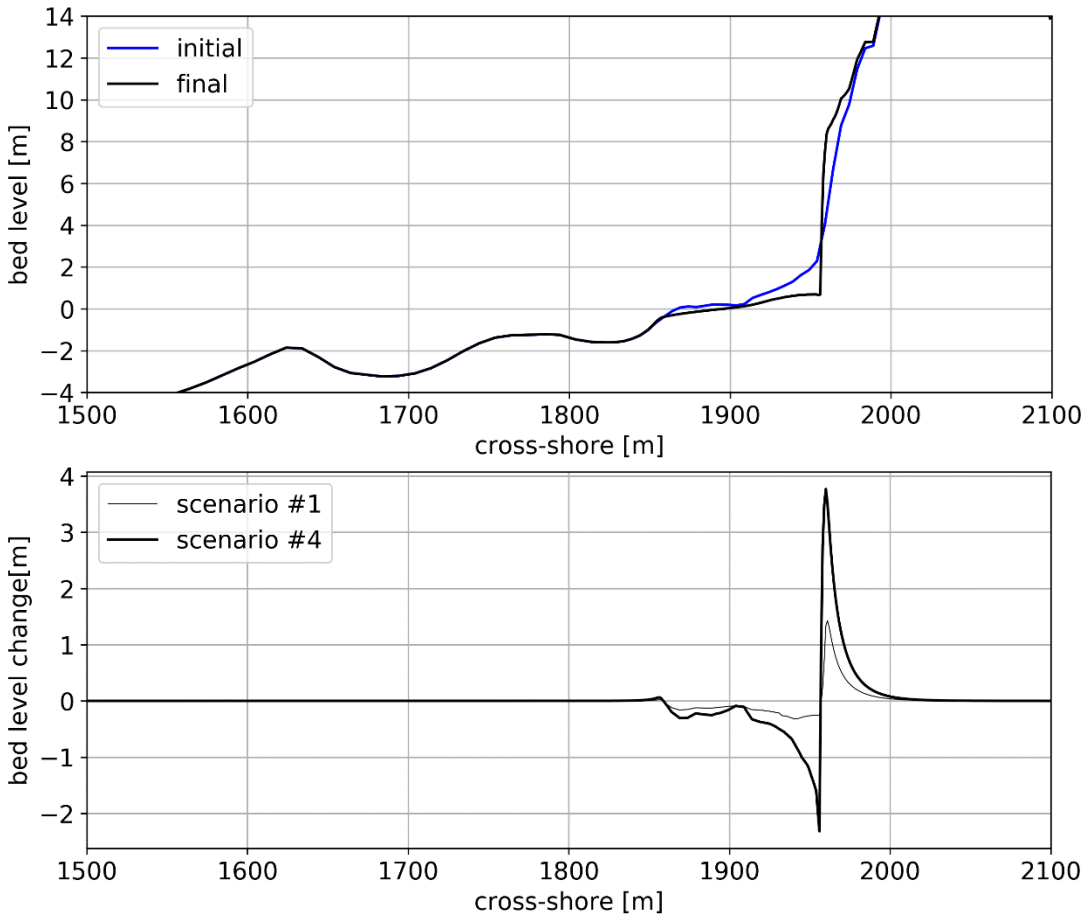

Figure 30. Resultant profiles and bed level change of the scenario #4. Top panel is the enlarged view of the initial and final profile of the concerned transect. Bottom panel shows the bed level change, where both scenarios #1 and #4 are shown for convenient comparison.

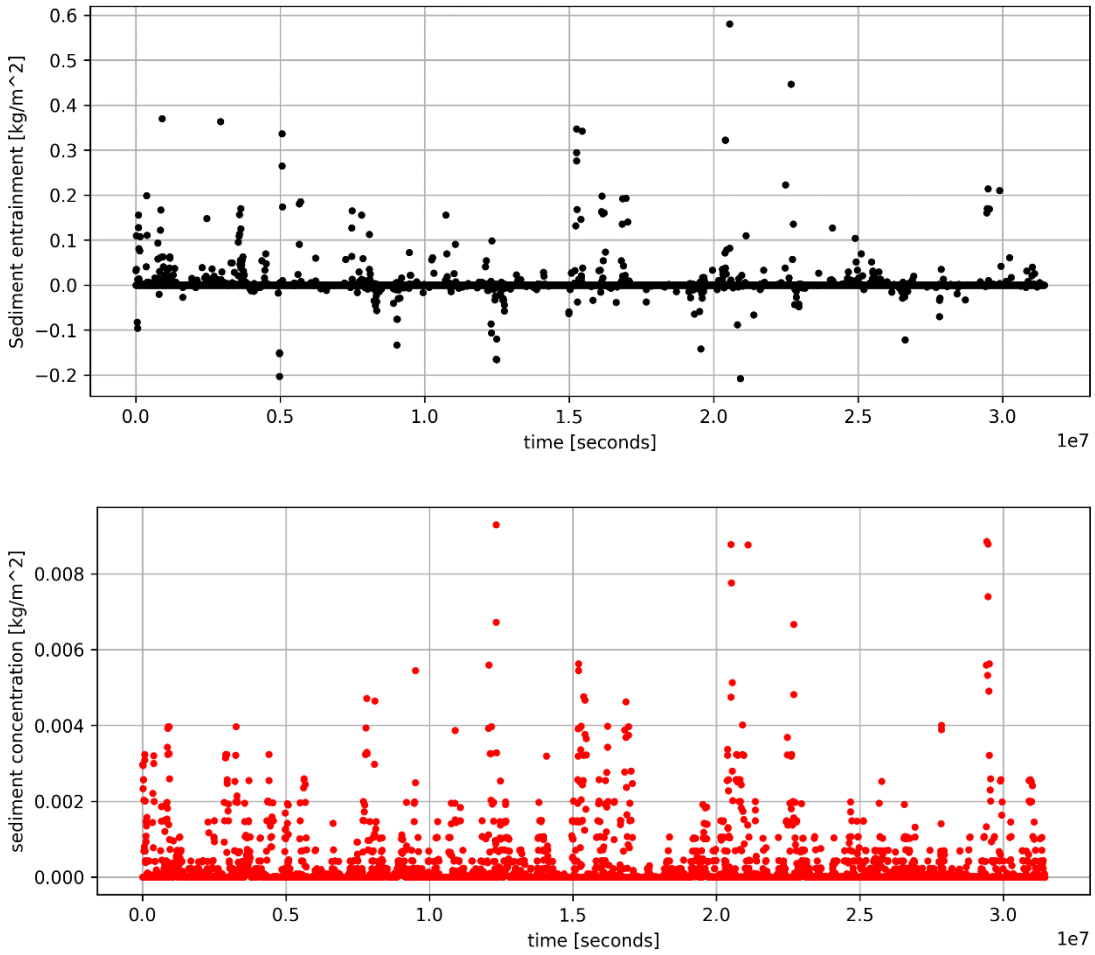

Figure 31. Time series of sediment entrainment (top panel), concentration (bottom panel) result of the smaller grain size fraction for the scenario #4. The chosen location is x = 1930. Total length of the horizontal axis in seconds equals 1 year.

The difference in erosion and deposition extent is due to the only difference in model input between scenarios #1 and #4: having both erodible and nonerodible fractions or only having erodible fraction. And it is related to sediment sorting and beach armoring. For scenario #1 which has two sediment fractions (0.0003m and 0.0320m), erosion and deposition are nonuniform over these two fractions. The smaller grain size fraction has smaller wind shear velocity threshold and is considered erodible while the larger fraction with high velocity threshold is considered nonerodible. In the upwind grid cell, the fines are eroded while the coarse elements remain, leading to coarsening of the bed surface layer. As erosion continues, more and more nonerodible elements emerge from the bed and cover more area, sheltering the fines from erosion. Gradually sediment availability and entrainment get reduced, leading to armoring of the beach surface. Therefore the erosion and deposition are relatively small for scenario #1 with two fractions. However, only with fine sediment fraction, scenario #4 does not experience sediment sorting and beach armoring. Nonerodible roughness elements are not available to shelter the fines and reduce sediment availability. Therefore erosion continues without restriction, resulting in much more serious erosion and deposition.

5.4.2. Influence of the grain size distribution of nonerodible roughness elements

The occurrence of sediment sorting and beach armoring is due to the emergence of nonerodible roughness element. How the grain size distribution of these nonerodible elements affect the aeolian sediment transport could also be an interesting issue. So scenario #5 with higher percentage of coarse sediment is simulated and analyzed. Scenario #5 still has two sediment fractions, while the corresponding grain sizes distribution is 85% and 15% for the grain size fractions 0.0003m and 0.0320m respectively, rather than 95% and 5% in the scenario #1. Figure 32 shows the profile results and the corresponding bed level change. From the figure it's recognized that both the erosion and deposition for scenario #5 get reduced compared to scenario #1 (see Figure 25). The dune accretion volume derived from the bed level change for scenario #5 is $7.88\mathrm{m}^3/\mathrm{yr}/\mathrm{m}$, which is only half of the accretion volume of $15.83\mathrm{m}^3/\mathrm{yr}/\mathrm{m}$ for scenario #1. This can be explained by the imposed roughness elements with higher percentage. During the processes of sediment sorting and beach armoring, higher percentage of nonerodible elements may cover more area and shelter more fine elements, reducing the sediment availability. Then the erosion and deposition extents of scenario #5 get weakened. On the other hand, the results of scenario #5 also imply that when modelling aeolian sediment transport, the determination of the grain size distribution of roughness elements is vital for simulating sediment sorting and beach armoring well and truly. Field survey may be an appropriate solution.

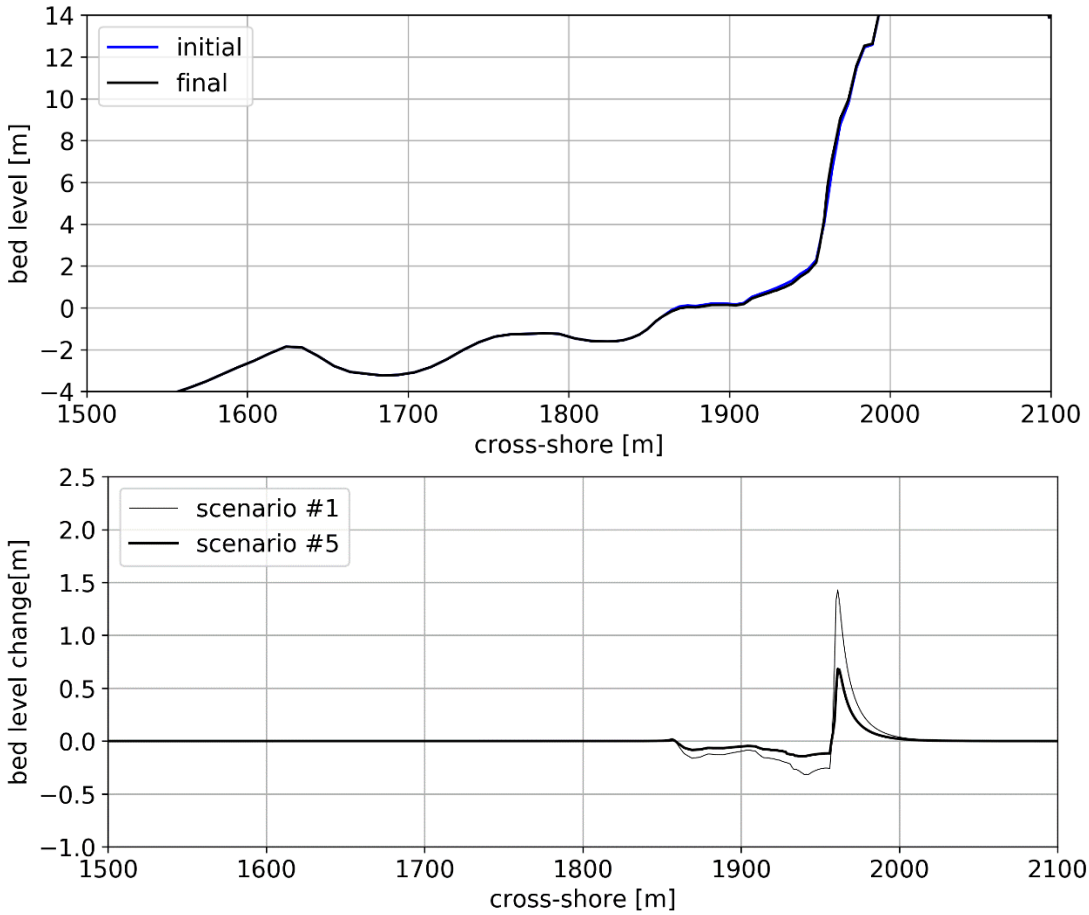

Figure 32. Resultant profiles and bed level change of the scenario #5. Top panel is the enlarged view of the initial and final profile of the concerned transect. Bottom panel shows the bed level change, where both scenarios #1 and #5 are shown for convenient comparison.

5.5. Influence of offshore wind

In an aeolian system, onshore wind and offshore wind may exist at the same time. However, only the onshore wind can pick up and transport sediment, and then build the dunes. The offshore wind effects on aeolian sediment transport and dune behavior deserves more research. Here in this section the influences of offshore wind on the aeolian system will be explored for onshore wind dominant system and offshore wind dominant system respectively. And the performance of the AeoLiS model in accounting offshore wind will be discussed.

5.5.1. Influence of offshore wind in onshore wind dominant system

Considering the wind condition and the coastal orientation, Rijnland is regarded as an onshore wind dominant system. Scenario #6 is set to test the influence of the offshore wind, in which the offshore wind is all filtered out using the method stated in previous chapter. Figure 33 shows the results of scenario #6 including the initial and final profiles as well as the bed level change. The bed level change curve for scenario #6 is very close to the curve for scenario #1. Actually, the dune accretion volume derived from the bed level change for scenario #6 is $16.26\mathrm{m}^3/\mathrm{yr}/\mathrm{m}$, which is a little bit larger than the accretion volume of $15.83\mathrm{m}^3/\mathrm{yr}/\mathrm{m}$ for scenario #1.

Based on the comparison above, it seems that during the simulation of the base scenario a small part of the onshore transport effect has been counteracted by the offshore wind. The offshore wind generated a small amount of offshore aeolian transport and eroded the dune with a small volume. Therefore in onshore wind dominant system, the pattern of onshore aeolian transport and dune accretion can be reproduced by the model but the offshore wind could also erode the dune with a small volume. In order to focus on onshore aeolian transport and dune accretion, this thesis will use the results of scenario #8 later to be compared with measured dune growth rates, where the offshore wind component in scenario #8 being filtered out.

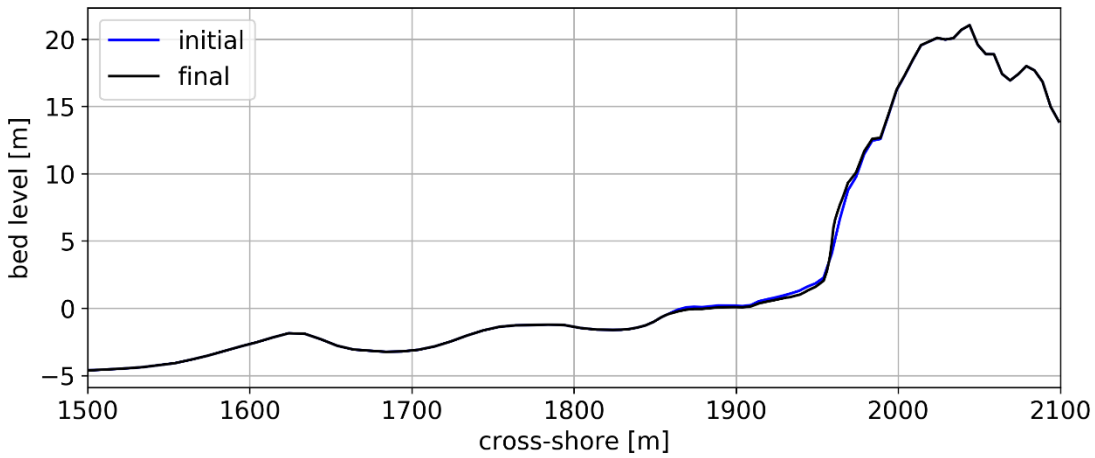

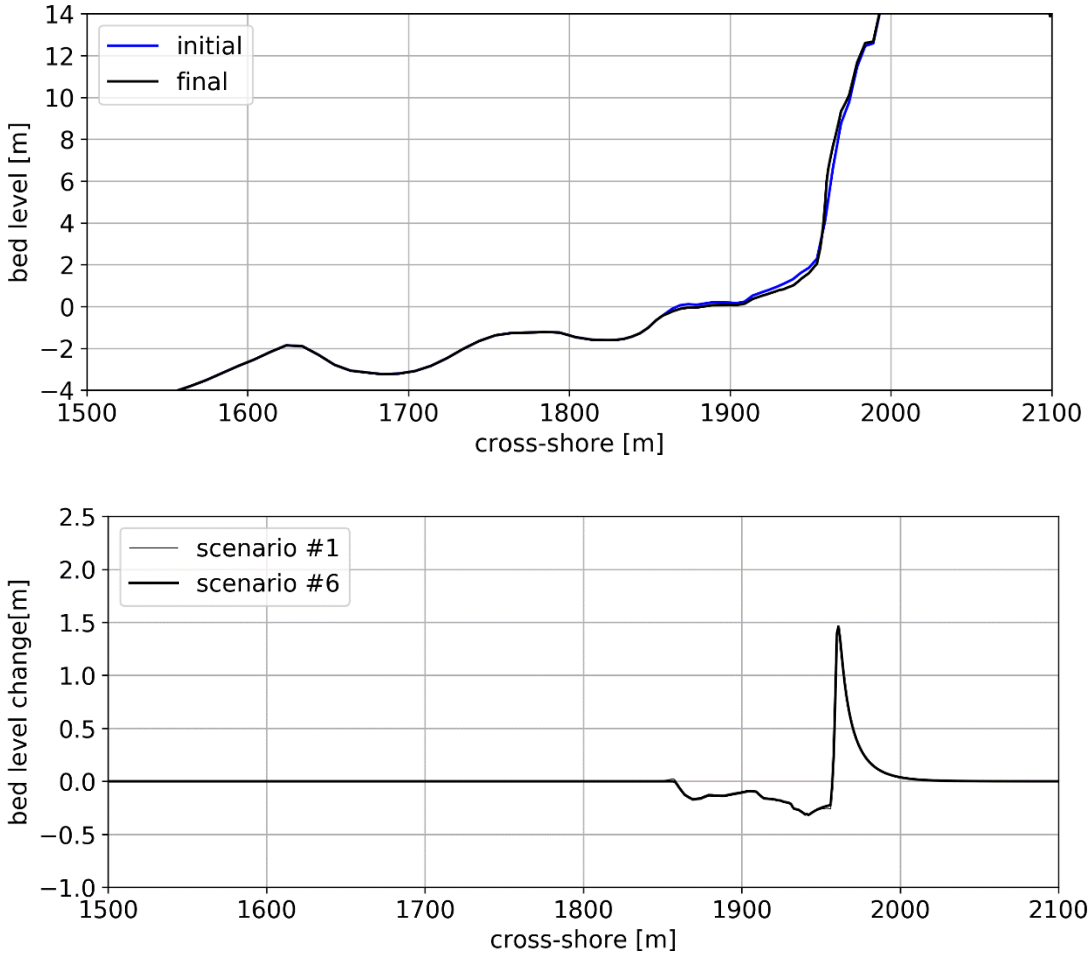

Figure 33. Resultant profiles and bed level change of the scenario #6. Top panel is the enlarged view of the initial and final profile of the concerned transect. Bottom panel shows the bed level change, where both scenarios #1 and #6 are shown for convenient comparison.

5.5.2. Influence of offshore wind in offshore wind dominant system

The Ameland coast is a typical example of offshore wind dominant system, considering the relation between dominant wind direction and coastal orientation. By comparing the results of scenarios #9 and #10, the influence of offshore wind on the aeolian system in an offshore wind dominant system is discussed. In scenario #9 a transect on Ameland (id = 3000900) is simulated using full wind field, while in scenario #10 the same transect is simulated with all the offshore winds being filtered out.

The results of scenario #9 for Ameland are shown in Figure 34 including the initial and final profiles as well as the corresponding bed level change. From the figures it is found that the beach close to the dunefoot gets eroded. The eroded sediment is then transported seaward and deposited around the waterline. Although nonerodible roughness elements have been imposed in the scenario input, the offshore wind could still erode the dry beach continuously and transport the sediment seaward.

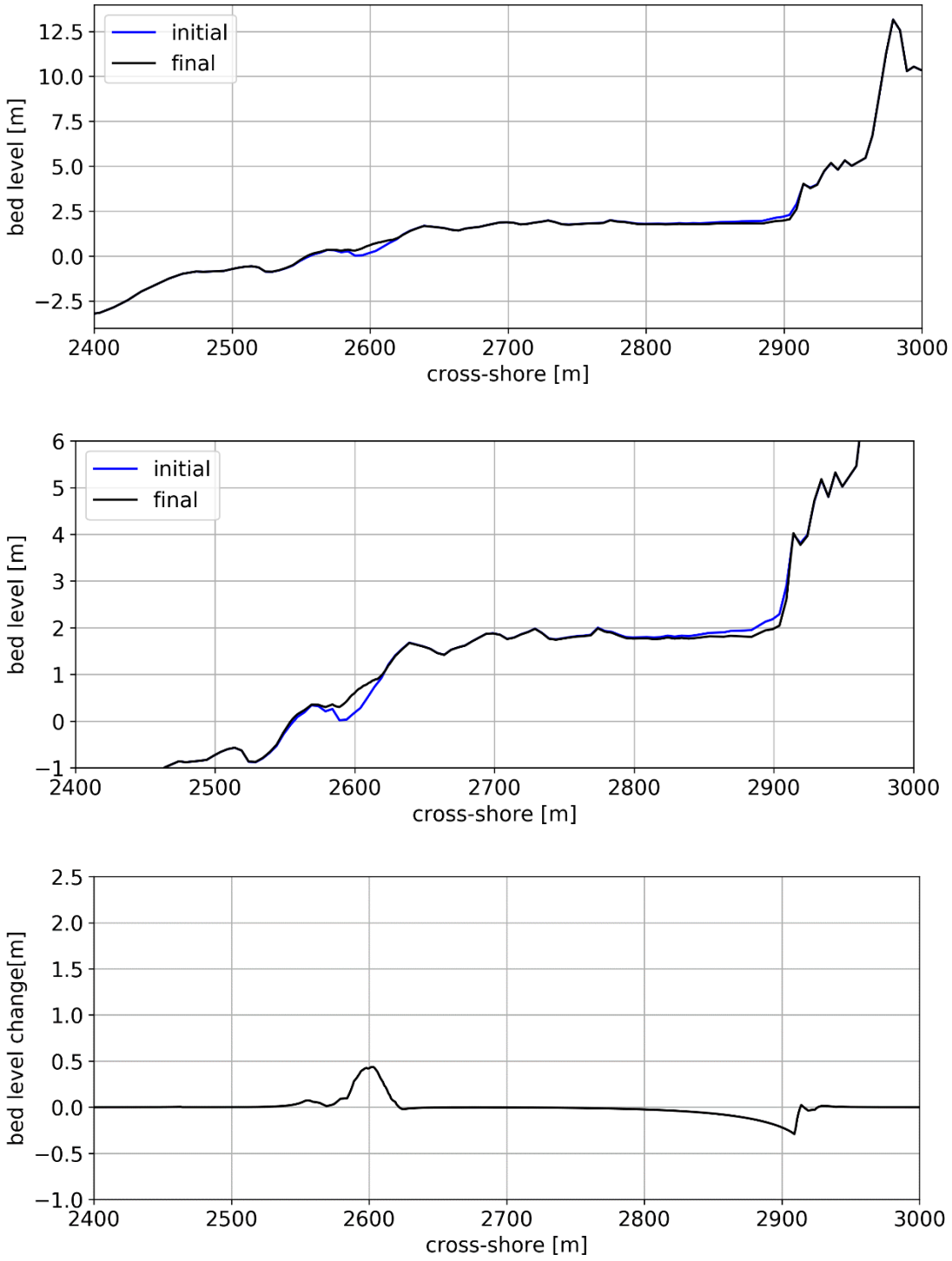

Figure 34. Resultant profiles and bed level change of the scenario #9. Top panel is the initial and final profile of the concerned transect. Middle panel is the enlarged view of the top panel. Bottom panel shows the bed level change.

The results of scenario #10 for Ameland with all the offshore wind filtered out are shown in Figure 35. The bed level change figure shows the pattern of erosion at the water line and deposition on the dune. The model reproduce the onshore aeolian transport and the resultant dune accretion again, which is similar to the pattern for Rijnland. The dune accretion volume derived from the bed

level change for scenario #10 is only $3.55\mathrm{m}^3/\mathrm{yr}/\mathrm{m}$, which is considered relatively small. That's because the onshore wind components on the Ameland coast, which is offshore wind dominant, are relatively small and therefore the erosion capability declines.

By comparing the results above, it is found that in onshore wind dominant system, the pattern of onshore aeolian transport and dune accretion can be reproduced by the model. The offshore wind component could reduce the dune accretion with a small amount. In offshore wind dominant system, in order to reproduce the pattern of onshore transport and dune accretion, the offshore winds need to be filtered out. More discussions about the performance of the AeoLiS model regarding the coexistence of onshore and offshore wind will be presented in the discussion chapter.

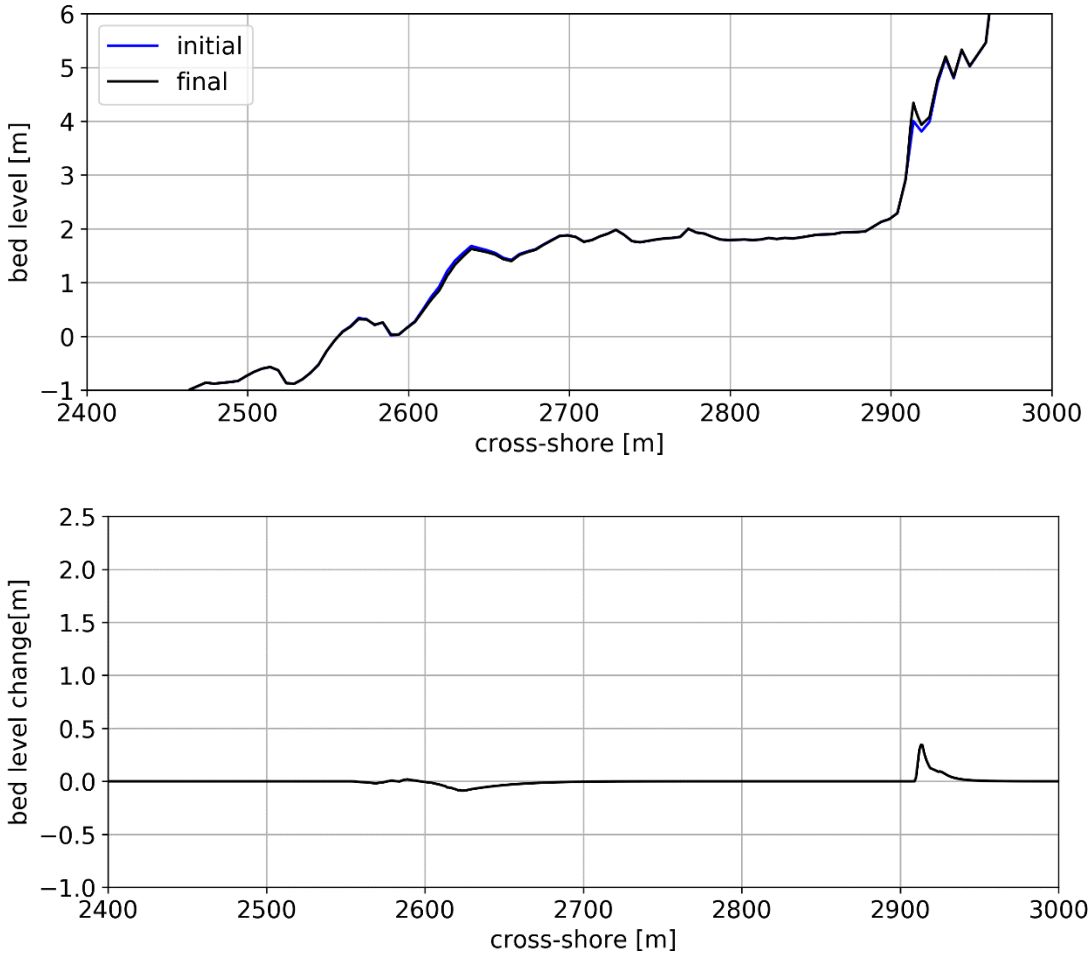

Figure 35. Resultant profiles and bed level change of the scenario #10. Top panel is the enlarged view of the initial and final profile of the chosen transect. Bottom panel shows the bed level change.

5.6. Scenario #7 – Varying wind speeds

Wind is the driving force for aeolian sediment transport. Scenario #7 is set to test the influence of varying wind speeds on aeolian sediment transport. The wind speed used in scenario #7 is 20% larger than the wind speed used in the base scenario. Figure 36 shows the initial and final profile as well as the corresponding bed level change of scenario #7. Compared to the results of scenario

#1 in Figure 25, scenario #7 experiences larger erosion and deposition. The maximum erosion and deposition of scenario #7 are around 0.5m and 2.2m respectively while the ones for scenario #1 are about 0.3m and 1.4m. The dune accretion volume derived from the bed level change for scenario #7 is $27.58\mathrm{m}^3/\mathrm{yr}/\mathrm{m}$, which is much larger than the accretion volume of $15.83\mathrm{m}^3/\mathrm{yr}/\mathrm{m}$ for scenario #1. Figure 37 shows the pickup and concentration time series results of scenario #7. The location is x = 1930m, a point in the intertidal zone. Compared to the results of scenario #1 in Figure 25, more elements are entrained in scenario #7 and the concentration is also high. That explains the larger erosion and deposition of scenario #7. The wind with higher speed picks up more fines, resulting in higher sediment concentration and deeper erosion hole. More fines are transported downwind and deposit when approaching the vegetation area with high velocity threshold. Therefore, for the case with enough available sediment, increasing wind speed can give larger aeolian transport and dune deposition. It can also be concluded that in most of time, the aeolian transport in the base scenario could still be strengthened if the present wind speed is higher.

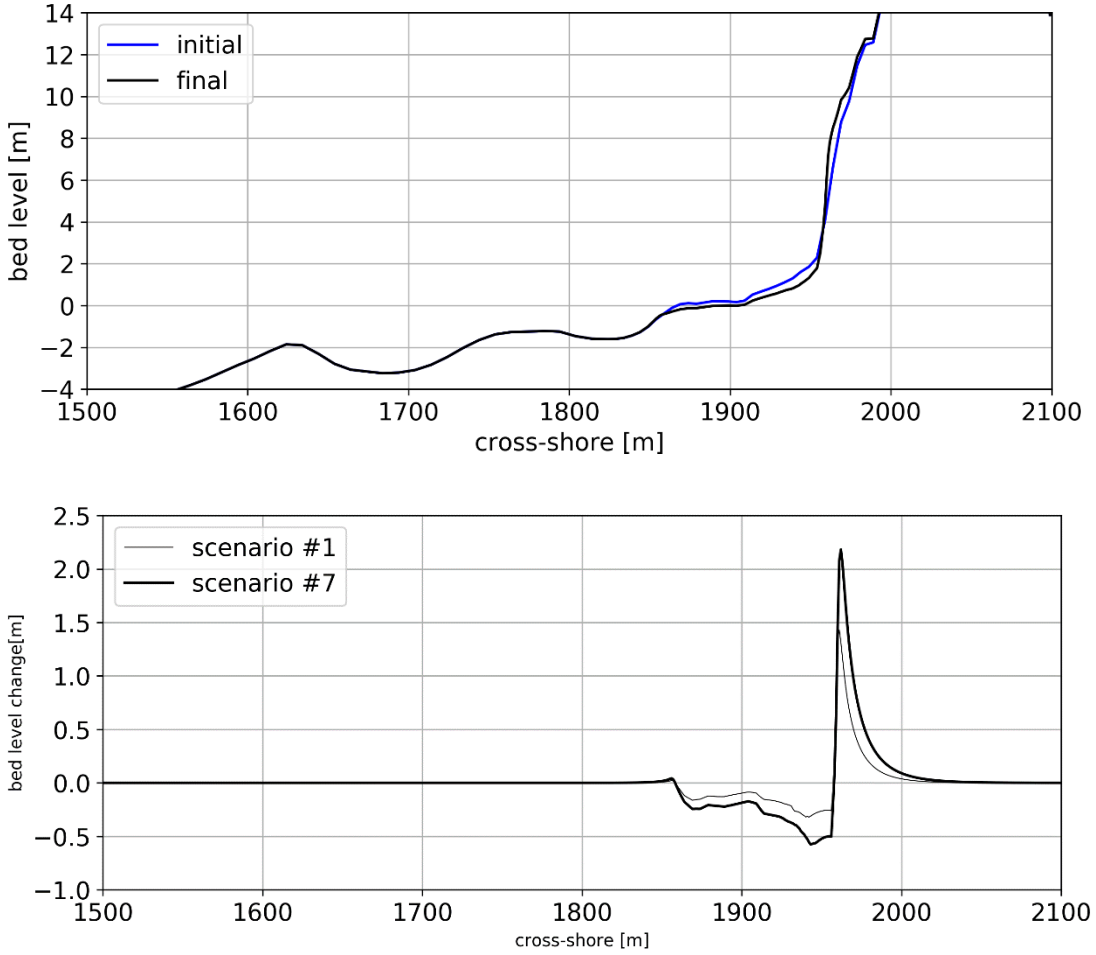

Figure 36. Resultant profiles and bed level change of the scenario #7. Top panel is the enlarged view of the initial and final profile of the concerned transect. Bottom panel shows the bed level change, where both scenarios #1 and #7 are shown for convenient comparison.

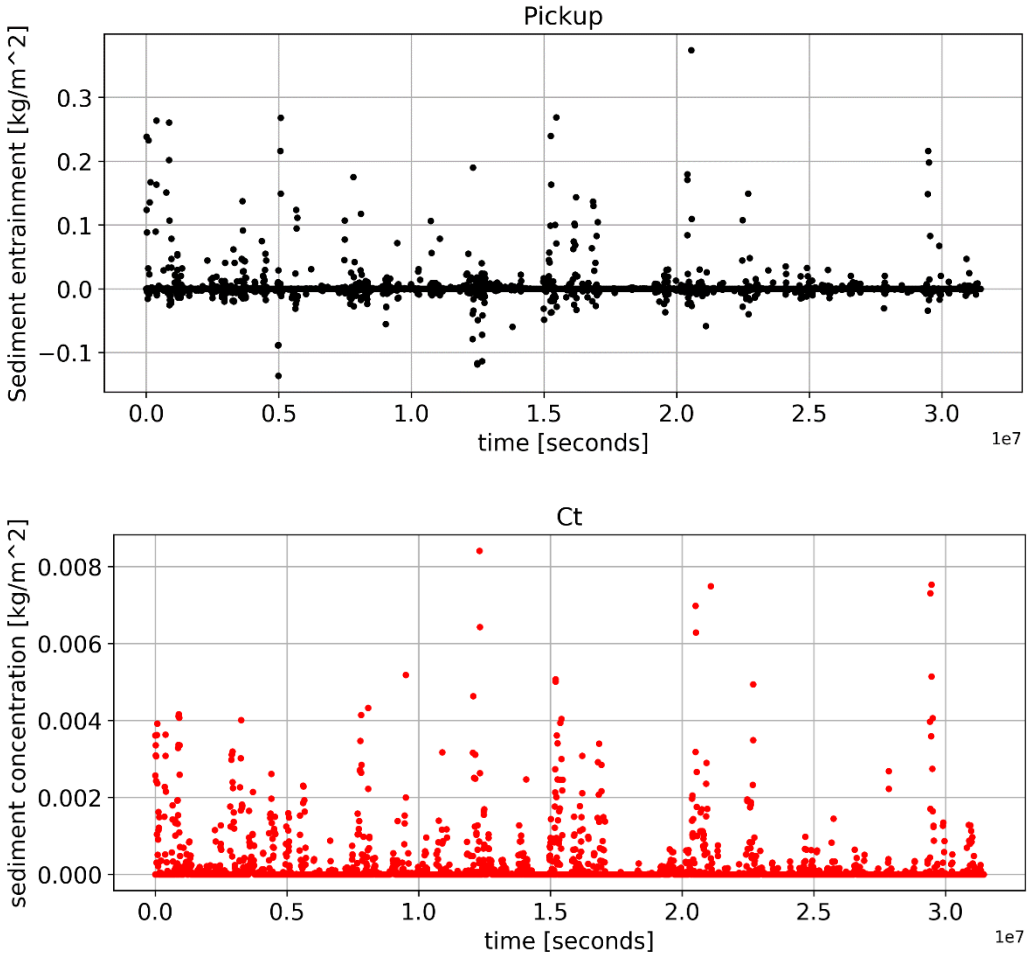

Figure 37. Time series of sediment entrainment (top panel), concentration (bottom panel) result of the smaller grain size fraction for the scenario #7. The chosen location is x = 1930. Total length of the horizontal axis in seconds equals 1 year.

5.7. Development of erosion over time

Previous sections have shown the final profile for each scenario. How the erosion depth develop over time is of interest, too. Figure 38 shows the development of the erosion depths for each scenario. All the lines are for the location of x = 1930m, a point on beach in front of the dunefoot. Here the main concern is how fast the erosion develops for each scenario. The red line represents scenario #1, the base scenario. By comparing lines of other scenarios with the line of the base scenario, the influences of certain input parameters on erosion development can be identified.

Generally speaking, the development of erosion for all the scenarios in the figure slow down over time. But different scenario has different patterns of development. Compared to the base scenario, the yellow line in the figure (scenario #4) vibrates very fiercely and the erosion develops quite fast over time. That may be explained by the absence of nonerodible roughness elements in scenario #4. Without the shelter provided by nonerodible elements, beach armoring cannot form. The availability of fines does not get reduced over time, leading to relatively fast erosion. With the fine sediment on bed surface completely exposed to the air, the fines are more vulnerable to the

varying wind speed which results in a much dynamic development pattern. It can also be proved by the blue line, scenario #5. The blue line develops slower and less dynamically. With increased percentage of nonerodible elements in scenario #5, the fines on the bed are relatively well protected by the roughness grains. Therefore, a well armored beach may be less vulnerable to the varying wind and show less dynamic characteristics. The orange and green lines show similar pattern compared to the red line, though the values are not equal. So the factors like layer thickness and offshore wind can affect the erosion depth but cannot really change the aeolian transport characteristics.

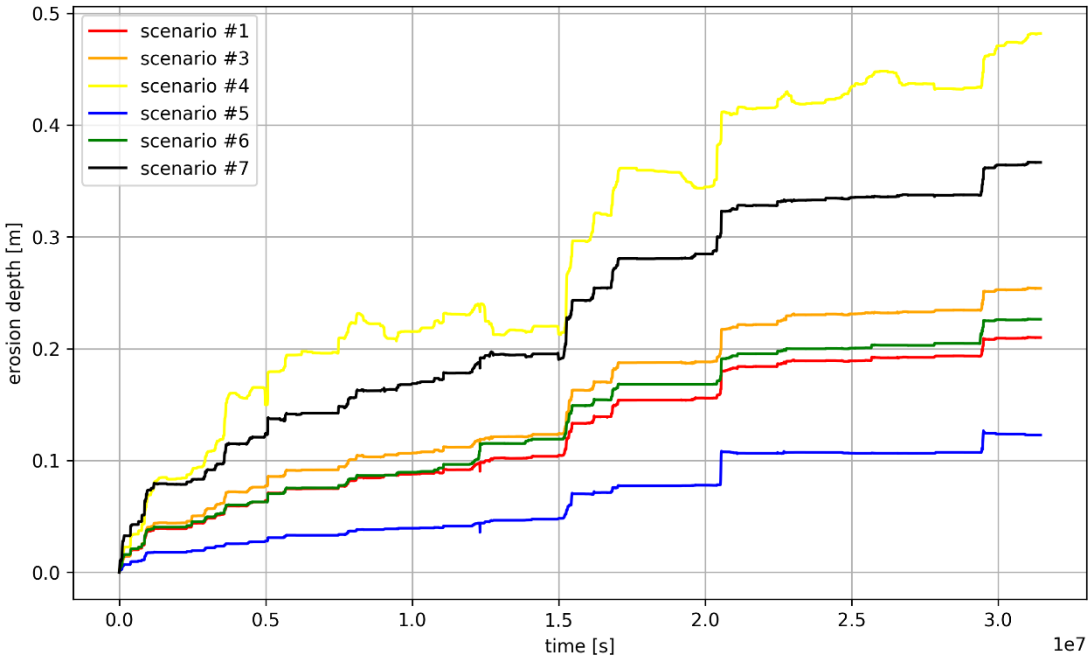

Figure 38. Development of the erosion depths for each scenario at the location of x = 1930m in the intertidal zone.

5.8. Comparing the model results with the results of data analysis

In Part I of the thesis concerning the data analysis, the alongshore distributions of dune growth rates have been calculated and plotted for both the Rijnland and Ameland coasts. Here the results of dune growth rate based on the data analysis will be compared with the dune accretion volumes calculated by the AeoLiS model. The dune growth rates presented in the data analysis are derived based on the profile measurements from 2006 to 2016. The resultant values are the volumes of dune accretion (sometimes dune erosion) per year. In the modeling study, the periods of input data like tide and wind are from July 1, 2016 till June 30, 2017 and the model simulation time is one year. The model results give dune accretion volumes at the end of one year. Therefore it is considered the dune accretion volumes from the data analysis and the model simulation are comparable. In the following subsections, the comparisons will be discussed for Rijnland and Ameland respectively.

5.8.1. Comparing the modeled and measured dune accretion volumes on the Rijnland coast

In the modeling study, the transect with the transect id of 8007350 has been used as the model topography for all the scenarios concerning Rijnland. To compare with the data analysis, scenario #8 has been set and simulated for one year. In scenario #8 all the offshore winds are filtered out to focus on the dune accretion caused by the onshore winds. To keep the simulation as close to the real world as possible, the sediment fraction setting for scenario #8 uses Pattern 4, which consisting of 11 sediment fractions (see Figure 21 for the grain size and grainsize distribution). Figure 39 shows the initial and final profile (enlarged view) and the corresponding bed level change of the results of scenario #8. From the bed level change figure, the dune accretion volume on the front dune slope is calculated as $21.70\mathrm{m}^3/\mathrm{yr}/\mathrm{m}$. In the data analysis part, the dune growth rates have been calculated for every transect location along the Rijnland coast, see Figure 11. For the chosen transect with id = 8007350, the dune accretion volume based on the data analysis is $8.92\mathrm{m}^3/\mathrm{yr}/\mathrm{m}$.

It is found that the simulated dune accretion volume is twice as large as the volume based on the data analysis. Several reasons may explain this inconsistency between the modeled and measured results. The first one is that the settings of sand bed in the model may not reproduce the reality perfectly. In the model, the sand bed is discretized into three layers with the thickness of 0.05m. Maybe this thickness is larger than the movable layer thickness in reality, resulting in more available fine sediment in the model. And with relatively large wind applied in the model on Rijnland (see Figure 20, top right panel), the inaccuracy in bed setting is enlarged which results in more dune accretion in the model. The second reason could be that the vegetation strategies applied in the model are not perfect enough. In the model, the dune area is imposed with locally increased wind shear velocity threshold (see Figure 23). The threshold values are very high around the top of the dune, which forces all the fine sediment will deposit on the dune without leaving the domain. But in reality, some sediment could still be transported over dunes (Kostaschuk et al., 2008), which reduces the dune accretion volume in reality. In addition, the intermittent erosion which may happen in reality during the concerned period of data analysis from 2006 to 2016 could be another reason. The dunes could be eroded by wave run up and storm surge. The narrow beach on Rijnland also increases the risk of dune erosion because of storm surge and wave run up. With relatively larger and more frequent onshore wind, the dune may grow too fast, resulting in very steep slope and slope slide which also reduce dune accretion. In addition, the precipitation is not considered in the model. In reality, when sand grains get wet because of the precipitation, they are difficult to be picked up and transported. Although the simulation is not perfect, it is still considered that the dune accretion volumes from the data analysis and the model simulation are in the same order of magnitude. More discussions about the difference between the modeled and measured dune accretion are presented in the discussion chapter regarding model performance.

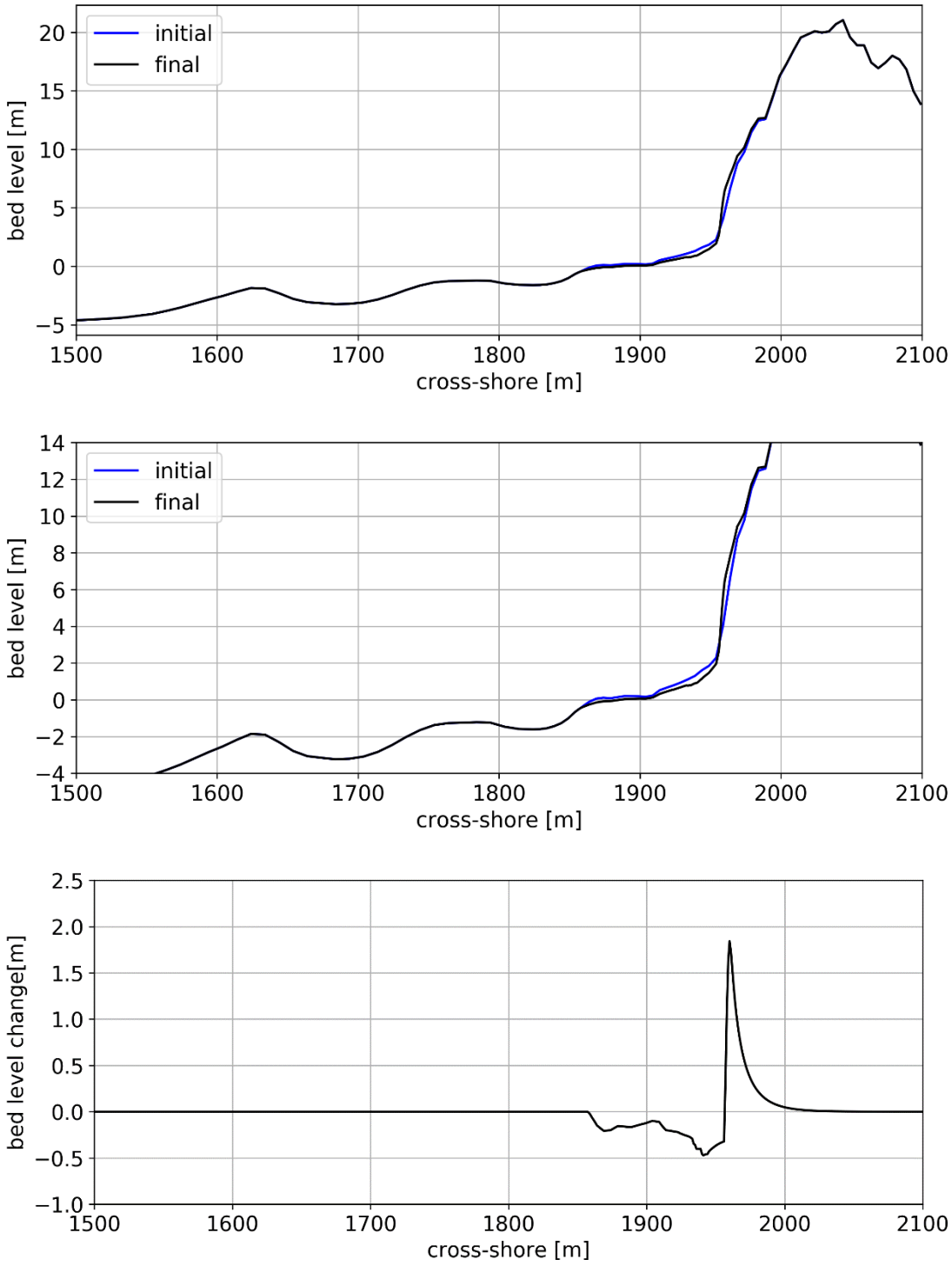

Figure 39. Resultant profiles and bed level change of the scenario #8. Top panel is the enlarged view of the initial and final profile of the chosen transect. Bottom panel shows the bed level change.

5.8.2. Comparing the modeled and measured dune accretion volumes on the Ameland coast

For the model simulation of Ameland, the transect of id = 3000900 has been used as the model topography. Here the results of scenario #11 are used to compare with the results of data analysis. Similar to scenario #8 for Rijnland, scenario #11 for Ameland also uses Pattern 4 for the sediment

fraction setting to make the simulation approaching the real world, see Figure 21 for the grain size and distribution. And scenario #11 has filtered out all the offshore winds to focus on the onshore aeolian sediment transport and the resultant dune accretion.

Figure 40 shows the results of scenario #11, including the initial and final profile (enlarged view) and the corresponding bed level change. From the bed level change results, the dune accretion volume is calculated as $3.36\mathrm{m}^3/\mathrm{yr}/\mathrm{m}$. The data analysis gives the alongshore distribution of the dune growth rates for the Ameland coast, see Figure 10. For the chosen transect with id = 3000900, the data analysis gives the dune accretion volume of $4.50\mathrm{m}^3/\mathrm{yr}/\mathrm{m}$. Different from the Rijnland coast, the dune accretion volume calculated by the model for Ameland is close to the volume derived from the data analysis. It may be because that with smaller and less frequent onshore winds for Ameland (see Figure 20, bottom right panel) than for Rijnland, the difference between the bed settings in the model and the ones in reality has not been enlarged. And the aeolian sediment transport and unrealistic vegetation strategies are not that important any more. The slope slide also seldom happens in reality because the dune accretion is less. The relatively wide beach on Ameland also reduces the dune erosion because of the possible wave run up. Therefore the inconsistency between the modeled dune accretion volume and the one derived from the data analysis remains small. More applications of AeoLiS in offshore wind dominant systems can help further evaluate the performance of the model in such kind of situation. More discussions about the model performance in offshore wind dominant system are presented in the discussion chapter.

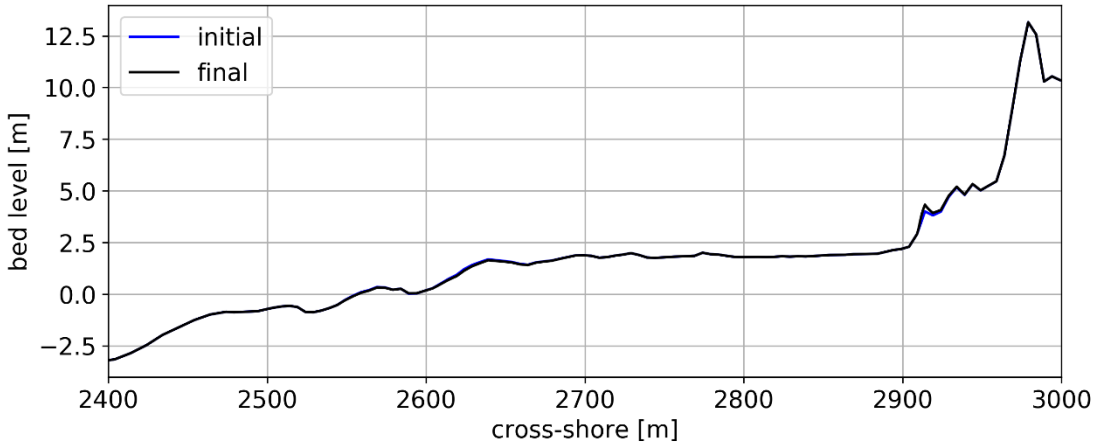

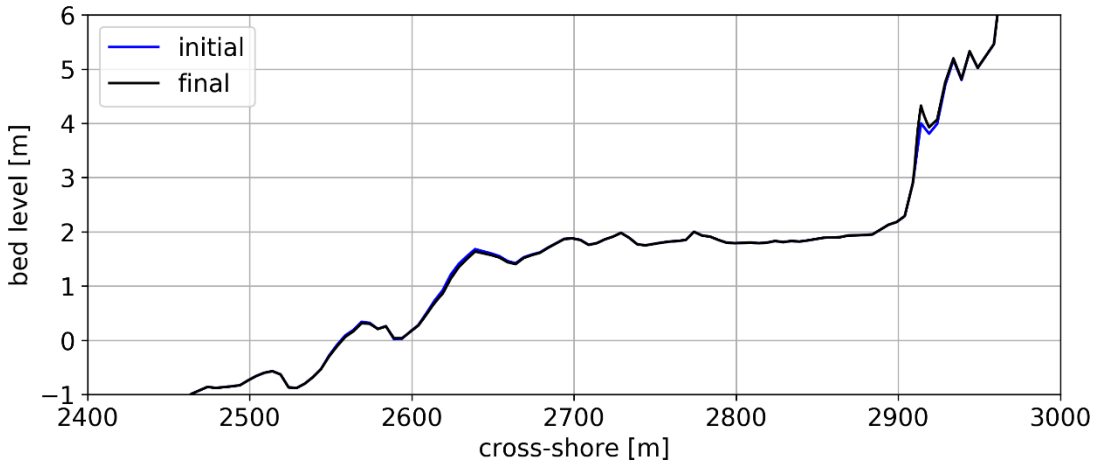

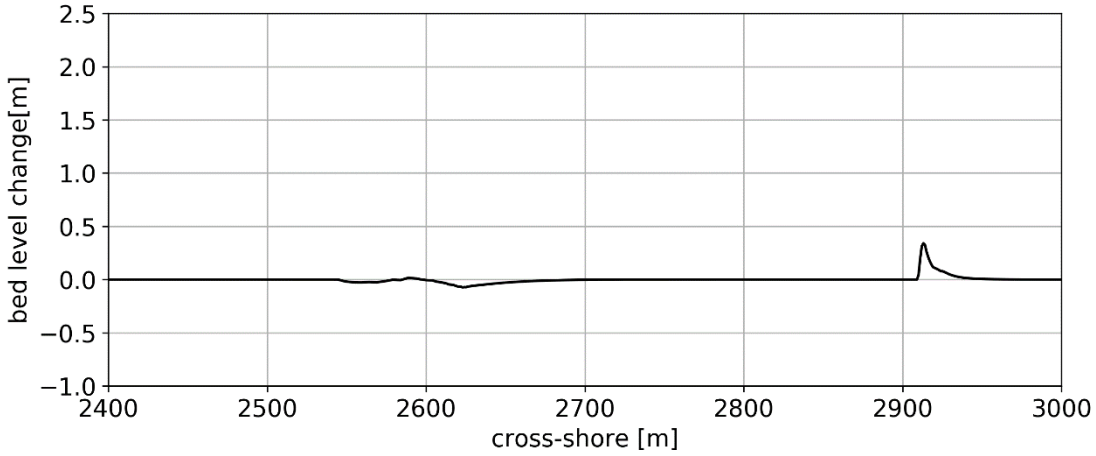

Figure 40. Resultant profiles and bed level change of the scenario #11. Top panel is the enlarged view of the initial and final profile of the concerned transect. Bottom panel shows the bed level change.

5.8.3. Difference between Rijnland and Ameland in comparing the model results with the data analysis results and its correlation to the coastal orientations

In Part I of the thesis which concerns data analysis, the theoretical wind transport capacity and the actual dune growth rates have been calculated for Rijnland and Ameland based on the measurements from the JARKUS dataset. In Part II which discusses modeling study, the dune accretion volumes for the two concerned coasts have been calculated from the model results of scenario #8 and scenario #11 respectively. Here these three kinds of results for Rijnland and Ameland are compared with each other and the influences of the different coastal orientations between the two places on the aeolian sediment transport will be explored further.

As presented in section 3.1.1, the theoretical onshore wind transport capacity values are $24.6m^3/yr\ /m$ for Rijnland and $7.7m^3/yr\ /m$ for Ameland. According to the results of actual dune growth rates (see Figure 11 and Figure 10), the measured dune accretion volume for the transect belonging to Rijnland with id = 8007350 is $8.92m^3/yr\ /m$ while the value for the Ameland transect with id = 3000900 is $4.50m^3/yr\ /m$. As for the results from the modeling study, the Rijnland transect (id = 8007350) gets a dune accretion volume of $21.70m^3/yr\ /m$ while the Ameland transect (id = 3000900) gains a dune accretion volume of $3.36m^3/yr\ /m$. See Table 3 for the summary of the results.

The onshore wind transport capacity, the measured dune growth rates and the simulated dune accretion volumes all show a similar pattern: the results for Rijnland are larger than the ones for Ameland. The different coastal orientations between Rijnland and Ameland can be a possible reason for this pattern. As discussed in section 3.1.2 and section 3.2.3, the coastal orientations can explain why the wind transport capacity and measured dune accretion for Rijnland are often larger than the ones for Ameland. Here the results of the simulated dune accretion volumes for Rijnland and Ameland have proved the influence of coastal orientation. When the coastal orientation of a coast (the normal direction of coastline) approaches the local dominant wind direction which makes more strong winds being considered as onshore rather than offshore, the onshore aeolian

sediment transport and the resultant dune accretion are relatively large. When the coastal orientation of a coast approaches the opposite direction of the local dominant wind direction which leads to more strong winds being considered offshore, the onshore aeolian sediment transport and the resultant dune accretion are relatively small.

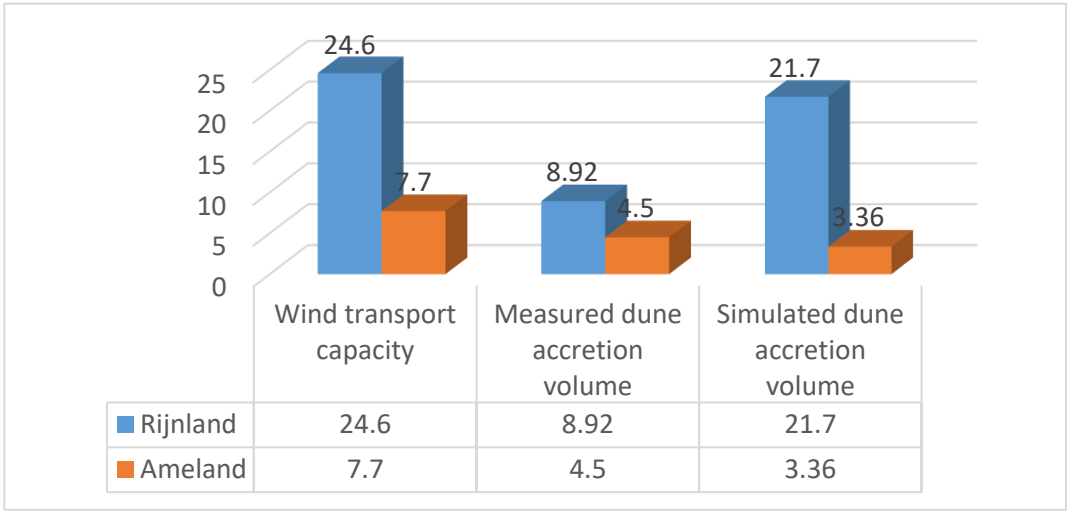

Table 3. Summary of wind transport capacity, measured dune accretion and simulated dune accretion for Rijnland and Ameland. Note that the wind transport capacity is the average over the concerned coast. The measured and simulated dune accretion are for certain transects: transect with id = 8007350 for Rijnland and transect with id = 3000900 for Ameland.

5.9. Conclusions modeling study

The AeoLiS model has been applied with 11 scenarios to further explore the influences of relevant processes on the aeolian sediment transport. Vegetation strategies which locally increase the wind shear velocity threshold have been applied to some of the scenarios to account for the effects of dune vegetation. The influences of the offshore wind on the aeolian system have been assessed by comparing the model results between the simulations with and without offshore wind.

Based on the results of modeling study, it is found that sediment sorting and beach armoring can largely reduce the beach erosion and the onshore aeolian transport. With more nonerodible elements existing in the bed, the effects of beach armoring get strengthened. The parameter of layer thickness in the model could also affect aeolian transport, where a thicker layer can lead to larger dune accretion. As for the influences of wind, higher wind speed may induce stronger aeolian sediment transport. The existence of offshore wind can reduce the dune accretion in onshore wind dominant system. In offshore wind dominant system, the offshore wind needs to be filtered out to enable the model to reproduce the pattern of onshore transport and dune accretion. When the wind condition is very favorable for onshore transport like Rijnland, the modeled dune accretion is relatively larger than the measured dune accretion. When the wind condition is not favorable for dune accretion like Ameland, the modeled and measured dune accretion volumes are in the same range. The modeled dune accretion volume for the Rijnland transect are larger than the one for Ameland, which again demonstrates the influence of coastal orientations on the aeolian transport.

Part III

DISCUSSION AND CONCLUSIONS

6. Discussion

During the course of this research a few of topics of interest have come up which are open for discussion. First the model performance for Rijnland and Ameland cases is discussed, including the model ability in onshore and offshore wind dominant systems and the inconsistency between modeled and measured dune accretion. Then, model validation and calibration are discussed as well.

6.1. Model performance

In Part II of the thesis, the AeoLiS model has been applied for 11 scenarios on the Rijnland and Ameland coasts. Based on the results of some scenarios, here the performance of the AeoLiS model in this thesis study will be evaluated for Rijnland and Ameland respectively.

6.1.1. Model performance on the Rijnland coast

As discussed before, the Rijnland coast is considered as an onshore wind dominant system because of its coastal orientation. Scenario #1 with 'full wind field' obtained a dune accretion volume of $15.83 m^3/yr\ /m$. Scenario # 6 with all the offshore winds being filtered out obtained a dune accretion of $16.26 m^3/yr\ /m$, which is larger than the volume of scenario #1. That is to say the offshore winds in the imposed wind field can reduce the onshore aeolian sediment transport, and the resultant beach erosion and dune accretion. However, this reduction effect of the offshore winds is not expected in the constructed model of this thesis study. With high wind shear velocity threshold resulted from the vegetation, the dune accretion is not expected to be eroded again by the offshore winds. Without sediment source from the landward boundary of the model domain, the beach erosion in the intertidal area is not expected to be reduced by the offshore winds either. Therefore based on the findings of this thesis study, to focus on the aeolian transport and dune accretion caused by the onshore winds, it is recommended to filter out all the offshore winds in an onshore wind dominant system like Rijnland.

Another aspect which deserves discussion is the relatively large inconsistency between the modeled and measured dune accretion volume on the Rijnland coast. Based on the data analysis, the measured dune accretion for the Rijnland transect is only $8.92 m^3/yr\ /m$. Based on the modeling study, the modeled dune accretion for scenario #8 which uses the sediment fraction settings of the Sand Motor and the wind field without offshore wind is $21.70 m^3/yr\ /m$. Other scenarios for Rijnland also give high value for the dune accretion: scenarios #1, #3, #4, #6, #7 all got dune accretion larger than $15.00 m^3/yr\ /m$. In other words, the errors between the modeled and measured dune accretion for Rijnland are usually big and the modeled volumes are usually larger. Therefore the performance of the AeoLiS model for this case is not excellent enough. Here for Rijnland as an onshore wind dominant system, most of the winds are onshore and the wind speeds are high. Intuitively, with more large onshore winds, the dune accretion will be large and the model results seem to be correct. However, in reality, dune accretion usually cannot reach a very high value. The front dune slope with fast and large dune accretion may become too steep to

grow further. Slope slide may happen which limits the dune accretion. But in the model, dune accretion can be very large as long as the wind condition is favorable. Therefore, it is recommended that for the cases with very favorable wind condition for dune accretion, some mechanisms should be included to account for the factors which limits the dune accretion and keep the dune accretion to a realistic level.

6.1.2. Model performance on the Ameland coast

The constructed model has also been applied to the Ameland coast. As the coastal orientation towards the north while the dominant wind from the southwest, the Ameland coast is considered as an offshore wind dominant system. When applying the 'full wind field', the model cannot reproduce the dune accretion which happens in reality any more, see the results of scenario #9 in Figure 34. After filtering out all the offshore winds, scenario #10 reproduces the onshore aeolian transport and dune accretion again. Therefore in an offshore wind dominant system, it is necessary to filter out the offshore winds to enable the model to reproduce the onshore wind transport and dune accretion in the real world.

The measured dune accretion volume based on the data analysis has been compared to the modeled dune accretion in section 5.8.2. The measured dune accretion based on the data analysis is $4.50 m^3/yr/m$. In the modeling study, scenario #11 which uses the sediment fraction settings of the Sand Motor and the wind field without offshore wind get a dune accretion volume of $3.36 m^3/yr/m$. Compared to Rijnland, the difference between measured and modeled dune accretion volumes for Ameland is relatively small. As the onshore wind for Ameland happens much less frequently, the dune accretion is relatively slow. Mechanisms like slope slide is not that important anymore. The inaccuracy of the sediment fraction settings is not enlarged either. The modeled results can be very close to the measured results. Therefore, for the cases with unfavorable wind condition for dune accretion, the model can give relatively accurate results compared to the measurements.

6.2. Validation

With the fact that the hydraulic mixing, drying rate and bed interaction being included and the spatiotemporal varying sediment availability being simulated rather than parameterized through the velocity threshold, the model should already reproduce the true nature of aeolian sediment transport much better than the existing models. The AeoLiS model has been validated for the Sand Motor in The Netherlands. The results show that the aeolian sediment transport simulated by the constructed model correspond well with the measurements. The comparison between the measured and simulated dune accretion in this thesis study could also be seen as an attempt of validation of the model, where the modeled dune accretion corresponds well with the measurement for Ameland while the modeled dune accretion for Rijnland is larger than the measurement. More practice of validation is ongoing, which may help to make the model more robust and accurate.

6.3. Calibration

The constructed model has used some input obtained from the measurements, such as tide, wind and bed level. Some other parameters applied in this model approach needs calibration, which has been done pragmatically and can be improved. For example, *Tdry* is the adaptation time scale for soil drying, which has been chosen as 7200 seconds (2hours). The AeoLiS model uses simplified functions for infiltration and evaporation to simulate the soil drying on the beach (Hoonhout & de Vries, 2016). An increase in *Tdry* means the sediment after getting wet needs more time to be dried, then picked up and transported, because of the high shear velocity threshold of the wet sand. Lowering the drying time makes the adaptation of soil drying faster. However, in the constructed model, no wave or precipitation input was applied. Only the tidal forcing can moisten the sediment. And the time scale of the tidal forcing (12 hours) is much larger than the chosen time scale of soil drying (2 hours). Small variations to the drying time do not lead to significant differences in aeolian sediment transport in this model, making the results of model simulation can be seen as representative.

The bed interaction parameter indicates the exchange of momentum between different sediment fractions, weighing the contribution of the grainsize distribution in the bed and in the air to the grain size distribution for erosion and deposition. The bed interaction parameter varies between 0 and 1, where low values means the grain size distribution in the bed is less important and high values indicates the transport depends more on the grain size distribution in the bed. In the model of the thesis, the bed interaction parameter *bi* is set to 0.05, lower than the default value of 1.0. A lower value of *bi* is used in order to weaken the influence of the grain size distribution on the aeolian sediment transport. A comprehensive calibration of the applied *bi* value in the model needs detailed measurements of grain size distributions in the bed. This has not been executed for this thesis study and can be a point to be improved.

7. Conclusions and recommendations

In this chapter, the conclusions and recommendations regarding this Master thesis research are presented. They are all based on the findings of this thesis.

7.1. Conclusions

Here in this chapter the conclusions and answers to the research questions of this Master thesis research are listed. The alongshore distributions of dune growth rate for the Rijnland coast and the Ameland coast have been derived from the JARKUS dataset and the spatial variability in the distributions has been analyzed. The spatial variability in coastal morphology along the Rijnland coast has been assessed and the relationship between coastal morphology and dune growth rate has been explored. The topography obtained from the data analysis has been used as input for the AeoLiS model. By using this model 11 simulations have been conducted in order to explore the influences of sediment supply and some other parameters on the aeolian system. Based on the results of data analysis and model study, the influence of coastal orientations on the dune behavior has been assessed.

1. What parameters represent/quantify dune behavior?

The dune behavior has been represented by a series of parameters. The dimension of a dune is assessed quantitatively by the dune volume. Here the dune volume is considered as the volume of the active dune, which is defined as the dune section where the profiles show distinctly large temporal variability over years. A fitted line for the time series of the calculated dune volumes can be determined based on regression analysis. Then the slope of the fitted line gives the average dune growth rate, which assesses quantitatively the rate the dune volume changing over the concerned period.

2. What are the theoretical aeolian transport capacity and the dune growth rates along the Dutch coast under different coastal orientations and how do they compare with each other?

The dune growth rates for both Ameland and Rijnland show large spatial variability along the two coasts. For both coasts, the measured dune growth rates are smaller than the onshore components of the respective theoretical wind transport capacity. Between the two concerned coasts, both the theoretical and the measured aeolian sediment transport have very different results: the theoretical aeolian transport capacity for Rijnland is in the onshore direction while the one for Ameland is considered offshore; the onshore wind transport capacity for Rijnland is more than three times as large as the one for Ameland; the actual aeolian sediment transport values reflected by the dune growth rates along the Rijnland coast are generally much higher than the ones for Ameland. One of the major factors which may account for these differences is the difference in coastal orientations between the two places, which makes Rijnland an onshore wind dominant system while Ameland an offshore wind dominant system.

3. How do the spatial variations existing in coastal morphology correlate to the alongshore varying dune behavior?

The measured positions in the cross shore direction of the waterline, dunefoot and active dune's landward boundary can vary widely along a coast, resulting in large alongshore morphologic variability in the coastal beach-dune system. The width of active dune and the dune growth rate have a positive correlation: a larger dune accretion is usually linked to a wider active dune. As for the beach width, no necessary association can be distinguished between the beach width and the dune growth rate along the studied coast.

4. How to simulate aeolian sediment transport, dune volume changes and the combined effect of erosive and accretive processes?

The AeoLiS model has been used with 11 different scenarios to explore the aeolian sediment transport and the role of sediment supply. The model topography was obtained from the results of data analysis while the hydrodynamic and meteorological input were acquired from the nearby measuring stations. The effects of dune vegetation on the aeolian sediment transport were accounted for by increasing the local wind shear velocity threshold within the dune area. The influence of the offshore wind on the aeolian system was assessed by comparing the model results between the simulations with and without offshore wind.

5. How do relevant processes affect the aeolian sediment transport and what is the role of sediment supply in the aeolian system?

The generic process of the aeolian sediment transport has been reproduced: sediment in the intertidal zone gets entrained and transported towards the dune by the onshore wind, and then gets deposited on the dune because of the high velocity threshold resulted from the dune vegetation. The simulation of dune vegetation is important for realizing dune accretion in the constructed model.

Sediment sorting develops over time as the fines get eroded and transported continuously by the wind. More nonerodible roughness elements emerge from the bed and the beach gets armored, resulting in the reduction of onshore wind transport and dune accretion. When more nonerodible elements exist in the bed, the effects of sediment sorting and beach armoring on reducing the aeolian sediment transport get strengthened.

As another influential factor, higher wind speed may also results in stronger sediment entrainment and aeolian transport. The existence of the offshore wind in onshore wind dominant system can reduce the effect of aeolian sediment transport caused by the onshore wind, resulting in less beach erosion and less dune accretion in the model. In offshore wind dominant system, the offshore wind needs to be filtered out to enable the model to reproduce the pattern of onshore wind transport and dune accretion. For the case where the wind condition is very favorable for dune accretion like the Rijnland coast, the modeled dune accretion is relatively larger than the measured dune growth. For the case where the wind condition is not favorable for dune accretion such as Ameland, the difference between the modeled and measured dune accretion is small. Under the different coastal

orientations, the simulated dune accretion for the Rijnland transect is larger than the value for Ameland.

7.2. Recommendations

This section provides the recommendations regarding the conducted research, for both data analysis and modeling study. More work can be done in the future to understand coastal dune behavior and aeolian sediment transport.

Recommendations for data analysis:

- Investigation about nourishments and erosion events

The conducted data analysis in this thesis derived dune growth rates from the time series of dune volume, which was calculated based on the yearly measured profiles. Nourishments and erosion events like storm surge may have happened in the concerned period. They could bring relatively large and sudden change to the coastal beach-dune system. An investigation of the happened nourishments and erosion events in the concern period will benefit this thesis as well as other studies which conduct similar data analysis.

- Combining data analysis with monitoring techniques

In this thesis research, the data analysis obtained the profiles from the JARKUS dataset, with the temporal resolution of one year. Recently more innovative monitoring techniques have been developed and applied, such as GPS surveying, laser scanning, etc. These relatively new techniques may provide measurements with higher temporal and spatial resolutions. Combining the data analysis based on the JARKUS dataset with other monitoring techniques may give a more comprehensive understanding of the coastal beach-dune system.

Recommendations for modeling study:

- Sediment survey

As shown in section 5.4, sediment availability of the bed could have significant influences on aeolian sediment transport and the resultant dune accretion. However, no measurements about the grain size distribution on the Rijnland and Ameland coasts were available. A sediment sample survey may enhance the reliability and accuracy of the model when reproducing the real world. It will help choosing appropriate input parameters such as grain size distribution and layer thickness as well.

- Influence of offshore wind

As discussed in section 5.5 and 6.1, the existence of offshore wind will affect the aeolian sediment transport and the dune accretion in the model. Based on this thesis study, for modeling studies which focus on onshore aeolian transport and dune accretion, it is recommended to filter out all

the offshore winds for both onshore and offshore wind dominant systems. The exact role of offshore wind in modeling the aeolian transport in coastal system is still not yet well-known and deserves more research. Especially for offshore wind dominant system, more applications are needed to improve the model performance.

- Correction of the dune accretion under favorable onshore wind condition

When onshore winds were very large and frequent, the dune in the model grew fast which resulted in large dune accretion value. However, the measured dune accretion in reality obtained smaller value, see section 5.8. The inconsistency between the modeled and measured dune accretion inspires more model applications for the cases with favorable onshore wind condition. Some mechanisms like front dune slope slide could be introduced to limit the modeled dune accretion to a more realistic level. The distribution of the sediment being deposited over the dune surface deserves more research as well.

- Modeling 3D situations

The modeling study of this thesis has only chosen one transect for each concerned coast to establish a 2DV profile model. The situations for other transects along the coasts have not been tested. Modeling 3D situations which takes all the transects into account may give a more comprehensive understanding of the aeolian system.

iv. APPENDICES

Part IV

APPENDICES

Appendix A. Summary of dune accretion volumes in the modeling study

In Part II of the thesis, 11 scenarios have been simulated and analyzed. Table 4 shows a summary of the dune accretion volumes obtained from the model results. The settings of the scenarios can be found in section 4.2. In Chapter 5, the results of different scenarios have already been compared in order to discuss the influences of different processes on the aeolian sediment transport. Below the table a brief review is given by comparing the dune accretion volumes in Table 4.

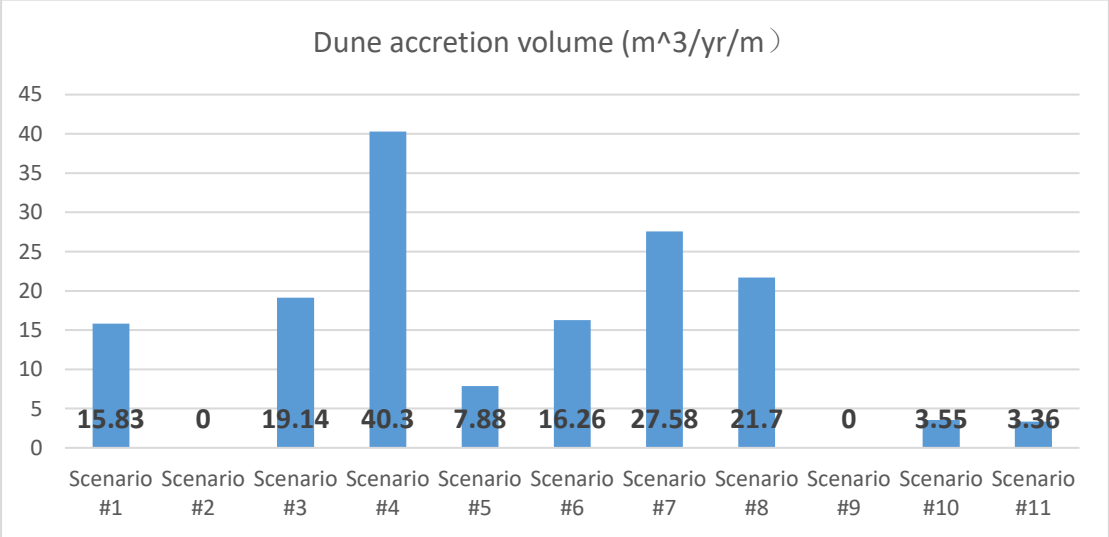

Table 4. Summary of the dune accretion volumes for all the scenarios.

Scenario #1 is regarded as the base scenario, which has a dune accretion volume of $15.83 m^3/yr/m$. Scenario #2 has zero dune accretion because no vegetation is applied in scenario #2. Scenario #3 has larger dune accretion than scenario #1, showing that larger layer thickness in the model gives larger onshore aeolian transport and dune accretion. Scenario #4 without nonerodible roughness elements has very large dune accretion, indicating the effect of sediment sorting and beach armoring on reducing aeolian sediment transport. Scenario #5 proves that a bed with more nonerodible elements will gain less dune accretion. Scenario #6 shows that when modeling an onshore wind dominant system, the offshore winds will reduce the onshore transport and the dune accretion in the model. Comparing scenario #9 and #10 shows that when modeling an offshore wind dominant system, it is necessary to filter out all the offshore winds to enable the model to reproduce onshore aeolian transport and dune accretion. Scenario #7 indicates that larger wind can increase aeolian transport and dune accretion. By comparing scenarios #8 and #11 which both use Pattern 4 as sediment fraction settings and let the offshore winds filtered out, the influences of coastal orientations on the aeolian sediment transport are considered to be important. If the orientation of a coast (the normal direction of the coastline) is more approaching the dominant wind direction which makes more large winds considered onshore, the onshore aeolian transport and resultant dune accretion are larger.

Appendix B. Results from the data analysis for the chosen transects in the modeling study

In the modeling study, the transect with id = 8007350 was chosen for the Rijnland coast and the transect with id = 3000900 was chosen for Ameland. In section 5.8, the modeled results for these two transects were compared with the measured results based on the previous data analysis. In order to give a comprehensive impression, here more details for these two transects derived from the data analysis are shown.

Figure 41 shows the results of data analysis for the Rijnland transect, including the profile evolution over years and the corresponding variance (top panel) and the dune volume time series (bottom panel). When the top panel is considered, the curves with different colors are the transect profiles for each year from 2006 to 2016. The variance calculated from the profile evolution is shown below it. The right hand side is the sea side while the left side is the land side. It is found only a small section in the middle shows large variations and this section is considered as the active dune. The point where the variance becomes neglected again (from the sea side towards the land) is taken as the landward boundary of the active dune. The bottom panel shows the time series of the active dune volumes and the fitted line. The slope of the fitted line is taken as the dune growth rate. Actually the dune growth rate for this Rijnland transect is $21.70 m^3/yr/m$.

Similarly, Figure 42 shows the results of data analysis for the Ameland transect. The top panel shows the profile evolution and the corresponding variance, where the section with relatively large variance (in the middle) is taken as the active dune. The bottom panel shows the time series of the active dune volumes, where the slope of the fitted line indicates the dune growth rate of this transect is $3.36 m^3/yr/m$.

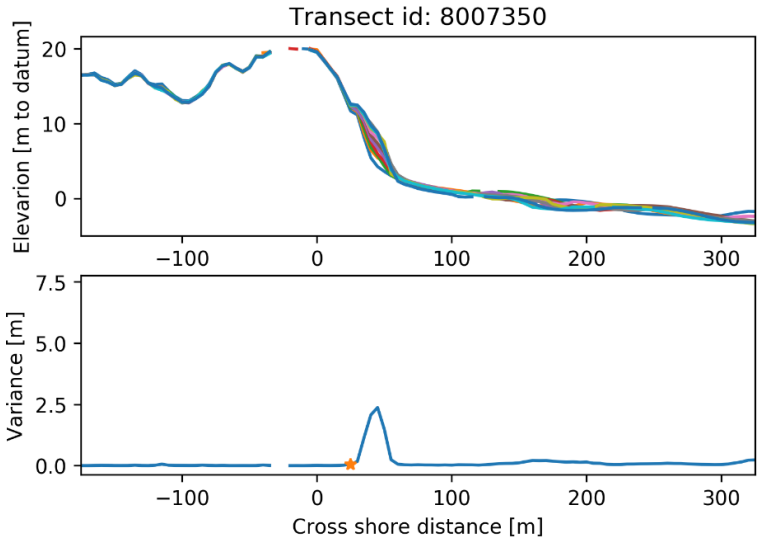

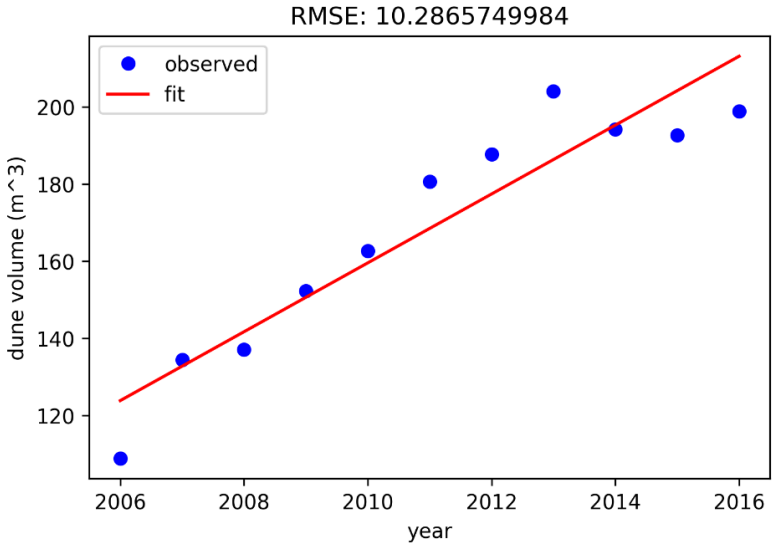

Figure 41. Results of data analysis for the Rijnland transect (id = 8007350), including the profile evolution and the calculated variance (top panel) and the dune volume time series (bottom panel).

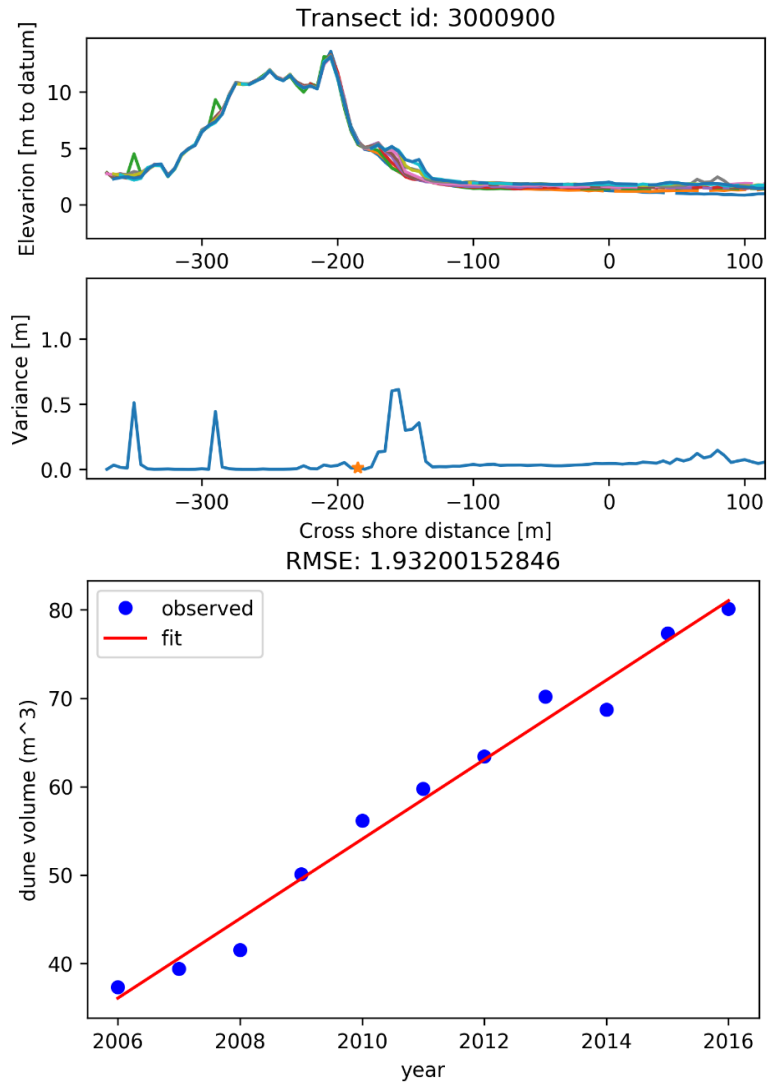

Figure 42. Results of data analysis for the Ameland transect (id = 3000900), including the profile evolution and the calculated variance (top panel) and the dune volume time series (bottom panel).

Appendix C. Results of dune volume and dune growth rate from the data analysis for the period from 1980 to 1990

1. Results of dune volume and dune growth rate on the Ameland coast

The dune volume values have been calculated for all transect locations of the entire Ameland coast for the period from 1980 to 1990, using the methods mentioned in chapter 2. From the slope of the fitted line of the dune volume time series, the dune growth rates have been obtained and plotted alongshore, shown in Figure 43. The vertical axis represents the dune growth rate per year per running meter $(\mathrm{m}^3/\mathrm{yr}/\mathrm{m})$, while the horizontal axis represents the alongshore identifier of transect (id) which corresponds to alongshore coordinate. The locations with the small id (left side of the figure) are in the west part of the Ameland coast, while the large values of id (right side of the figure) represent the east part of the coast.

From the Figure 43, a relatively large spatial variation alongshore for the dune growth rate can be recognized from the west to the east for the Ameland coast. The locations with the id around 3000200 experience serious erosion, where the values being able to reach $-40\ \mathrm{m}^3/\mathrm{yr}/\mathrm{m}$. For the locations with the id in the range of 3000500 to 3001000, the coastal dunes experience strong accretion with the growth rates around $10\ \mathrm{m}^3/\mathrm{yr}/\mathrm{m}$. The dunes located in the section with the id from 3001150 to 3001800 obtain mostly erosion, with the rates in the order of 5 to 10 $\mathrm{m}^3/\mathrm{yr}/\mathrm{m}$. The area with the id around 3002000 experience strong accretion again. For the coast from id=3000350 to the east, erosion and accretion appear alternatively. And generally the accretion is stronger than erosion. Considering the entire Ameland coast, the coastal dunes experience a trend (but not a strong trend) of growing.

2. Results of dune volume and dune growth rate on the Rijnland coast

Similar to the Ameland coast, the dune volume values and dune growth rates have also been calculated for all transect locations for the entire Rijnland coast for the period from 1980 to 1990. The dune growth rates alongshore has been plotted and shown in Figure 44. Again the vertical axis is the dune growth rate value in $[\mathrm{m}^3/\mathrm{yr}/\mathrm{m}]$, while the horizontal axis is the alongshore identifier of transect (id) corresponding to alongshore coordinate. The locations with small id (left side of the figure) are in the north side of the Rijnland coast, while large id (right side of the figure) represent the south part.

First consider the right part of the figure, from the location with id=8006300 to the right (to the south). Within this part, the spatial variation for the dune growth rate is relatively small. Dune erosion seldom happen in this part of the Rijnland coast. Oppositely, most of the area experience dune accretion or volume balance. The section from approximately id=8006900 to id=8008200 experience dune accretion with the dune growth rates in the order of 5 to 8 $\mathrm{m}^3/\mathrm{yr}/\mathrm{m}$. Some other part, for example around id=8006500, neither experience dune accretion nor dune erosion with the dune growth rate values more or less equal 0. When considering the left hand side of the figure

from id=8006300 to the left (north part of the coast), the dune growth rates show two peaks. The very left side until id=8005950 shows relatively large dune accretion, while the locations from id=8005950 to id=8006300 show strong dune erosion.

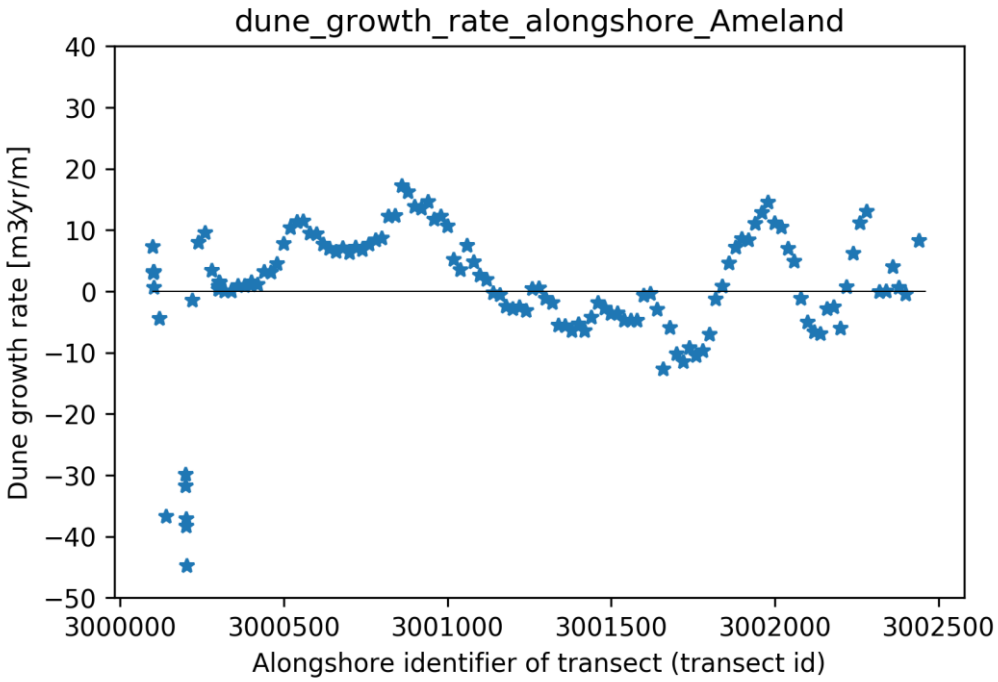

Figure 43. Dune growth rates along the Ameland Coast for the period from 1980 to 1990.

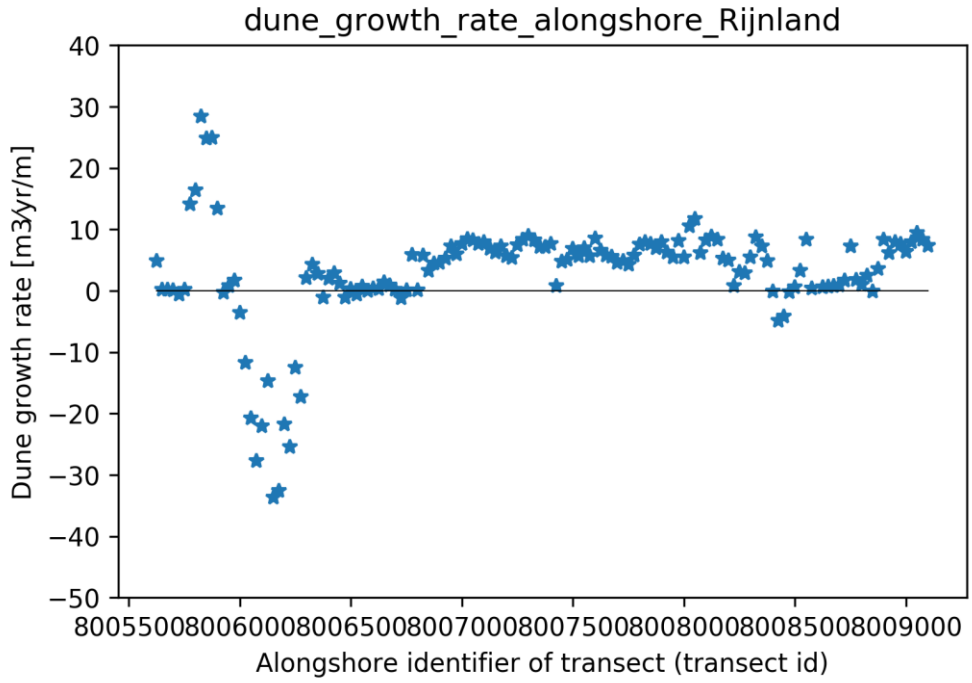

Figure 44. Dune growth rates along the Rijnland Coast for the period from 1980 to 1990.

References

Aagaard, T., Davidson-Arnott, R., Greenwood, B., Nielsen, J., 2004. Sediment supply from shoreface to dunes: linking sediment transport measurements and long-term morphological evolution. Geomorpology, 60 (1), pp. 205-224.

Aarninkhof, S., van Dalfsen, J.A., Mulder, J., Rijks, D., May 2010. Sustainable development of nourished shorelines: innovations in project design and realization. Proceedings of PIANC MMX Congress. Liverpool UK.

Arens, S.M., 1996. Rates of aeolian transport on a beach in a temperate humid climate. Geomorphology, 17 (1–3), pp. 3–18.

Bagnold, R., 1937. The transport of sand by wind. Geogr. J., 89, pp. 409–438.

Bagnold, R., 1954. The Physics of Blown Sand and Desert Dunes, (2nd Edition) Methuen, Lonon.

Bauer, B.O., Davidson-Arnott, R.G.D., Hesp, P. A., Namikas, S. L., Ollerhead, J., Walker, I. J., 2009. Aeolian sediment transport on a beach: Surface moisture, wind fetch, and mean transport. Geomorphology, 105, pp. 106–116.

Bochev-van der Burgh, L., Wijnberg, K., Hulscher, S., 2011. Decadal-scale morphologic variability of managed coastal dunes. Coastal Engineering, 58 (9), pp. 927–936.

Callaghan, D.P., Nielsen, P., Short, A., Ranasinghe, R., 2008. Statistical simulation of wave climate and extreme beach erosion. Coastal Engineering, 55 (5), pp. 375–390.

Cheng, H., Liu, C., Zou, X., Li, J., He, J., Liu, B., Wu, Y., Kang, L., Fang, Y., 2015. Aeolian creeping mass of different grain sizes over sand beds of varying length. J. Geophys. Res. Earth Surf., 120, pp. 1404–1417.

Davidson-Arnott, R.G.D., Yang, Y., Ollerhead, J., Hesp, P.A., Walker, I.J., 2008. The effects of surface moisture on aeolian sediment transport threshold and mass flux on a beach. Earth Surface Processes and Landforms, 33 (1), pp. 55–74.

de Vries, S., Southgate, H.N., Kanning, W., Ranasinghe, R., 2012. Dune behavior and aeolian transport on decadal timescales. Coastal Engineering, 67, pp. 41-53.

de Vries, S., van Thiel de Vries, J.S.M., van Rijn, L.C., Arens, S. M., Ranasinghe, R., 2014. Aeolian sediment transport in supply limited situations. Aeolian Res., 12, pp. 75–85.

den Heijer, C., Baart, F., van Koningsveld, M., 2012. Assessment of dune failure along the Dutch coast using a fully probabilistic approach. Geomorphology, 143–144, pp. 95–103.

Dong, Z., Wang, H., Liu, X., Wang, X., 2004. A wind tunnel investigation of the influences of fetch length on the flux profile of a sand cloud blowing over a gravel surface. Earth Surf. Processes Landforms, 29(13), pp. 1613–1626.

Fryberger, S., 1979. Dune forms and wind regime. A study of global sand seas. USGS Professional Paper, 1052, pp. 137–169.

Gillies, J.A., Nickling, W.G., King, J., 2006. Aeolian sediment transport through large patches of roughness in the atmospheric inertial sublayer. J. Geophys. Res., 111, F02006.

Guillen, J., Stive, M.J.F., Capobianco, M., 1999. Shoreline evolution of the Holland coast on a decadal scale. Earth Surface Processes and Landforms, 24 (6), pp. 517–536.

Hoonhout, B.M., de Vries, S., 2016. A process-based model for aeolian sediment transport and spatiotemporal varying sediment availability. J. Geophys. Res. Earth Surf., 121, pp. 1555–1575.

Hoonhout, B.M., de Vries, S., 2017. Aeolian sediment supply at a mega nourishment. Coastal

Engineering, 123, pp. 11-20.
Hotta, S., Kubota, S., Katori, S., Horikawa, K., 1984. Sand transport by wind on a wet sand beach, in Proceedings of the 19th Conference on Coastal Engineering, ASCE, Houston, Tex, pp. 1264–1281.
Iversen, J.D., Rasmussen, K.R., 1994. The effect of surface slope on saltation threshold. Sedimentology, 41 (4), pp. 721–728.
Janssen, T., 2016. Aeolian transport on a beach: Testing the AeoLiS aeolian sediment transport model against the observed recovery of Fire Island. MSc thesis, Delft University of Technology, Delft.
Jungerius, P.D., Witter, J.V., Boxel, J.H.V., 1991. The effects of changing wind regimes on the development of blowouts in the coastal dunes of the Netherlands. Landscape Ecology, 6, pp. 41–48.
Kawamura, 1951. Study on sand movement by wind. Reports of Physical Sciences Research Institute of Tokyo University, 5 (3–4), pp. 95–112.
Keijsers J.G.S., Poortinga A., Riksen M.J.P.M., Maroulis J., 2014. Spatio-temporal variability in accretion and erosion of coastal foredunes in the Netherlands: Regional climate and local topography. PloS ONE 9 (3): e91115.
King, J., Nickling, W.G., Gillies, J.A., 2005. Representation of vegetation and other nonerodible elements in Aeolian shear stress partitioning models for predicting transport threshold. J. Geophys. Res., 110, F04015.
Kocurek, G., Lancaster, N., 1999. Aeolian system sediment state: Theory and Mojave Desert Kelso dune field example. Sedimentology, 46(3), pp. 505–515.
Kostaschuk, R., Shugar, D.H., Best, J.L., Parsons, D.R., Lane, S.N., Hardy, R.J., 2008. Suspended sediment transport over a dune. MARID (Marine and River Dune Dynamics) 2008 Workshop, 1-3 April 2008, University of Leeds, United Kingdom, pp. 197-201.
Kriebel, D.L., Dean, R.G., 1985. Numerical simulation of time-dependent beach and dune erosion. Coastal Engineering, 9 (3), pp. 221–245.
Larson, M., Erikson, L., Hanson, H., 2004. An analytical model to predict dune erosion due to wave impact. Coastal Engineering, 51 (8–9), pp. 675–696.
Lynch, K., Jackson, D.W., Cooper, J.A.G., 2016. The fetch effect on aeolian sediment transport on a sandy beach: a case study from Magilligan Strand, Northern Ireland. Earth Surf. Process. Landf., 41(8), pp. 1129-1135.
McCall, R.T., van Thiel de Vries, J.S.M., Plant, N.G., van Dongeren, A.R., Roelvink, J.A., Thompson, D.M., Reniers, A.J.H.M., 2010. Two-dimensional time dependent hurricane overwash and erosion modeling at Santa Rosa Island. Coastal Eng., 57(7), pp. 668–683.
McKenna Neuman, C., Li, B., Nash, D., 2012. Micro-topographic analysis of shell pavements formed by aeolian transport in a wind tunnel simulation. J. Geophys. Res., 117, F04003.
Nickling, W., Davidson-Arnott, R., 1990. Aeolian sediment transport on beaches and coastal sand dunes. Canadian Symposium on Coastal Sand Dunes, Canadian Coastal Science and Engineering Association, Guelph, Ontario.
Nickling, W., McKenna Neuman, C., 1995. Development of deflation lag surfaces. Sedimentology, 42(3), pp. 403–414.
Nickling, W.G., Ecclestone, M., 1981. The effects of soluble salts on the threshold shear velocity of fine sand. Sedimentology, 28, pp. 505–510.
Okin, G.S., 2008. A new model of wind erosion in the presence of vegetation. J. Geophys. Res., 113, F02S10.

Pye, K., Blott, S.J., 2008. Decadal-scale variation in dune erosion and accretion rates: an investigation of the significance of changing storm tide frequency and magnitude on the Sefton coast, UK. Geomorphology, 102 (3–4), pp. 652–666.
Raupach, M., Gillette, D., Leys, J., 1993. The effect of roughness elements on wind erosion threshold. J. Geophys. Res., 98(D2), pp. 3023–3029.
Roelvink, D., Reniers, A., van Dongeren, A., van Thiel de Vries, J., McCall, R., Lescinski, J., 2009. Modelling storm impacts on beaches, dunes and barrier islands. Coastal Eng., 56(11–12), pp. 1133–1152.
Ruessink, B.G., Jeuken, M.C.J.L., 2002. Dunefoot dynamics along the Dutch coast. Earth Surface Processes and Landforms, 27 (10), pp. 1043–1056.
Sherman, D.J., Li, B., 2012. Predicting aeolian sand transport rates: A reevaluation of models. Aeolian Res., 3(4), pp. 371–378.
Sørensen, M. 2004. On the rate of aeolian sand transport. Geomorphology, 59(1), pp. 53–62.
Southgate, H.N., 2011. Data-based yearly forecasting of beach volumes along the Dutch North Sea coast. Coastal Engineering, 58 (8), pp. 749–760.
Stout, J.E. 2004. A method for establishing the critical threshold for aeolian transport in the field. Earth Surf. Processes Landforms, 29(10), pp. 1195–1207.
Tan, L., Zhang, W., Qu, J., Zhang, K., An, Z., Wang, X., 2013. Aeolian sand transport over Gobi with different gravel coverages under limited sand supply: A mobile wind tunnel investigation. Aeolian Res., 11, pp. 67–74.
Turpin, C., Badr, T., Harion, J. L., 2010. Numerical modelling of aeolian erosion over rough surfaces. Earth Surf. Processes Landforms, 35(12), pp. 1418–1429.
van de Graaff, J., 1977. Dune erosion during a storm surge. Coastal Engineering, 1, pp. 99–134.
van der Wal, D., 1998. The impact of the grain-size distribution of nourishment sand on aeolian sand transport. J. Coastal Res., 14, pp. 620–631.
van Straaten, L., 1961. Directional effects of winds, waves and currents along the Dutch North Sea coast. Geologie en Mijnbouw, 40, pp. 333–346 (Part 1) and 363–391 (Part 2).
van Thiel de Vries, J.S.M., 2010. Dune erosion during storm surges. PhD Thesis. Delft University of Technology, Delft.
Velhorst, R.L.C., 2017. Towards a coupled morphodynamic model of the nearshore zone and the beach at the Sand Engine: Combining waves, tide, morphodynamics and aeolian sediment transport into a process-based model. MSc Thesis. Delft University of Technology, Delft.
Vellinga, P., 1986. Beach and dune erosion during storm surges. Ph.D. thesis, Delft University of Technology.
WL/Delft Hydraulics, 1978. (in Dutch) Duinafslag ten gevolge van de stormvloed op 3 januari 1976. Tech. rep., Waterloopkundig Laboratorium.
WL/Delft Hydraulics, 1984. (in Dutch) Duinafslag ten gevolge van de stormvloed op 1 en 2 februari 1983. Tech. rep., Waterloopkundig Laboratorium.